Jasmonates in the model lycophyte *Selaginella moellendorffii*: biosynthesis, metabolism, and functions

(イヌカタヒバにおけるジャスモン酸類の同定および機能解析)

A Dissertation Presented

by

Putri Pratiwi

Laboratory of Natural Product Chemistry

Division of Bio-system Sustainability

Graduate School of Agriculture

Hokkaido University

Japan

Jasmonates in the model lycophyte *Selaginella moellendorffii*: biosynthesis, metabolism, and functions

(イヌカタヒバにおけるジャスモン酸類の同定および機能解析)

by

Putri Pratiwi

A dissertation submitted to the Special Postgraduate English Program in Biosphere Sustainability Science, Graduate School of Agriculture, Hokkaido University, Japan.

Approved as to style and content by,

_____

Professor Dr. Hideyuki Matsuura

_____

Professor Dr. Yasuyuki Hashidoko

_____

Lecturer Dr. Kosaku Takahashi

Sapporo, Japan

September 2017

TABLE OF CONTENTS

LIST OF FIGURES

LIST OF TABLES

LIST OF ABBREVIATIONS

α -LeA	:	α –linolenic acid
12-OPDA	:	12-oxo-phytodienoic acid
13(*S*)-HPOT	:	13(*S*)-hydroperoxyoctadecatrienoic acid
13-LOX	:	13-lipoxygenase
12,13(*S*)-EOT	:	12,13(*S*)-epoxyoctadecatrienoic acid
A. thaliana	:	*Arabidopsis thaliana*
ABA	:	abscisic acid
ACX	:	acyl-CoA oxidase
AOC	:	allene oxide cyclase
AOS	:	allene oxide synthase
aq	:	aqueous
bp	:	base pair
cDNA	:	complimentary DNA
COI1	:	coronatine insensitive 1
dH_2O	:	distilled water
DNA	:	deoxyribonucleic acid
DAD1	:	defective in anther dehiscence 1
GC-MS	:	gas chromatography-mass spectrometry
GFP	:	green fluorescent protein
His	:	histidine
His-tag	:	hexa histidine-tag
Ile	:	isoleucine
IPTG	:	isopropyl β–D-1-thiogalactopyranoside
JA	:	jasmonic acid
JA-Ile	:	(+)-7-*iso*-jasmonyl-L-isoleucine
JAR1	:	jasmonic acid resistant 1
JAZ	:	jasmonate-zim domain
KAT	:	L-3-ketoacyl-CoA thiolase
kDa	:	kilodalton
MFP	:	multifunctional protein
Mya	:	million years ago

M. polmorpha	:	*Marchantia polymorpha*
NINJA	:	novel interactor of jasmonate-zim domain
Ni-NTA	:	nickel-nitrilotriacetic acid
OPC-8:0	:	3-oxo-2-(2'(*Z*)-pentenyl)-cyclopentane-1-octanoic acid
OPR	:	12-oxo-phytodienoic acid reductase
ORF	:	open reading frame
PEG	:	polyethylene glycol
PL	:	phospholipase
P. patens	:	*Physcomitrella patens*
PI	:	isoelectric point
RT-PCR	:	reverse transcription-polymerase chain reaction
SCF	:	Skp-cullin-F box
SDS-PAGE	:	sodium dodecylsulfate-polyacrylamide gel electrophoresis
S. moellendorffii	:	*Selaginella moellendorffii*
TE	:	thioesterase
TPL	:	topless
UPLC/MS-MS	:	ultra-performance liquid chromatography tandem mass-spectrometry
UV	:	ultraviolet
µm	:	micrometer
µM	:	micromolar concentration

CHAPTER I

GENERAL INTRODUCTION

The natural characteristic of plants as sessile organisms makes them vulnerable from different environmental stresses. These stresses cause changes in biological system that potentially damage and likely reduce its fitness. As their defense mechanisms, plants response in various ways, such as acclimation, change in hormone-modulated biochemical and physiological changes, and/or developmental changes in morphology. If the individual response cannot fully recover from the stress, the plant fitness is reduced and evolutionary (genetic changes) at population level may occur. Thus, these changes result in alteration of one or more of the hormonal, physiological, or developmental responses.

The early evolution of land plants was occurred in the mid-Palaeozoic era (between 480 and 360 Mya) and remarked the important history of life. From the aquatic environment, early land plants have evolved in several innovations to sustain their life. Elaboration of two phase life cycle, the complex organs and tissue systems, specialization of vascular tissue, and diverse seed are among the plant innovation to keep them survived (Kenrick and Crane 1997). These adjustments attracted researcher to study more detail of the mechanisms. In recent years, many analyses regarding to plant defense mechanisms and growth regulators have been investigated especially upon plant hormones (known as phytohoromones). Hormones are secreted chemical signals to regulate the coordinate expression of multiple physiological and morphological phenotypes to optimize the individual fitness. The binding of plant hormones to their own receptors located in target tissues is important to lead the

alteration of cell physiology or changes in genes expression and transcription level (Livingstone 2014).

Phytohormones occur in low concentration and play an important role in regulating plant growth and development, and also protective response against biotic or abiotic stresses. The first discovery of phytohormones is auxin in 1926 (Swarup and Péret 2012). Since that time, several phytohormones such as cytokinins, abscisic acid, gibberellins, ethylene, and jasmonic acid (JA) have been reported. Among those of phytohormones, JA and its methyl ester (MeJA), commonly known as jasmonates, have been attracted much interest in the last three decades. In 1962, MeJA was firstly extracted from the essential oil of *Jasminum grandiflorum* (Demole et al. 1962) and has become an important ingredient in parfume industry. JA was first identified as a plant growth inhibitor after its isolation from fungus culture of *Lasiodiplodia theobromae* (Aldridge et al. 1971). Jasmonates are widely distributed in the plant kingdom (Creelman and Mullet 1997) and responsible for the alteration of gene expression in various plants in responding to biotic and abiotic stresses, as well as plant development, especially in reproduction (Wasternack et al. 1997; Ishiguro et al. 2001; Wasternack 2007). Jasmonates and other plant oxylipins (e.g., hydroxy fatty acids, keto fatty acids, peroxy fatty acids, epoxides, ketoles, divinyl ethers and volatile aldehydes) are the results of oxygenation of unsaturated fatty acids (Mosblech et al. 2009).

Like other plant hormones, jasmonates exhibit a broad spectrum of physiological activities. Under abiotic stresses, such as wounding, UV irradiation, and ozone treatment, jasmonate levels are tended to accumulate. Similarly, the amount of jasmonates increases in response to attack by herbivore, infection by pathogens, or other biotic stresses (Wasternack 2007; Schaller and Stintzi 2008). In addition, jasmonates also play a role as a regulator for root growth, flower development, seed

germination, tendril coiling, senescence, and carbon portioning in healthy plant (Wasternack and Kombrink 2010; Kombrink 2012). All these mechanisms are important for plant survival against adverse environmental conditions. In most cases, such challenges require a prompt physiological response to allow plants to survive and reproduce with success in their natural environment.

1.1 Jasmonic acid biosynthesis

The series of enzymatic reactions to synthesize JA is often referred to as the octadecanoid pathway because JA is derived from octadecatrienoic acid (Fig. 1). Biosynthesis of JA through octadecanoid pathway was first elucidated in 1980's by Vick and Zimmerman (1983). The structures of jasmonates are similar to those of prostaglandins, important signaling molecules in animal kingdom. JA biosynthesis is started by the release of a fatty acid substrate, α-linolenic acid (α-LeA, C18:3), from galactolipids of chloroplast membrane by phospholipases (PL) such as DAD1 (Wasternack and Hause 2013). This α-LeA is oxygenated by specific lipoxygenase (LOX) at C13 to 13(*S*)-hydroperoxyoctadecatrienoic acid (13-HPOT). The first committed step of the JA pathway is performed by allene oxide synthase (AOS). AOS catalyzes the dehydration of 13-HPOT to the unstable allene oxide 12,13(*S*)-epoxy-octadecatrienoic acid (12,13(*S*)-EOT). This unstable 12,13(*S*)-EOT can spontaneously convert to α-ketol, γ-ketol, and racemic 12-oxo-phytodienoic acid (OPDA). As opposed to spontaneous cyclization that results in the production of racemic OPDA, allene oxide cyclase (AOC) ensures the cyclization of the optically pure *cis*-(+)-12-oxo-phytodienoic acid ((9*S*,13*S*)-OPDA). This is the end product of JA biosynthesis pathway that localizes in chloroplast membrane.

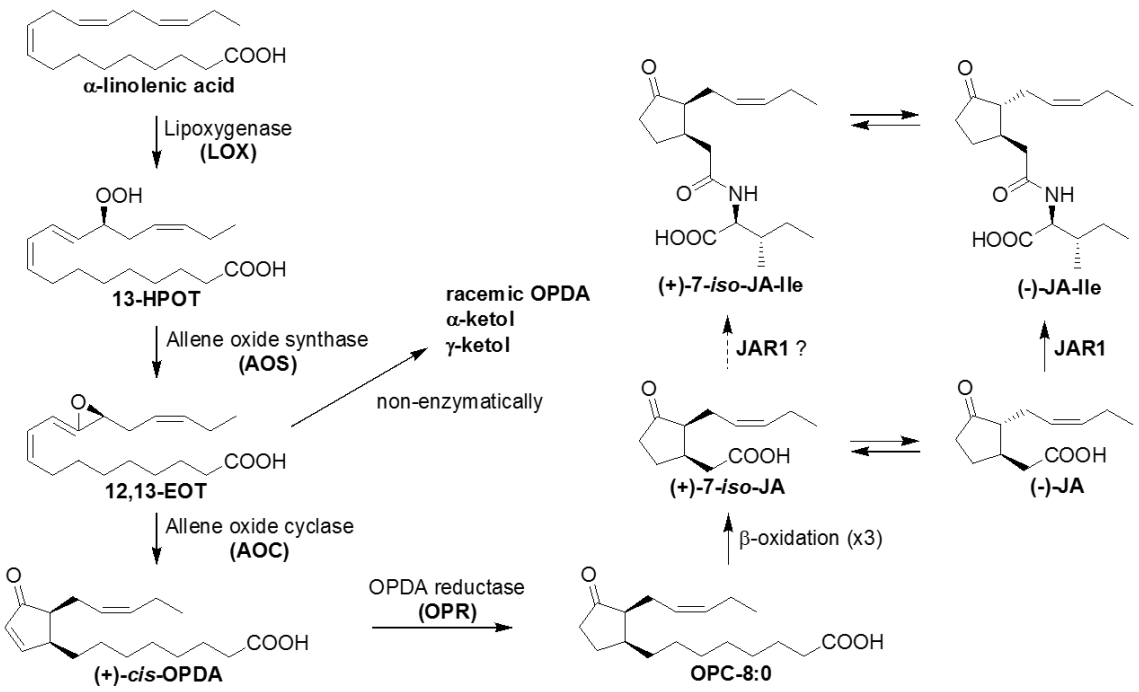

Fig. 1. The biosynthesis of JA and JA-Ile.

The next step for JA biosynthesis occurs in peroxisome. However, little is known about how OPDA is transferred from chloroplast to peroxisome. Recently, it is predicted to be mediated by the ABC transporter COMATOSE (CTS, also known as PXA1/ PED3) and/or ion trapping mechanisms. Once within peroxisomes, (9*S*,13*S*)-OPDA is reduced by OPDA reductase (OPR3) to yield 3-oxo-2-(2'(*Z*)-pentenyl)-cyclopentan-1-octanoic acid (OPC-8:0). The octanoic acid side chain in OPC-8:0 is shortened by three rounds of β–oxidation. Before entering the cycle, the carboxylic moiety requires to be activated to the corresponding CoA ester. β–Oxidation machinery involves three core enzymes, acyl-CoA oxidase (ACX), multifunctional protein (MFP), and L-3-ketoacyl CoA thiolase (KAT) that will lead to the end product of jasmonyl-CoA. Jasmonyl-CoA is cleaved by a putative thioesterase (TE) giving rise to (+)-7-*iso*-JA (Schaller and Stintzi 2009; Wasternack and Kombrink 2010). (+)-7-*iso*-JA immediately epimerizes into more stable (−)-*trans*-JA or undergoes modifications to produce other

JA derivatives including MeJA and (+)-7-*iso*-JA-Ile. (+)-7-*Iso*-JA-Ile, bioactive form of JA, is produced by conjugation of JA and L-isoleucine by JA-Ile synthase (JAR1) (Yan et al. 2013).

1.2 JA biosynthetic enzymes

1.2.1 13-Lipoxygenase (LOX)

The generation of oxylipins is started with the oxygenation of α-LeA. The oxygen needs to be inserted at the C-13 position by a lipoxygenase (LOX), which forms hydroperoxides from α-LeA (18:3) or linoleic acid (18:2). With α-LeA as the substrate, (13*S*)-hydroperoxyoctadecatrienoic acid (13-HPOT) or (9*S*)-hydroperoxyoctadecatrienoic acid (9-HPOT) are formed. Four of six Arabidopsis LOXs are 13-LOXs (LOX2, LOX3, LOX4, and LOX6) (Bannenberg et al. 2009) and involved in wound-induced JA formation with specific activity: (1) a dominant role in wounding (LOX2); (2) lipid peroxidation (LOX2); (3) early wound response of xylem cells (LOX6); (4) wound response in vascular tissue (LOX3, LOX4); (5) natural and dark-induced senescence (LOX2); (6) fertility and flower development (LOX3, LOX4) (Wasternack and Hause 2013). The remaining LOX1 and LOX5 are 9-LOXs that are involved in cell death process by formation of phytoalexins such as death acids (Christensen et al. 2015).

The LOX-catalyzed reaction can be distinguished by the selective formation of the (*S*)-isomers. The LOX products, 13-HPOT or 9-HPOT, represent branch points of LOX pathway. There are seven different groups of compounds that are formed by individual enzyme families by using LOX products as their substrate (Fig. 2): (1) octadecanoid and jasmonates originating from 13-AOS activity; (2) epoxyhydroxy-polyunsaturated fatty acids (PUFAs) formed by peroxygenases (POX); (3) aldehydes,

ω-oxo fatty acids and alcohols formed by hydroperoxy lyases (HPL); (4) divinyl ether-containing PUFAs synthesized by divinyl synthases (DES); (5) epoxyhydroxy PUFAs formed by epoxy alcohol synthases (EAS); (6) keto-PUFAs formed by LOX; and (7) hydroxyl PUFAs formed by reductases (Feussner and Wasternack 2002).

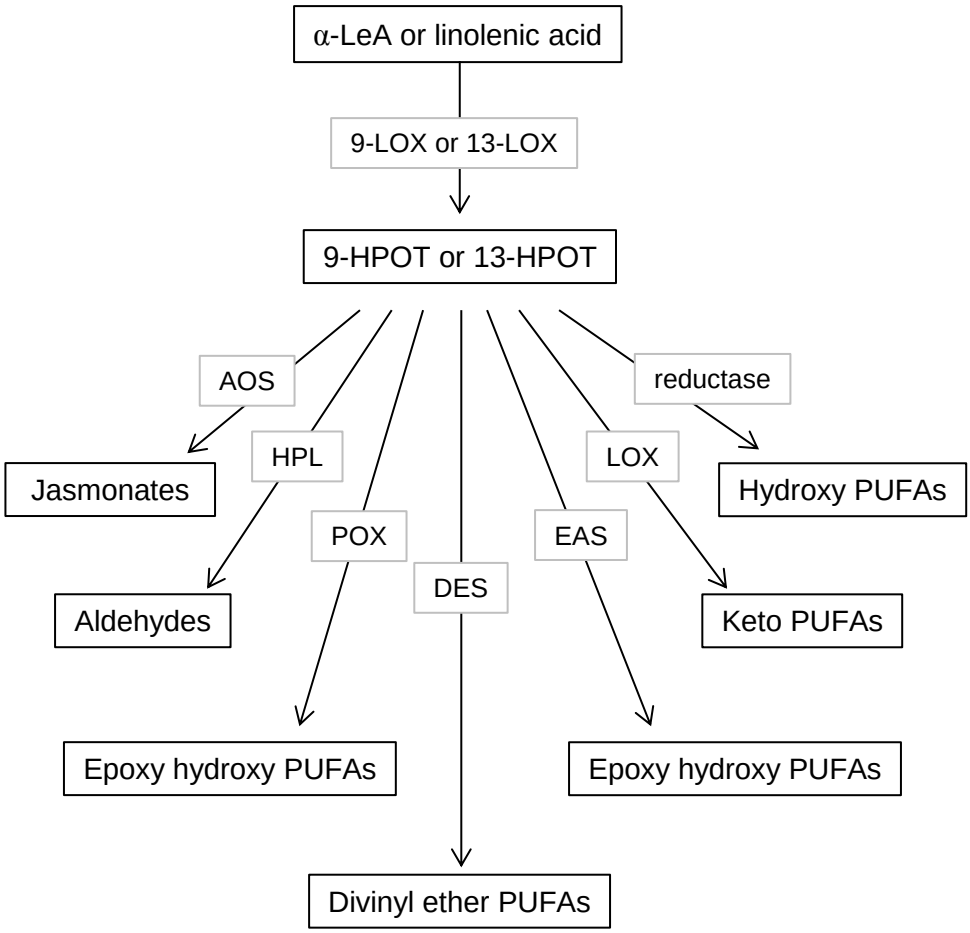

Fig. 2. The LOX pathway.

1.2.2 Allene oxide synthase (AOS)

Among the seven different branches of the LOX pathway, only the AOS branch leads to JA formation. AOS (hydroperoxide dehydratase, EC 4.2.1.92) belongs to CYP74 family, the cytochrome P450. All HPLs, DESs, and AOSs directly utilize LOX products, hydroperoxy fatty acid. Unlike other P450, they have a unique reaction

mechanism that does not require molecular oxygen or NAD(P)H as cofactors but uses their hydroperoxide substrates as source for reducing equivalents and as oxygen donor. The 9-, 9/13- and 13-AOSs belong to the CYP74A clade. The 13-AOS is a key enzyme in the octadecanoid pathway leading to JA biosynthesis by converting the substrate 13-HPOT into the unstable allene oxide. After the first report on isolation of *AOS* from flax (*Linum usitatissimum*), more than twenty *AOS* genes from other plant species have been cloned. These AOSs are divided into two groups, 9-AOS and 13-AOS (Stumpe and Feussner 2006). Most of them demonstrate the specificity for 13-hydroperoxides, except of the barley (*Hordeum vulgare*) AOS that is able to metabolize both 9- and 13-hydroperoxides (Maucher et al. 2000). All of the 13-AOSs carry a plastid transit peptide, except the AOS of guayule (*Parthenium argentatum*) (Pan et al. 1995) and barley (*Hordeum vulgare*) (Maucher et al. 2000). This compartmentation corresponds to the plastidal location of 13-LOX whereas 9-LOX activity was found in cytosol (Feussner and Wasternack 2002). Phylogenetic analysis and characterization of AOS from the liverwort *Marchantia polymorpha* and green microalgae *Klebsormidium flaccidum* showed that the CYP74 enzymes in bryophyets and algae are separated from CYP74 subfamily at the early stage of plant evolution; thus suggested the acquisition of the CYP74 enzymes (AOS, HPL, and DES) in plants may have occurred during the evolution from Chlorophyte to Charophyta, followed by a gene duplication event in the CYP74 family (Koeduka et al. 2015).

1.2.3 Allene oxide cyclase (AOC)

AOC (EC 5.3.99.6) catalyzes the stereospecific cyclization of the unstable allene oxide 12,13(*S*)-EOT, the product of AOS, to yield *cis*-(+)-OPDA, the only precursor for biologically active of JA (Schaller 2001; Yan et al. 2013). Thus, the AOC-catalyzed

step is crucially important in octadecanoid pathway to establish the enantiomeric structure of the cyclopentenone ring (Schaller et al. 2000; Ziegler et al. 2000). In 1990, AOC was first identified as a soluble enzyme in corn (*Zea mays*) with an apparent dimer about 45 kDa (Hamberg and Fahlstadius 1990). The full-length cDNA coding for *AOC* was first isolated from tomato (Ziegler et al. 2000). To date, *AOC* genes are successfully isolated and identified from *Arabidopsis* (Stenzel et al. 2003), *Leymus mollis* (Habora et al. 2013), *Torenia fournieri* (Liu et al. 2012), *Humulus lupulus* (Fortes et al. 2005), *Camptotheca cuminata* (Pi et al. 2008), moss of *Physomitrella patens* (Stumpe et al. 2010; Hashimoto et al. 2011), and *M. polymorpha* (Yamamoto et al. 2015). The extremely short half-life of EOT (< 30 s in water) and the accumulation of pure (9*S*,13*S*)-OPDA suggest a tight coupling of the AOS and AOC reaction, possibly in a synthase-cyclase complex, to avoid needless spontaneous chemical conversion of the unstable intermediate (Schaller and Stintzi 2009; Wasternack and Kombrink 2010).

1.2.4 OPDA reductase 3 (OPR3)

All OPRs catalyze the conversion of cyclopentenones into cyclopentanones. OPR enzyme (EC 1.3.1.42) belongs to Flavin-dependent oxidoreductase and is encoded by small gene families in plants (Strassner et al. 2002). OPR was identified as a protein with a molecular mass about 54 kDa and a preference for NADPH as the reducing agent. OPR was first purified from cell cultures of *Corydalis sempervirens* (Schaller and Weiler 1997) and the sequence information derived from this enzyme lead to the cloning of a first OPR cDNA (*AtOPR1*) from *Arabidopsis* (Schaller and Weiler 1997). Plant OPRs can be classified into two groups (I and II) according to their substrate specificity (Zhang et al. 2005; Tani et al. 2008). OPR I group (e.g. AtOPR1, AtOPR2,

and OsOPR1) has a very low affinity to *cis*-(+)-OPDA, the only natural precursor of JA, and are unlikely to be involved in JA biosynthesis. Members of OPR II (e.g. AtOPR3, SlOPR3, and OsOPR7) group are required for the formation of JA because they reduce exclusively *cis*-(+)-OPDA over *cis*-(-)-OPDA (Schaller et al. 2000). Among the six *OPR*s found in *Arabidopsis*, only OPR3 reduces (9*S*, 13*S*)-OPDA to OPC-8:0 while OPR1 and OPR2 have a broad substrate acceptability and their physiological function remains obscure (Schaller et al. 2000).

The specificity of OPR3 is strongly supported by the crystal structures of OPR3 and OPR1. This analysis provided the imaging of the enzymes active site and their stereoselectivity. The active site of the enzyme is located above the non-covalently bound flavin mononucleotide (FMN). The gate to access the active site in OPR1 is maintained by two large amino acid residues, Tyr246 and Tyr78, while in OPR3, these positions are substituted by the smaller residues, His244 and Phe74. Thereafter, OPR3 imposes less restriction on substrate entry into the active site cavity, resulting in its relaxed specificity with respect to the different OPDA isomers (Breithaupt et al. 2009).

The JA-deficient line *opr3* and *dde1* in *Arabidopsis* revealed that OPR3 cannot be substituted by other type of OPRs (Sanders et al. 2000; Stintzi and Browse 2000). Initially, the loss-of-function mutant *opr3* carried a 17-kb T-DNA insertion in an *OPR3* intron had a resistant ability against *Alternaria brassicicola.* It was suggested the direct role of OPDA in pathogen defense (Stintzi et al. 2001). Thus, this mutant was used to distinguish between OPDA- and JA-dependent signalings. However, *opr3* is not a null mutant and is able to transcript full-length of *OPR3* by splicing the T-DNA containing intron under specific conditions. Chehab et al. (2011) found that *Botrytis cinerea* infection leads to JA accumulation in *opr3* mutant. Therefore, under certain conditions, *opr3* is not an ideal mutant for dissection OPDA-specific signaling. Other groups used

double mutant *opr7opr8* from maize (*Zea mays*) that dramatically reduced levels of JA in all organs tested and displayed strong defects in development, including formation of a feminized tassel and the elongation of ear shanks. However, these defects can be restored by exogenous JA application (Yan et al. 2012).

1.3 Jasmonic acid signaling pathway

JA level in plants varies in every developmental stage, organs, and also in response to different environmental stresses. For example, endogenous concentrations of jasmonate such as OPDA, JA, and JA-Ile increase rapidly in response to mechanical perturbations especially when suffer from wounding (Creelman and Mullet 1995; Yan et al. 2013).

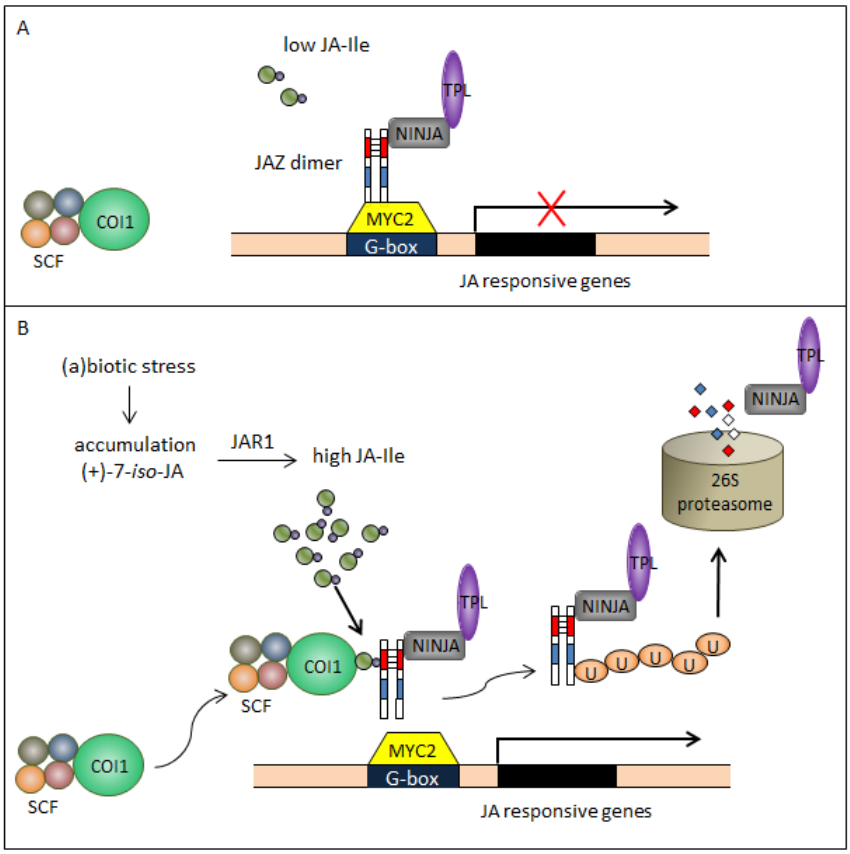

Fig. 3. Model for JA signaling.

This model was cited from Santino et al. (2013) with some modifications.

In JA signaling pathway, JA responses are controlled by a group of nuclear proteins, called jasmonate-zim domain (JAZ) repressors. JAZ repressors interact with coronatine insensitive1 (COI1) as an F-box protein that functions as the substrate-recruiting element of the Skp-Cullin-F-box protein (SCF) ubiquitin E3 ligase complex. Among the bioactive JA derivatives forms, JA, OPDA, MeJA, and JA-Ile, only the last derivative functions as a ligand for COI1-JAZ interaction (Thines et al. 2007). In the low level of (+)-7-*iso*-JA-L-Ile, JAZ repressor complex, including co-repressor topless (TPL) and adaptor protein novel interactor of JAZ (NINJA), actively blocks JA-responsive transcription factors (e.g. MYC2), which bind to *cis*-acting elements of jasmonate-response genes, resulting in prevention of transcription activity (Fig. 3A). Under stress conditions such as wounding, the accumulation of (+)-7-*iso*-JA-L-Ile stimulates the specific binding of JAZ proteins to COI1 leading to poly-ubiquitination that subsequently degrades the JAZ protein by 26S proteasome. Finally, the JA responsive genes can be expressed (Fig. 3B) (Santino et al. 2013; Yan et al. 2013).

1.4 Metabolism of jasmonates

Up to now, six metabolic routes are known that convert JA into active, inactive and/or partially active JA derivatives (Fig. 4):

- Adenylation at the carboxylic end of JA by JAR1 leads to the formation of amino acid conjugates (Staswick and Tiryaki 2004).
- Hydroxylation at C-11 or C-12 of the pentenyl side chain followed by *O*-glucosylation (Sembdner and Parthier 1993; Swiatek et al. 2004) or sulphation (Gidda et al. 2003).
- Decarboxylation to *cis*-jasmone (Koch et al. 1997).

- Methylation at the carboxy group by a JA-specific methyl transferase (Seo et al. 2001).
- Formation of jasmonoyl-1-β-gentibiose and hydroxyjasmonoyl-1-β-glucose (Swiatek et al. 2004).
- Reduction of the keto group ot the cyclopentanone ring leading to cucurbic acids (Sembdner and Parthier 1993).

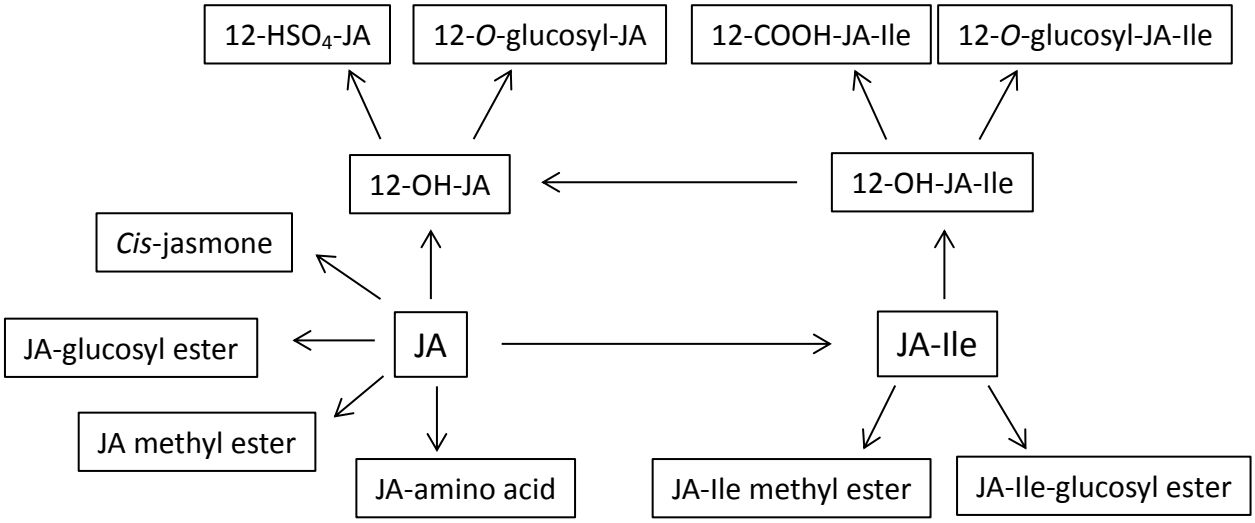

Fig. 4. Jasmonate metabolism.

Among these modifications, formation of amino acid conjugates by JAR1 (a JA-Ile synthase) and hydroxylation of JA-Ile by cytochrome P450 enzymes will be described in detail. This metabolism, which is known as JA-Ile homoestasis, is a crucial mechanism in plants to sustain the balance level of active and inactive forms of JA. A better understanding of JA-Ile homeostasis is important to comprehend more about plant physiology.

1.4.1 Conjugation with amino acid

JA-amino acid conjugates are permanent constituents of plant tissues and their level increase upon stress-induced (Kramell et al. 1995). Among the various conjugates, JA-Ile become the most biologically active JA compound. JA-Ile acts as a ligand to mediate the promotion of SCF^{COI1}-JAZ co-receptor complex formation (Thines et al. 2007; Sheard et al. 2010). Both of JA and JA-Ile play an important regulatory role for all JA-dependent process. Under mechanical wounding stress, *Arabidopsis* accumulates JA and JA-Ile within minutes in tissue damage. The rapid response of jasmonates suggests that all JA-Ile biosynthetic enzymes are present in healthy tissues prior to stimulation. JA-Ile mainly accumulates in leaves, flowers, and mycorrhizal roots. JA-Ile biosynthesis is tightly correlated with environmental cues and involves the adenylation of JA, followed by the exchange of AMP with isoleucine. This conversion is catalyzed by the enzyme JAR1 to conjugate JA with amino acids.

JAR1 is a member of the GRETCHEN HAGEN 3 (GH3) family, which belongs to the large group of enzymes forming acyl-adenylate/ thioester intermediates. The cloning of *JAR1* gene was a breakthrough in the research field of JA. This enzyme finalizes the catalytic step of a bioactive form of JA, JA-Ile (Staswick and Tiryaki 2004). The identification of (+)-7-*iso*-JA-Ile as the ligand of the COI1-JAZ co-receptor complex (Fonseca et al. 2009) and the crystallization of the receptor complex provided mechanistic explanation for JA/JA-Ile perception. Group I GH3 protein, AtJAR1 from *Arabidopsis* encodes an ATP-dependent JA-amino synthase producing JA-amino acid conjugates, such as JA-Ile, JA-Leu, and JA-Val (Staswick and Tiryaki 2004). Group II GH3 protein produces indole-3-acetic acid (IAA) amino acid conjugates, such as IAA-Asp, IAA-Ala, and IAA-Glu (Staswick et al. 2005). The *Arabidopsis jar1* mutant showed a decreased sensitivity to exogenous JA and decrease endogenous levels of JA-Ile. The expression of rice *OsJAR1* and *OsJAR2*, which encode the functional JA-Ile

synthases, are similar to *AtJAR1* in terms of JA-Ile accumulation after wounding and pathogen attack (Wakuta et al. 2011).

JAR1 from tomato (*Solanum lycopersicum*) prefers to conjugate (+)-7-*iso*-JA over (-)-JA and isoleucine over other amino acids (Suza and Staswick 2008; Suza et al. 2010), suggesting that JAR1 activity is tightly coupled to (+)-7-*iso*-JA formation before its epimerization occurs, and leads to the prominent bioactivity of (+)-7-*iso*-JA-L-Ile in comparison with (-)-JA-L-Ile. Inactivation of (+)-7-*iso*-JA-L-Ile signaling was recently proposed through two major pathways: the cleavage of jasmonoyl-residue from isoleucine by specific amido-hydrolases (Woldemariam et al. 2012; Widemann et al. 2013) or sequential oxidation of the ω-end of the pentenyl group by cytochrome P450 monooxygenase subfamily CYP94 such as CYP94B1, CYP94B3, and CYP94C1 (Kitaoka et al. 2011; Koo et al. 2011; Heitz et al. 2012).

1.4.2 Hydroxylation and carboxylation

Formation of COI1-JAZ co-receptor complex *via* JA-Ile controls the growth, development, and defense mechanism in plants. However, little is known about the JA-Ile catabolism and inactivation mechanism of JA-Ile signaling until recently. The turnover of JA-Ile is mediated by an ω-oxidation, which are catalyzed by members of the CYP94 subfamily of cytochrome P450. CYP94B3 prefers to hydroxylate JA-Ile to 12-hydroxyJA-Ile (Kitaoka et al. 2011; Koo et al. 2011) while CYP94C1 catalyzes the subsequent oxidation, yielding to 12-carboxyJA-Ile (Heitz et al. 2012). Phenotypic analysis of *CYP94B3* mutant demonstrates an importance of JA-Ile catabolism in plant. Overexpressing of *CYP94B3* gene showed a severe deficient in wound-induced JA-Ile accumulation, which causes JA-Ile deficiency, including increasing susceptibility to insect herbivores, resistance to JA-mediated root growth inhibition, and defects in

anther and pollen development (Koo et al. 2011; Koo and Howe 2012). In contrast, the wounded *cyp94b3* and *cyp94b3 cyp94c1* double mutant-plants exhibited higher expression of JA-responsive genes and increased sensitivity to JA-mediated root growth inhibition (Heitz et al. 2012). These data demonstrates that hydroxylation and carboxylation of JA-Ile by CYP94 family function to switch off JA/ JA-Ile signaling. Thus, oxidation of JA-Ile affects the physiological processes in roots, leaves, and reproductive tissue.

1.5 Lycophytes

Terrestrial plants can be classified into two divisions: Bryophyta (liverworts, mosses, and hornworts) that lacks of vascular tissue and Tracheophyta (lycophytes and euphyllophytes), vascular plants, has vascular conducting tissue (xylem and phloem) to transport water, mineral, and sugar. Lycophytes consists of clubmosses, quillworts, and spikemosses (*Selaginella* sp.), and euphyllophytes consists of ferns, gymnosperms, and angiosperms (Fig. 5) (Futuyma 1998; Banks et al. 2011).

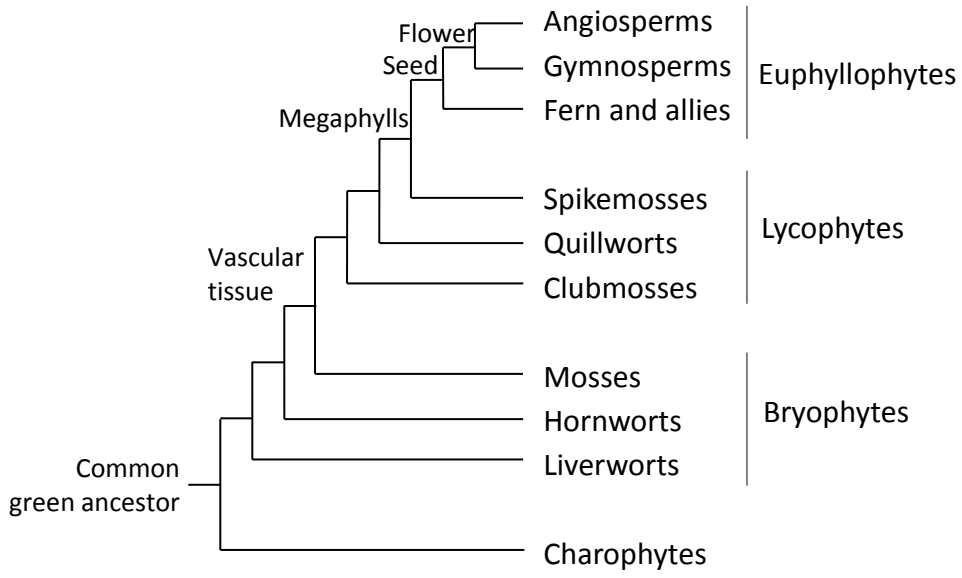

Fig. 5. Plant evolution.

Lycophytes are considered to be the oldest vascular plants and appeared in the middle Silurian period (439-409 million years ago) long before gymnosperm and angiosperm. The fossil record shows that lycophytes diversified into two main groups: zosterophylls that becomes extinct by the end of the Devonian period, and lycopods, which diversified through the Devonian, consists of about 1250 species currently living on Earth (Livingstone 2014). The majority of these species belongs to the genus of spikemoss, *Selaginella*, which includes approximately 700 species. The still existing lycophytes possesses a tremendous ability to adapt to the constantly changing environment. However, compared to angiosperms, lycophytes has received relatively little attention as a subject of functional genomic research, which yet offers the novel insight into plant evolution and discovers the ancient core of genes common to all vascular plants.

1.5.1 *Selaginella moellendorffii*

Selaginella, commonly known as spikemoss, is one of the genus that belongs to the lycophytes clade. Like other lycophytes groups, *Selaginella* has a unique leaves called microphylls, that have only one vein that runs down the length of the leaf. The above ground part is almost entirely green, including stems. The stems of lycophytes are densely packed at the ends of the branches that forming a strobilus. They are primitive plants that lack seeds, wood, fruit, and flowers.

Recently the genome of *S. moellendorffii* (Fig. 6) has been successfully sequenced by the group from Department of Energy Joint Genome Institute (JGI) (Banks et al. 2011). *S. moellendorffii* has a genome size of approximately 110 Mbp, the smallest size compared to those of known vascular plants (Wang et al. 2005). The revealed genome

sequence of this spikemoss can be used to decipher the evolution of physiological, biochemical, and developmental processes unique to land plants.

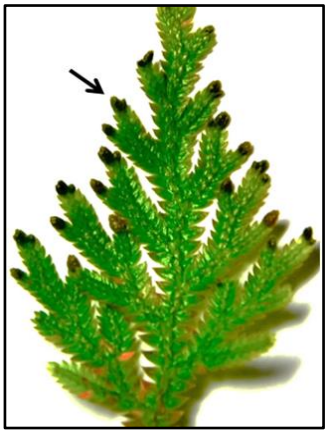

Fig. 6. The morphology of microphyll of *S. moellendorffii*.
The arrow indicates a bulbil.

1.6 Objective

With the recent achievement of *S. moellendorffiii* genome sequence, we are able to study the first insight of appearance of JA and JA derivatives in a model lycophyte, and attempt the elucidation of a physiology effect of jasmsonates in this plant. Moreover, cloning and characterization of important enzymes in the biosynthesis of JA and JA-Ile, and catabolism of JA-Ile were also carried out. This study, not only demonstrates the role of the committed enzymes in regulating the octadecanoid pathway upon wounding stresses, but also represents a leading indicator in our understanding about evolution of land plants.

CHAPTER II

IDENTIFICATION OF JASMONATES IN *SELAGINELLA MOELLENDORFFII*

2.1 Introduction

The tremendous amount of experiment results has shed a new light into how plants respond to biotic or abiotic stress and how growth and development mechanisms process in plant life cycle. Plant adapts and responds to external stimulus by induction of numerous genes that is mediated by small molecules like plant hormones (e.g. abscic acid, ethylene, salicylic acid, and JA). Thereafter, those plant hormones are considered to be important in regulating the adaptive response. In this study, JA and its derivatives will be described in detail especially in answering to the question of the first appearance of the bioactive jasmonates during plant evolutionary history in order to adapt to environmental changes.

After initial identification of methyl jasmonates (MeJA) as an odor in flowering plants, jasmonates have attracted much interest and are detected ubiquitously in land plants. Jasmonates occur in algae, mosses, gymnosperms, and angiosperms in different derivatives. In most of higher plants, JA and JA-Ile act as a signaling molecule for defense and development while in bryophytes only OPDA can be detected (Yamamoto et al. 2015). Thereafter, this current study focused on one of the oldest vascular plant *S. moellendorffii* to detect JA and JA-Ile which are probably acquired during the transition to vascular system.

2.2 Results and Discussion

2.2.1 Identification of OPDA, JA, and JA-Ile in *S. moellendorffii*

Seed plants can biosynthesize JA and JA-Ile; however, these compounds are absent in the model bryophytes *P. patens* and *M. polymorpha* (Stumpe et al. 2010; Yamamoto et al. 2015). In this study, *S. moellendorffii* which belongs to a lycophyte group that is taxonomically positioned between bryophytes and euphyllophyte (Fig. 5) was used to identify JA and its related compounds. The wounded *S. moellendorffii* produced OPDA, JA, and JA-Ile that were shown in UPLC-MS/MS analysis in MRM mode (Fig. 7). The OPDA analytical data revealed a predominant peak in the chromatogram of a *S. moellendorffii* extract (*m/z* 164.99 derived from the peak at *m/z* 291.37 $[M-H]^-$; Figs. 7A, 7B, and 7C). This peak overlapped with the *cis*-OPDA standard peak, which indicates that OPDA is present in *S. moellendorffii*. The minor peak that eluted before *cis*-OPDA was speculated to be either an unidentified OPDA-related compound or a *trans*-isomer of OPDA (Fig. 7B). The analytical JA data clearly demonstrated that the standard JA peak overlapped with the peak derived from an extract of *S. moellendorffii* (*m/z* 58.71 derived from the peak at *m/z* 209.09 $[M-H]^-$; Figs. 7D, 7E, and 7F). This result indicated the presence of JA in *S. moellendorffii*. Furthermore, an analysis of JA-Ile showed that the retention time of standard JA-Ile was the same as that of the peak derived from an extract of *S. moellendorffii* (*m/z* 129.68 derived from the peak at *m/z* 323.03 $[M-H]^-$; Figs. 7G, 7H, and 7I), suggesting that *S. moellendorffii* also biosynthesizes JA-Ile. The minor peak that was detected in the extract is potentially an unidentified contaminant that was not further analyzed (Fig. 7H). These data are the first evidence of OPDA, JA, and JA-Ile in *S. moellendorffii*.

2.2.2 Kinetic analysis of accumulation of OPDA, JA, and JA-Ile upon wounding stress

JA plays important roles in stress adaptation. Therefore, the accumulation of JA is considered a response to adverse environmental conditions involving both biotic and

abiotic stresses, especially in seed plants (Wasternack and Hause 2013). Wounding activates the octadecanoid pathway, which results in the accumulation of OPDA, JA, and JA-Ile in seed plants.

To illustrate the response of *S. moellendorffii* upon wounding stress, the photosynthesizing organs (stems and microphylls) were mechanically wounded and then analyzed at different time points. To perform kinetic analysis of OPDA, JA, and JA-Ile accumulations, the endogenous levels of OPDA, JA, and JA-Ile were analyzed using UPLC-MS/MS (Fig. 8). *S. moellendorffii* transiently produced a high level of OPDA within the first 10 min after wounding. OPDA was approximately 200-fold more abundant than JA at 10 min after wounding, whereas the JA level peaked at 30 min, after the initial increase at 10 min. In contrast to the rapid increase of OPDA and JA concentrations, JA-Ile accumulation was delayed and started at 180 min after wounding. Concentration of OPDA was much higher than concentrations of JA and JA-Ile. It is possible that OPDA is used as a main signaling molecule in response to wounding and/or is converted to other metabolites.

The increased levels of JA and JA-Ile were accompanied by a rapid decrease in the concentration of OPDA. The early accumulation of OPDA and JA within 10 min is probably due to the role of jasmonates in regulating responses to environmental stress in *S. moellendorffii.* Given that wounding also stimulated OPDA and JA in a fern *Pteridium aquilinum* (Radhika et al. 2012), the accumulation of JA in response to wounding is probably a common physiological response among all vascular plant species (Maucher et al. 2004). However, JA-Ile accumulated more slowly than OPDA and JA after wounding. It is possible that the early rise in JA levels within 30 min represents an early response, whereas the slow JA-Ile accumulation may be corresponded to a late stress response in this plant. Accordingly, environmental stress

probably activates the octadecanoid pathway. OPDA, JA, and JA-Ile seem to play a role in regulating the wounding responses in *S. moellendorffii*.

In studies of *P. patens* and *M. polymorpha*, only OPDA has been detected in both plants (Stumpe et al. 2010; Yamamoto et al. 2015). In contrast to vascular plants, it seems that JA is not important for the physiology of these model bryophytes. Hence, our data suggest that JA and JA-Ile biosynthesis first appeared after bryophytes in plant evolution (Figs. 7 and 8). Additionally, there is a significant difference between bryophytes and lycophytes. Lycophytes has a vascular system for the efficient transport of water, nutrients, and molecules, as well as for enhancing plant height and size. It is likely that the emergence of the JA biosynthetic pathway after OPDA is related to the acquisition of a vascular system by plants.

The transient increases of OPDA, JA, and JA-Ile after wounding in *S. moellendorffii* are similar to those observed in seed plants. It has been suggested that another metabolic pathway is required for inactivation of JA responses in *S. moellendorffii*. In *Arabidopsis*, the oxidation of JA-Ile, which decreases the JA-Ile concentration, is important in regulating JA activity (Kitaoka et al. 2011; Koo et al. 2011). A phylogenetic analysis of cytochrome P450s in *A. thaliana*, *P. patens*, and *S. moellendorffii* revealed that SmCYP94Js (SmCYP94J1, SmCYP94J2, SmCYP94J3, SmCYP94J5Pv1, and SmCYP94J5Pv2) are members of a cluster that includes AtCYP94B3 and AtCYP94C1 as enzymes responsible for the oxidation of JA-Ile and 12-OH-JA-Ile (Banks et al. 2011). SmCYP94Js are likely related to the oxidation of JA-Ile, leading to the inactivation of JA activity.

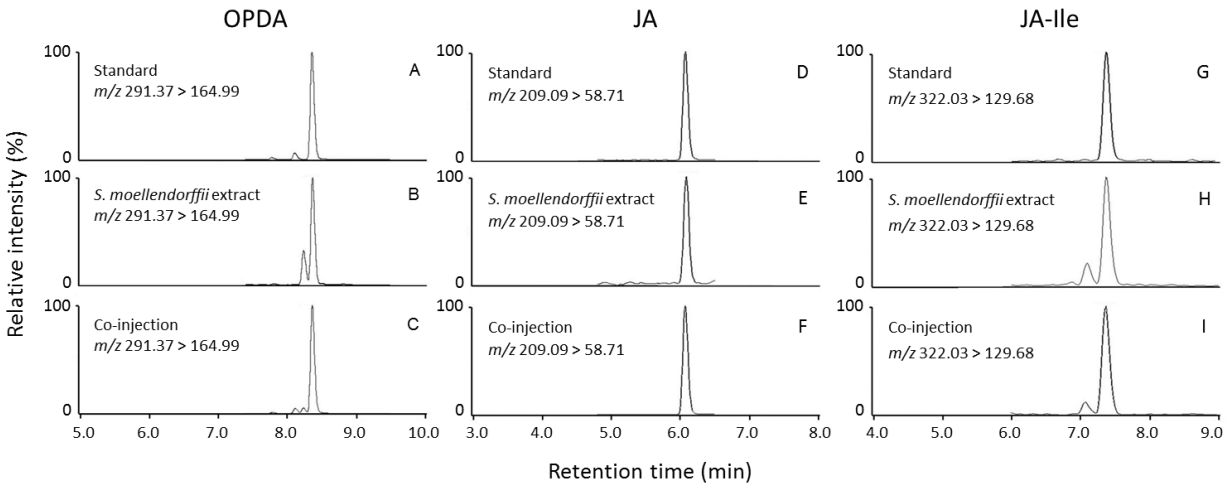

Fig. 7. UPLC-MS/MS analysis of OPDA, JA, and JA-Ile in wounded *S. moellendorffii*. (A-C) MRM mode analysis of a specific daughter peak at *m/z* 164.99 that was derived from the peak at *m/z* 291.37 $[M-H]^-$. (D-F) MRM mode analysis of a specific daughter peak at *m/z* 58.71 that was derived from the peak at *m/z* 209.09 $[M-H]^-$. (G-I) MRM mode analysis of a specific daughter peak at *m/z* 129.68 that was derived from the peak at *m/z* 322.03 $[M-H]^-$. (A, D, G) Standard. (B, E, H) *S. moellendorffii* extract. (C, F, I) Co-injection of the standard and *S. moellendorffii* extract.

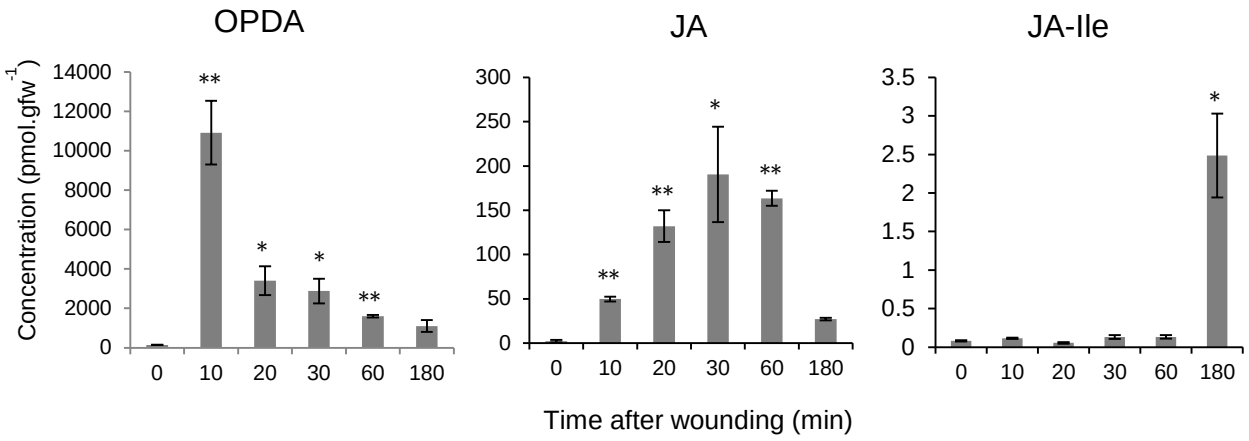

Fig. 8. Accumulation of OPDA, JA, and OPDA in *S. moellendorffii* after wounding.
S. moellendorffii was subjected to mechanical wounding and then collected at the indicated time after wounding. The concentrations of OPDA, JA, and JA-Ile were analyzed by UPLC-MS/MS. The data are presented as the mean ± SD (n = 3). The asterisks represent a significant difference between the treated and control plants (Student's t test, *$p < 0.05$, **$p < 0.01$).

2.3 Materials and Methods

2.3.1 Plant material

S. moellendorffii was grown in soil under 50-60 µmol photons m^{-2} s^{-1} continuous fluorescent light at 25°C.

2.3.2 Analysis of OPDA, JA, and JA-Ile

Concentration of OPDA, JA, and JA-Ile was analyzed by UPLC-MS/MS according to the method of Sato et al. (2011) with some modifications. After unwounded and wounded plants (8 h) (ca. 500 mg) were soaked in 20 ml of ethanol for 24 h, the resultant solution was extracted using solid phase extraction method before UPLC-MS/MS analysis. UPLC separation was performed using Waters ACQUITY ethylene-bridge (BEH) C18 1.7 µm column (2.1 x 100 mm; Waters, Milford, MA, USA) and Waters Micromass Quattro Premier Tandem Quadrupole Mass Spectrometer (Waters, Milford, MA, USA). The analytes were eluted with solvent A (20% aq. methanol with 0.05% acetic acid) and solvent B (methanol with 0.05% acetic acid) using linear gradient mode. The ratio of solvent A to solvent B was 100:0 from 0 min to 2 min, and linearly converted from 100:0 to 0:100 between 2 min to 8 min. Finally the column was eluted with solvent B from 8 min to 10 min at flow rate of 0.3 ml/min. The MRM transitions for tested compounds are given in Table 1.

2.3.3 Accumulation of OPDA, JA, and JA-Ile in *S. moellendorffii*

The microphylls and stems of *S. moellendorffii* (ca. 500 mg) were harvested 10, 20, 30, 60, or 180 min after wounding with tweezers and were homogenized under liquid nitrogen, followed by ethanol extraction for 24 h. UPLC-MS/MS analysis was performed according to the method described above.

Table 1. Conditions of MS optimization for MRM in negative mode.

Compound	$[M-H]^-$ (*m/z*)	Transition ion (*m/z*)	Cone voltage (V)	Collision energy (eV)
OPC-8-d_6	299.10	255.04	50	22
OPDA	291.37	164.99	50	22
JA-d_3	212.00	58.71	24	16
JA	209.00	58.71	24	16
JA-Ile-d_6	328.03	135.68	45	24
JA-Ile	322.03	129.68	45	24
12-OH-JA-[$^{13}C_6$]Ile	344.30	135.70	47	23
12-OH-JA-Ile	338.30	129.70	47	23
12-COOH-JA-[$^{2}H_3$]Leu	355.24	132.70	39	28
12-COOH-JA-Ile	352.24	129.70	39	28

CHAPTER 3

CLONING AND CHARACTERIZATION OF GENES ENCODE JASMONATES BIOSYNTHETIC ENZYMES

3.1 Introduction

JA biosynthesis starts from substrate α-LeA in chloroplast membrane. A series of oxidation, synthetase-cyclase reaction, reduction, and β-oxidation of the carboxylic acid leads to the formation of JA, and subsequently conjugation with amino acid to generate a bioactive form of JA-Ile. This chapter describes the JA biosynthetic enzymes in terms of gene families, enzymatic activity, location, substrate specificity and products particularly in *S. moellendorffii*. Moreover, genes encoding enzymes involved in JA-Ile biosynthesis that are known to be up-regulated in response to environmental signals in order to activate production of hormone were also observed. This transcriptional response demonstrates a positive feedback mechanism to amplify JA accumulation.

3.2 Results and discussion

3.2.1 Putative *AOS, AOC, OPR3,* and *JAR1* genes in *S. moellendorffii*

To further confirm the presence of OPDA, JA, and JA-Ile in *S. moellendorffii*, the characteristics of putative JA biosynthetic enzymes in *S. moellendorffii* were investigated. A genomic database analysis using Phytozome v 11.0 (https://phytozome.jgi.doe.gov/pz/portal.html) was performed to screen *AOS, AOC, OPR3,* and *JAR1* homologous genes in *S. moellendorffii* using amino acid sequences of these proteins from *Arabidopsis* as queries. As a result, the presence of putative *AOS* (*SmAOS1*, Sm_271334; *SmAOS2*, Sm_177201; *SmAOS3*, Sm_228572), *AOC* (*SmAOC1*,

Sm_91887), *OPR3* (*SmOPR1*, Sm_270843; *SmOPR5*, Sm_111662), and *JAR1* (*SmJAR1*, Sm_110439) genes were predicted in *S. moellendorffii* (Table 2).

3.2.2 Functional analysis of *SmAOS2*

One of the key enzymes in JA biosynthesis is AOS, which converts 13(*S*)-HPOT into unstable 12,13(*S*)-EOT. A genomic database analysis of Phytozome v 11.0 revealed the presence of nine putative *AOS* genes in *S. moellendorffii*. Amino acid sequence analysis of the SmAOS candidates showed that SmAOS1, SmAOS2, and SmAOS3 were promising candidates containing the important sequence motifs: the I-helix GXXX (F/L), EXLR motif, and heme-binding PXVXNKQCPG, all of which are the characteristic of CYP74 family members (Fig. 9) (Koeduka et al. 2015). Additionally, the amino acid sequences of SmAOS1, SmAOS2, and SmAOS3 are highly similar (Fig. 9). A phylogenetic tree analysis of the AOSs showed that the SmAOSs were separated from the seed plant AOSs (Fig. 10). Computational analysis using ChloroP v 1.1 (http://www.cbs.dtu.dk/services/ChloroP/) and iPSORT (http://ipsort.hgc.jp/) for subcellular localization predicted the absence of a transit peptide in SmAOS1, SmAOS2, and SmAOS3, whereas most known AOSs are localized in chloroplasts (Schaller and Stintzi 2009).

To confirm AOS activity in this plant, the production of these recombinant SmAOSs was attempted. However, only recombinant SmAOS2 fused with a His-tag was successfully synthesized in *E. coli*. SDS-PAGE analysis of a recombinant SmAOS2, which was purified by Ni-NTA affinity column chromatography, revealed a clear band of SmAOS2 with an expected molecular weight of approximately 50 kDa (Fig. 11). The AOS reaction converts 13(*S*)-HPOT to unstable 12,13(*S*)-EOT, which is non-enzymatically changed to racemic OPDA. Therefore, AOS enzymatic activity can

be determined by analyzing the presence of racemic OPDA. The recombinant SmAOS2 was incubated with 13(*S*)-HPOT, and then the products were extracted with ethyl acetate, followed by isomerization by alkaline treatment and methylation using ethereal diazomethane. Laudert et al. (1997) demonstrated that chiral GC-MS analysis of methylated OPDA can clearly separate the *trans*-isomers of methylated OPDA; therefore, isomerization was performed by conversion of *cis*-OPDA to *trans*-OPDA. Peaks of methylated (+)-*trans*-OPDA and methylated (-)-*trans*-OPDA were both identified in the SmAOS2 reaction products on the chiral GC-MS chromatogram (Fig. 12). Furthermore, an ion peak at *m/z* 306, corresponding to the molecular ion peak $[M]^+$ of OPDA methyl ester, was observed together with unique fragment ion peaks at *m/z* 275 ($[M\text{-}OCH_3]^+$), *m/z* 238 ($[M\text{-}C_5H_9]^+$), and *m/z* 149 ($[M\text{-}C_9H_{17}O_2]^+$) in the GC-MS spectral data of both methylated (+)-*trans*-OPDA and methylated (-)-*trans*-OPDA (Figs. 13-15, Laudert et al. 1997). These results indicated that SmAOS2 showed AOS activity similar to that of previously characterized AOSs.

AOS is classified as a member of the CYP74 family and requires an oxygenated fatty acid hydroperoxide as the substrate instead of oxygen or a redox partner. This study revealed three AOS candidate genes (*SmAOS1*, *SmAOS2*, and *SmAOS3*) in *S. moellendorffii* (Figs. 9 and 10). Among them, recombinant SmAOS2, which was successfully produced in *E. coli*, exhibiting an AOS activity similar to that of previously reported AOSs (Fig. 11). Computer programs analyzing protein subcellular localization did not predict any transit peptide in the N-terminus of SmAOS2. Because most known AOSs are localized in chloroplasts, SmAOS2 is likely located in chloroplasts for JA biosynthesis. Since the amino acid sequences of SmAOS1, SmAOS2, and SmAOS3 are similar, further investigation is needed to clarify the physiological functions of these SmAOSs, respectively.

3.2.3 Functional analysis of *SmAOC1*

Many *AOC* genes have been successfully cloned from seed plants, a moss, and a liverwort (Ziegler et al. 2000; Agrawal et al. 2003; Stenzel et al. 2003; Maucher et al. 2004; Farmaki et al. 2006; Pi et al. 2008; Stumpe et al. 2010; Hashimoto et al. 2011; Yamamoto et al. 2015). The 5'-UTR of *SmAOC1* was examined by 5'-RACE to obtain its full-length sequence. A computational analysis using ChloroP v 1.1 and iPSORT predicted that SmAOC1 has a chloroplast transit peptide at N-terminus. The amino acid sequence alignment of SmAOC1 and AOCs of other plants showed that SmAOC1 had high similarity to other AOCs (Fig. 16). The phylogenetic tree analysis of AOCs demonstrated that SmAOC1 was related to MpAOC from a liverwort *M. polymorpha* and AOCs in seed plants, while this enzyme was separated from PpAOC1 and PpAOC2 of a moss *P. patens* (Fig. 17).

AOC is a critical enzyme that establishes the enantiomeric structure of OPDA, which contributes to the basic structure of jasmonates. To determine whether SmAOC1 is involved in the production of OPDA, *SmAOC1* was cloned and overexpressed in *E. coli*. The recombinant SmAOC1 was fused with a His-tag at the N-terminus to replace the chloroplast signal peptide. After purifying SmAOC1 using Ni-NTA affinity column chromatography, a protein with the expected size of 22 kDa was clearly detected as a single band by SDS-PAGE analysis (Fig. 11). The purified recombinant SmAOC1 was used for enzymatic analysis.

Due to the instability of 12,13(*S*)-EOT, which is the substrate for the AOC reaction, the enzymatic activity of SmAOC1 was tested in a reaction mixture containing SmAOC1, PpAOS1, and 13(*S*)-HPOT as the substrates. For a control, only PpAOS1 and 13(*S*)-HPOT were used in a reaction mixture. After terminating the reaction, the

resulting *cis*-OPDA product was converted to *trans*-OPDA by alkaline treatment, which was followed by methylation using ethereal diazomethane. The resulting *trans*-OPDA methyl ester was finally analyzed by chiral GC-MS. The molecular ion peak of the OPDA methyl ester at *m/z* 306 $[M]^+$ was monitored to evaluate SmAOC1 activity (Laudert et al. 1997) (Fig. 18). The GC-MS analysis showed a predominant molecular ion peak (ca. 97%) in the reaction mixture containing SmAOC1 (Fig. 18B). The retention time of this peak coincided with the standard *trans*-(+)-OPDA methyl ester, which represents *cis*-(+)-OPDA. In contrast, two molecular ion peaks of the racemic *trans*-OPDA methyl esters were detected in the product of the PpAOS1 reaction (Fig. 18A). The enzymatic activity of SmAOC1 is required for the synthesis of naturally occurring OPDA (Fig. 18). The stereochemistry of OPDA in *S. moellendorffii* is the same as that in other studied plants.

The first three enzymes involved in JA biosynthesis (LOX, AOS, and AOC) have been reported to reside in chloroplasts (Schaller and Stintzi 2009). To examine whether SmAOC1 is localized in chloroplasts, a 35S::SmAOC1-GFP plasmid was constructed and introduced into *P. patens* protoplasts and was then finally observed by confocal laser scanning microscopy. The green fluorescent signal of SmAOC1 fused with GFP was clearly identified by the red auto-fluorescence of chlorophyll. The overlay data also strongly supported that SmAOC1 is located in chloroplasts, which is similar to the other characterized AOCs (Fig. 19). Accordingly, chloroplast could be the functional organelle in the biosynthesis of OPDA in *S. moellendorffii*. These results suggest that the first half of the octadecanoid pathway for synthesizing OPDA is present in the chloroplasts of *S. moellendorffii*. The presence of LOX, AOS, and AOC in chloroplasts may have been conserved during the process of land plant evolution.

3.2.4 Enzymatic activities of *SmOPR1* and *SmOPR5*

OPRs are classified into two groups based on their ability to reduce OPDA: OPR3-like enzymes (e.g., *Arabidopsis* AtOPR3, tomato SlOPR3, and rice OsOPR7) and OPR1-like enzymes (e.g., AtOPR1 and SlOPR1) (Breithaupt et al. 2009). OPR3-like enzymes catalyze the reduction of *cis*-(+)-OPDA, a natural JA precursor, and of *cis*-(-)-OPDA, which is not involved in JA biosynthesis. *Arabidopsis opr3* mutant shows male sterility and is desensitized to responses involving JA signaling. In contrast, OPR1-like enzymes preferentially reduce *cis*-(-)-OPDA rather than *cis*-(+)-OPDA; therefore, OPR1-like enzymes might function in pathways other than JA biosynthesis.

A genomic database search using Phytozome v 11.0 predicted the presence of six putative *OPR* genes in *S. moellendorffii*. All of the amino acid sequences of candidate SmOPRs were aligned with those of other known OPRs (Fig. 20). Based on a comparison of two critical amino acids for substrate binding and a phylogenetic tree analysis of SmOPRs (Fig. 21), two genes designated *SmOPR1* and *SmOPR5* were highly promising candidate genes encoding OPR3-like enzymes involved in JA biosynthesis. SmOPR1 harbors two important active-site residues, Phe and His, as an OPR3 motif in the active site, which is considered to be necessary to reduce the JA precursor *cis*-(+)-OPDA. However, SmOPR1 was grouped with the other SmOPRs in the cluster of OPR1-like enzymes (Fig. 21). In contrast, SmOPR5 was a member of the cluster of OPR3-like enzymes, such as AtOPR3, OsOPR7, SlOPR3, ZmOPR7, and ZmOPR8, which are active in JA biosynthesis (Fig. 21). Moreover, SmOPR5 shared 53% amino acid sequence identity with AtOPR3. Nonetheless, instead of Phe and His, which are considered unique to the OPR3 substrate filter, the active site residues of SmOPR5 are Trp and His. Therefore, these two genes were selected for further analysis to verify their enzymatic activity.

To confirm the enzymatic activities, recombinant SmOPR1 and SmOPR5 proteins fused with a His-tag were produced in *E. coli*. SDS-PAGE analysis showed that the recombinant SmOPR1 and SmOPR5 appeared as single bands with an expected molecular weight of approximately 40 kDa (Fig. 11). The enzymatic reactions were conducted according to the method of Schaller et al. (1998) with some modifications. Recombinant SmOPR1 and SmOPR5 were incubated in 50 mM potassium phosphate buffer (pH 7.4) containing NADPH and *cis*-(±)-OPDA. After terminating the OPR reactions, the *cis*-isomers of OPDA and OPC-8:0 in the OPR reaction solutions were converted into *trans*-isomers of OPDA and OPC-8:0 by alkaline treatment. The reaction products were finally analyzed by chiral GC-MS after methylation (Vick and Zimmerman 1983; Laudert et al. 1997). In the GC-MS chromatogram of SmOPR1 reaction products, only the peak of methylated *trans*-(-)-OPC-8:0, which was derived from the non-JA precursor *cis*-(-)-OPC-8:0, appeared. However, there was no peak for methylated *trans*-(+)-OPC-8:0, which would be derived from *cis*-(+)-OPDA, a natural JA biosynthetic intermediate (Fig. 22). Therefore, SmOPR1 does not participate in JA biosynthesis. In contrast, SmOPR5 catalyzed the reduction of both *cis*-(±)-OPDA enantiomers to both (±)-OPC-8:0 enantiomers (Fig. 22). The fragmentation of methylated *trans*-(+)-OPC-8:0 (Peak 1) derived from *cis*-(+)-OPDA was similar to that of standard methylated OPC-8:0 in the GC-MS spectral data (Figs. 23 and 24). These data indicated that *SmOPR5* encodes a functional OPR3 that participates in JA biosynthesis in *S. moellendorffii*.

The enzymatic analysis of SmOPR1 and SmOPR5 revealed that *S. moellendorffii* possesses two types of OPRs that are classified by substrate preference: OPR1-like enzymes and OPR3-like enzymes. SmOPR1 and SmOPR5 are similar in their molecular mass and isoelectric point (pI) (Table 3) but differ in their substrate specificity for *cis*-

OPDA isomers. Of these two SmOPRs, only SmOPR5 reduced *cis*-(±)-OPDA, including the endogenous substrate *cis*-(+)-OPDA, which is the natural JA precursor (Fig. 22). In contrast to SmOPR5, SmOPR1 reduced only *cis*-(-)-OPDA, which is the unnatural type (Fig. 22). SmOPR1 might instead be required for the other oxylipin metabolic pathways.

A structural comparison of tomato SlOPR1 and SlOPR3 indicated that two active site residues, Tyr78 and Tyr246 in SlOPR1 and Phe74 and His244 in SlOPR3, are critical for substrate specificity (Breithaupt et al. 2009). SlOPR3 is less enantioselective due to its two relatively smaller amino acid residues that form a larger substrate binding pocket. In contrast, the relatively larger amino acids (two Tyr residues) in SlOPR1 permit access to only *cis*-(-)-OPDA, the unnatural type, at the substrate binding site. This study showed that SmOPR5, but not SmOPR1, actively converts the endogenous substrate *cis*-(+)-OPDA to *cis*-(+)-OPC-8:0. This result contrasts with the prediction from the substrate preference analysis of their active site residues but agrees with the phylogenetic analysis of OPRs (Figs. 20 and 21). However, mutation of the important amino acids Phe and His into Tyr in SlOPR3 did not completely change the substrate specificity (Breithaupt et al. 2009). There might be other factors such as residues that are critical for dimer formation of OPR3 and strictly conserved in group II (Breithaupt et al. 2009).

Li et al. (2009) showed that OPR genes from the lower land plants *P. patens* (PpOPR1, PpOPR2, PpOPR4, and PpOPR5) and *S. moellendorffii* (SmOPR1, SmOPR2, SmOPR3, SmOPR4, and SmOPR6) clustered together in subgroup VI. Because SmOPR1 showed OPR1 activity, the other OPRs in subgroup VI may be unrelated to JA biosynthesis. In contrast, the other known OPR3-like enzymes are positioned in the

same cluster in subgroup II. It is most likely that OPR3-like enzymes independently evolved to expand the substrate binding pocket to accept *cis*-(+)-OPDA.

3.2.5 Enzymatic production of JA-Ile by SmJAR1

JAR1 is responsible for conjugating JA to amino acids. Because JA-Ile is a versatile molecule in JA signaling, JAR1 is necessary for JA-mediated physiological events in seed plants (Wasternack and Hause 2013). JAR1 is a member of the GH3 proteins, which are classified into three groups based on their enzymatic activity. Group I proteins, such as *Arabidopsis* AtJAR1, can synthesize the JA-amino acid conjugates JA-Ile, JA-Leu and JA-Val (Staswick and Tiryaki 2004). A group I GH3 protein from seed plants showed JA-Ile synthase activity, which functions in plant defense (Kang et al. 2006; Suza et al. 2010). Group II proteins conjugate IAA and SA to various amino acids (Staswick et al. 2005). Group III proteins accept benzoates as substrates for amino acid conjugation (Okrent et al. 2009).

An *Arabidopsis jar1* mutant, which is unable to produce JA-Ile, fails to trigger JA-mediated responses (Suza and Staswick 2008). Thus, JAR1 activity is necessary for JA signal transduction in seed plants. Here, 14 *JAR1* homologous genes are found in the Phytozome database using AtJAR1 as a query (Table 2). Multiple sequence alignment and phylogenetic analysis using Clustal Omega software were performed to show the relationship between these JAR1 homologous proteins of *S. moellendorffii* and the other existing JAR1 proteins (Figs. 25 and 26). As a result, the candidate Sm_110439, designated as SmJAR1, was most closely related to AtJAR1, OsJAR1 and OsJAR2, which can synthesize JA-Ile (Staswick and Tiryaki 2004; Wakuta et al. 2011). Moreover, SmJAR1 also has three short conserved motifs involved in ATP/AMP binding (Kai-Hsuan et al. 1997): SSGTSQGRPK (motif 1), YGSSE (motif 2), and

YRLGD (motif 3) (Fig. 25). To determine whether *SmJAR1* encodes functional JA-Ile synthase in *S. moellendorffii*, SmJAR1 was isolated to check its enzymatic activity.

The JAR1 activity was evaluated by using *E. coli* overexpressing *SmJAR1* was incubated with (-)−JA as a substrate. JA-Ile products in the culture supernatant of *E. coli* were analyzed by UPLC-MS/MS. The analytical data clearly showed that SmJAR1 catalyzes the conjugation of JA to Ile using endogenous ATP and Ile in *E. coli* (Fig. 27). To investigate the substrate specificity of SmJAR1, the conjugation of JA to other amino acids was also analyzed by UPLC-MS/MS. No peak derived from another conjugate of JA-Trp, JA-Phe, or JA-Val appeared in the culture supernatant of *E. coli* overexpressing *SmJAR1* (Fig. 28). Therefore, SmJAR1 was hypothesized to prefer Ile for conjugation to JA.

S. moellendorffii produces JA-Ile based on evidence of a functionally active SmJAR1 (Figs. 7 and 27). The identification of JA-Ile and an active SmJAR1 strongly suggests that JA-Ile-mediated signaling is functional in *S. moellendorffii.* Moreover, SmJAR1 was hypothesized to prefer Ile as a substrate for conjugation with JA (Figs. 27 and 28). The same characteristic was also found in AtJAR1 (Staswick and Tiryaki 2004; Suza and Staswick 2008). Considering the substrate specificity of SmJAR1, JA-Ile seems to be more important as a signaling molecule than the other JA-amino acid conjugates. Additionally, endogenous conjugates of JA with another amino acid, such as JA-Trp, JA-Phe, JA-Gly, JA-Leu, and JA-Val, have not been detected in *S. moellendorffii* (Fig. 29).

In the case of rice (*Oryza sativa*), OsJAR2 in the cluster of group II GH3 proteins can conjugate JA to Ile, similar to OsJAR1 in the cluster of group I GH3 proteins (Wakuta et al. 2011). The other thirteen of JAR1 homologs found in *S. moellendorffii* might also show JA-Ile synthetic activity. Given that GH3 proteins synthesize

conjugates of JA and amino acids in *P. patens* (Ludwig-Müller et al. 2009), land plants are suggested to have enzymes with ubiquitous JAR1 activity. JA synthesis and JAR1 activity might have evolved independently in land plants.

3.2.6 Expression of genes encoding key enzymes in JA-Ile under wounding stress and JA treatment

Wounding and JA induce the expression of a wide variety of genes in seed plants, such as defense-related genes and genes encoding enzymes involved in JA biosynthesis (Reymond and Farmer 1998). To examine whether wounding and JA treatment affect gene expression in *S. moellendorffii*, quantitative RT-PCR analysis was performed to analyze the expression of *SmAOC1*, *SmOPR5*, and *SmJAR1*. Wounding increased the transcriptional levels of *SmAOC1*, *SmOPR5*, and *SmJAR1* (Fig. 30). The expression of *SmAOC1* was transiently induced at 10 min after wounding and then decreased until 180 min. The accumulation of *SmOPR5* mRNA reached a maximum 20 min after wounding and decreased thereafter. By contrast, only weak expression was observed for *SmJAR1* until 60 min, followed by an increase in *SmJAR1* expression at 180 min. These results indicate that the expression patterns of *SmAOC1*, *SmOPR5*, and *SmJAR1* coincided with the accumulation profiles of OPDA, JA, and JA-Ile in wounded *S. moellendorffii*. Based on the *SmOPR5* expression level, the accumulation of *SmOPR5* appears to precede the production of OPDA. Additionally, the late accumulation of JA-Ile coincided with the late expression level of *SmJAR1* after wounding (Fig. 30). The expression profiles of *SmAOC1*, *SmOPR5*, and *SmJAR1* support the accumulation patterns of OPDA, JA, and JA-Ile (Fig. 8), probably due to the role of jasmonates in regulating responses to environmental stresses in S. *moellendorffii*.

The analytical data on *SmAOC1* and *SmOPR5* expression in JA-treated *S. moellendorffii* revealed an initial increase in transcriptional levels in the first 30 and 10 min, respectively (Fig. 31). The accumulation of *SmAOC1* continued to increase until 60 min after JA application and decreased thereafter, whereas the transcriptional level of *SmOPR5* decreased 30 min after the treatment. The expression profiles of *SmAOC1* and *SmOPR5* in the plants treated with JA were similar to those in the wounded plants. In contrast to *SmAOC1* and *SmOPR5*, the expression of *SmJAR1* was suppressed within 10 min after JA treatment and remained at a low level thereafter.

The present study demonstrated that JA induced the expression of *SmAOC1* and *SmOPR5* in *S. moellendorffii*. JA treatment led to the accumulation of genes encoding enzymes in the octadecanoid pathway, indicating positive feedback regulation of JA biosynthesis. The expression of *SmAOC1* and *SmOPR5* was enhanced upon JA application, and these expression patterns were similar to those observed under wounding treatment (Figs. 30 and 31). The JA-induced expression of *SmAOC1* and *SmOPR5* seems to indicate the presence of positive feedback regulation of JA biosynthesis in *S. moellendorffii*. In contrast to the up-regulation of *SmJAR1* by wounding (Fig. 30), JA inhibited *SmJAR1* expression at the transcriptional level (Fig. 31). Although the detailed JA signaling pathway has not been elucidated in *S. moellendorffii*, the suppression of *SmJAR1* expression by JA appears to function as negative feedback regulation of JA-Ile-mediated signaling, and/or an increase in JA signaling that is independent from JA-Ile. Wounding probably activates various signaling pathways that are JA-dependent and JA-independent. In the case of *SmJAR1* expression, integrated signaling was caused by wounding.

Table 2. Putative *AOS, AOC, OPR, JAR1* genes in *S. moellendorffii*.

Designation	Locus name	Location	Query (GenBank accession no.)
SmAOS1	271334	scaffold_38	*Arabidopsis* AOS (AED94842)
SmAOS2	177201	scaffold_38	*Arabidopsis* AOS (AED94842)
SmAOS3	228572	scaffold_38	*Arabidopsis* AOS (AED94842)
SmAOC1	91887	scaffold_12	*Arabidopsis* AOC (CAC83764)
*SmOPR1**	270843	scaffold_14	*Arabidopsis* OPR3 (AEC06000)
*SmOPR5**	111662	scaffold_41	*Arabidopsis* OPR3 (AEC06000)
SmJAR1	110439	scaffold_40	*Arabidopsis* JAR1 (AEC10684)

*The numbering of *SmOPRs* was previously described by Li et al. (2009).

Table 3. Properties of *SmAOS1*, *SmAOS2*, *SmAOS3*, *SmAOC1*, *SmOPR1*, *SmOPR5*, and *SmJAR1*.

Gene name	ORF length (bp)	Protein length (aa)	MW (Da)	Theoretical pI
SmAOS1	1458	485	54,107	6.01
SmAOS2	1404	467	52,079	6.35
SmAOS3	1458	485	54,071	5.89
SmAOC1	738	245	26,364	9.15
*SmOPR1**	1131	376	41,588	6.28
*SmOPR5**	1209	402	44,046	6.05
SmJAR1	1749	582	64,751	5.83

* The numbering of *SmOPRs* was previously described by Li et al. (2009).

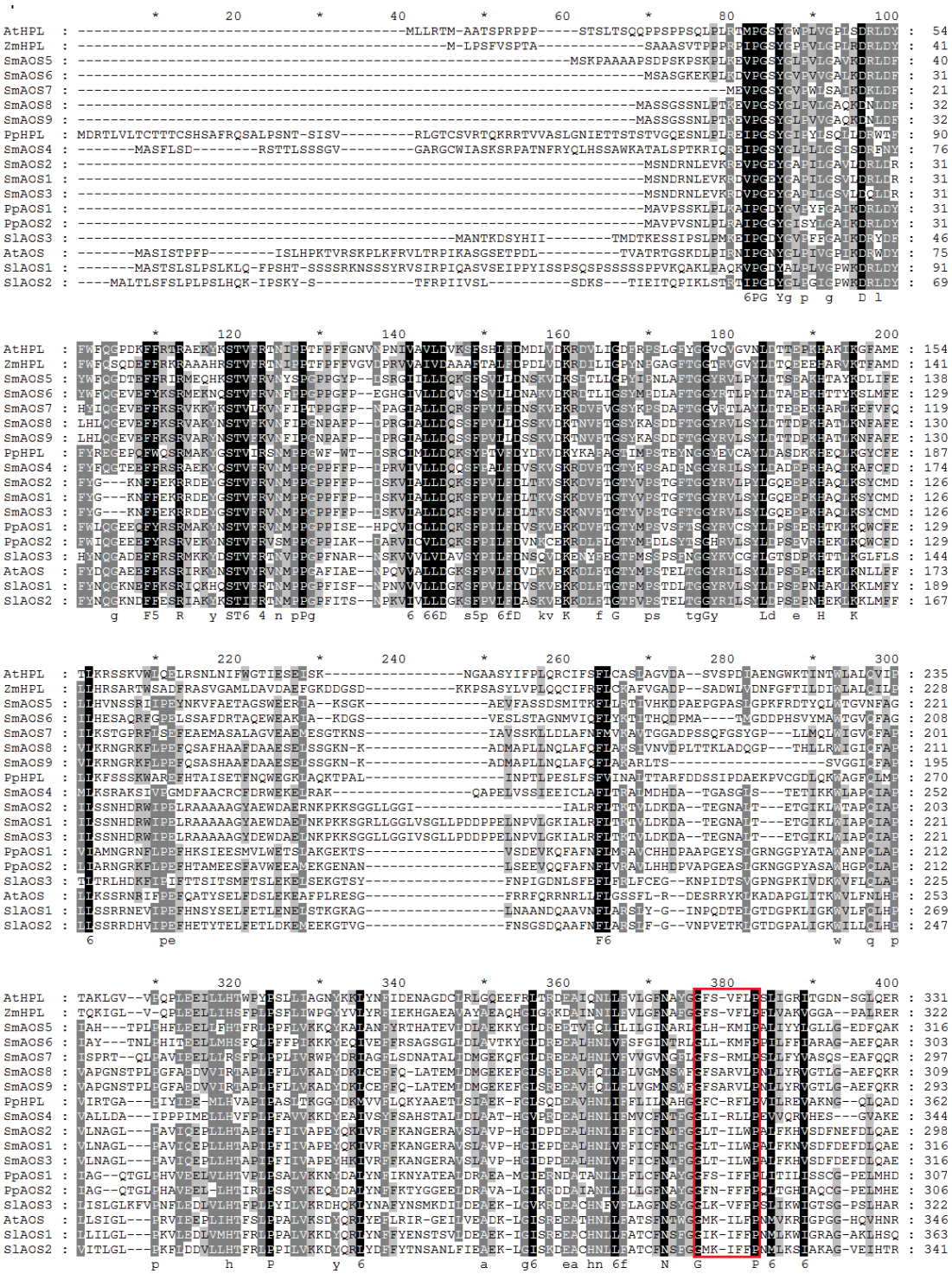

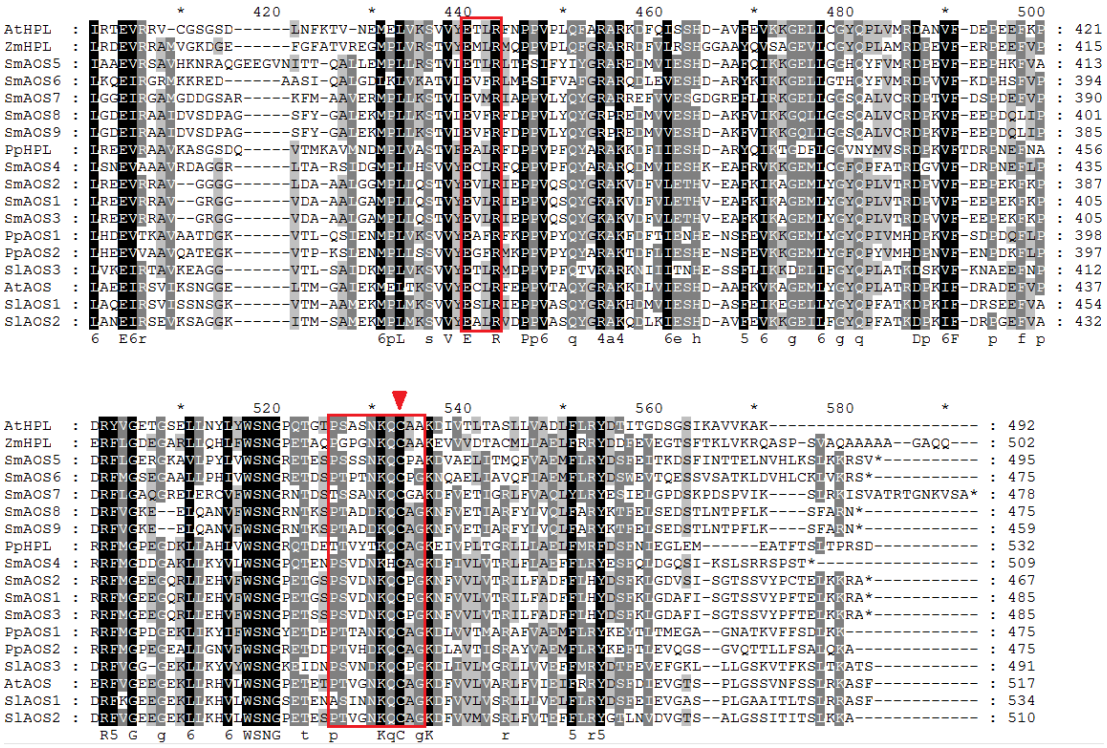

Fig. 9. Amino acid sequence alignment of SmAOSs with the previously reported AOSs. The Clustal Omega was used for the alignment. The conserved cysteine residue for heme-ligand binding is indicated with a red triangle. The I-helix GXXX(F/L), EXLR motif, and PXVXNKQCPG for heme-binding domain are in red box (Koeduka et al. 2015). The reported AOSs: PpAOS1 (*Physcomitrella patens*, CAC86919), PpAOS2 (*P. patens*, XP_001759629), SlAOS1 (*Solanum lycopersicum*, CAB88032), SlAOS2 (*S. lycopersicum*, AAF67141), SlAOS3 (*S. lycopersicum*, AAN76867), AtAOS (*Arabidopsis thaliana*, CAA63266), AtHPL (*A. thaliana*, AAC69871), ZmHPL (*Zea mays*, AAS47027), and PpHPL (*P. patens*, CAC86920). AOS homologues in *Selaginella moellendorffii*: SmAOS1 (SELMODRAFT_271334), SmAOS2 (SELMODRAFT_177201), SmAOS3 (SELMODRAFT_228572), SmAOS4 (SELMODRAFT_133317), SmAOS5 (SELMODRAFT_81998), SmAOS6 (SELMODRAFT_177485), SmAOS7 (SELMODRAFT_92382), SmAOS8 (SELMODRAFT_98717), and SmAOS9 (SELMODRAFT_41357).

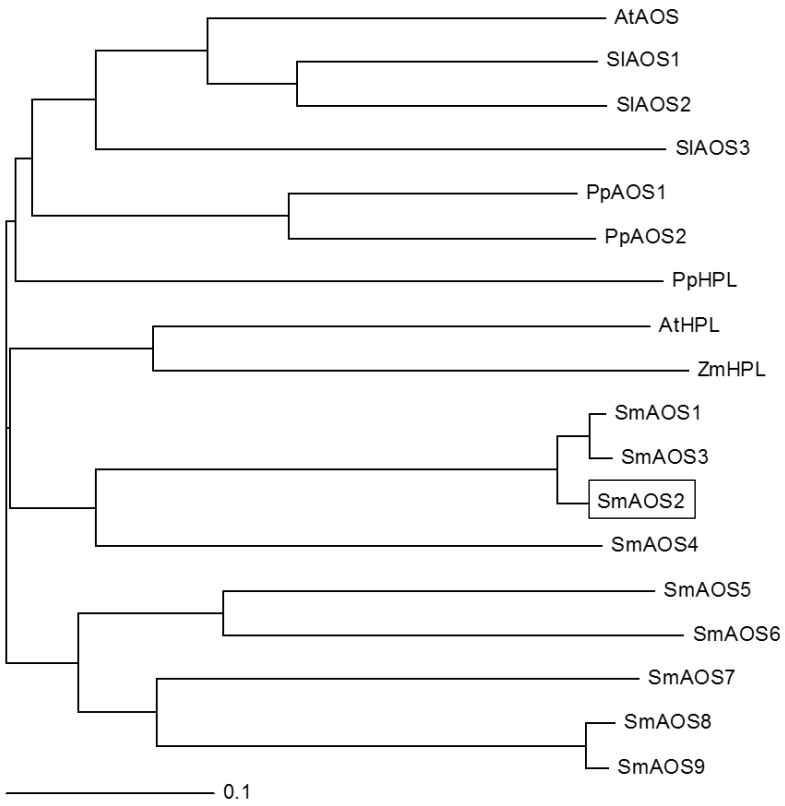

Fig. 10. Phylogenetic tree of SmAOSs and previously reported AOSs.

Phylogenetic tree was constructed using TreeView X program based on amino acid sequence alignment. The bars represent evolutionary distance. The reliability of the tree measured by bootstrap analysis with 1,000 replicates. The reported AOSs: PpAOS1 (*Physcomitrella patens*, CAC86919), PpAOS2 (*P. patens*, XP_001759629), SlAOS1 (*Solanum lycopersicum*, CAB88032), SlAOS2 (*S. lycopersicum*, AAF67141), SlAOS3 (*S. lycopersicum*, AAN76867), AtAOS (*Arabidopsis thaliana*, CAA63266), AtHPL (*A. thaliana*, AAC69871), ZmHPL (*Zea mays*, AAS47027), and PpHPL (*P. patens*, CAC86920). AOS homologous in *Selaginella moellendorffii*: SmAOS1 (SELMODRAFT_271334), SmAOS2 (SELMODRAFT_177201), SmAOS3 (SELMODRAFT_228572), SmAOS4 (SELMODRAFT_133317), SmAOS5 (SELMODRAFT_81998), SmAOS6 (SELMODRAFT_177485), SmAOS7 (SELMODRAFT_92382), SmAOS8 (SELMODRAFT_98717), and SmAOS9 (SELMODRAFT_41357).

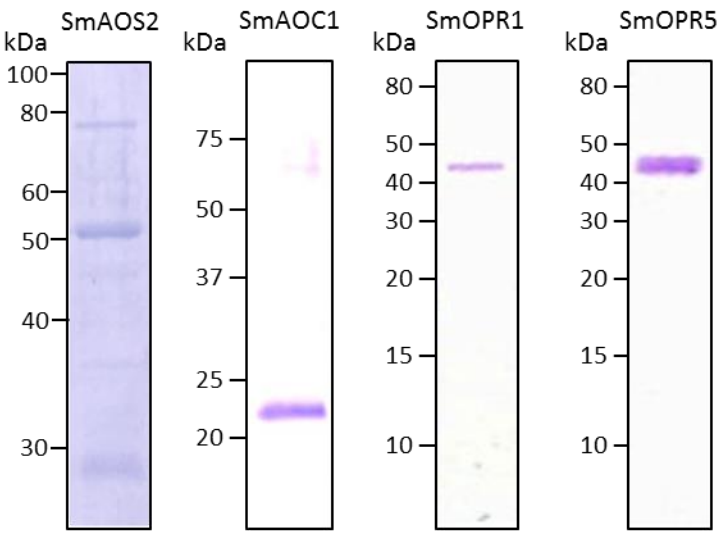

Fig. 11. SDS-PAGE analysis of recombinant SmAOS2, SmAOC1, SmOPR1 and SmOPR5.

The recombinant proteins fused with His-tag were overexpressed in *E. coli* and were purified using Ni-NTA agarose column chromatography. SmAOC1 was analyzed by 15% SDS-PAGE. SmAOS2, SmOPR1, and SmOPR5 were analyzed by 10% SDS-PAGE, respectively. Proteins were stained by Coomassie Brilliant Blue (CBB).

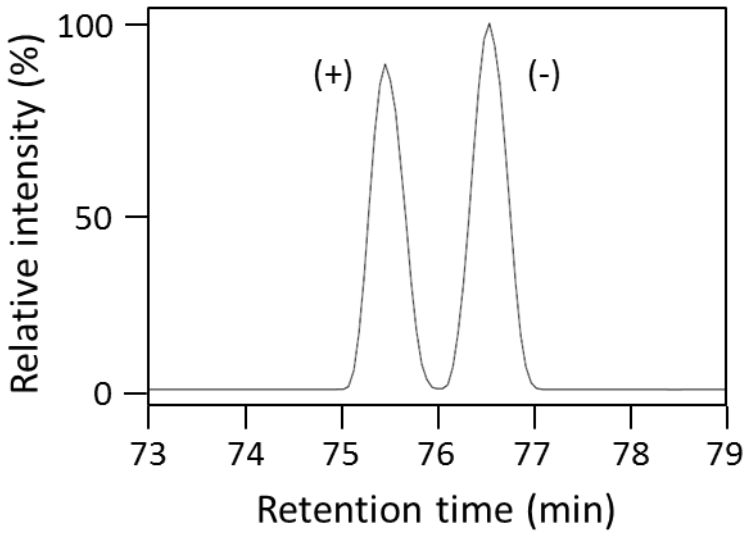

Fig. 12. Chiral GC-MS analysis of the products of SmAOS2 reaction .

Recombinant SmAOS2 was reacted with the substrate 13(*S*)-HPOT, directly treated with alkaline solution and then methylated by ethereal diazomethane. The methylated OPDA was analyzed by GC-MS equipped with a chiral capillary column. The former and latter peaks represent the *trans*-(+)- and (-)-OPDA methyl esters, respectively (Laudert et al. 1997).

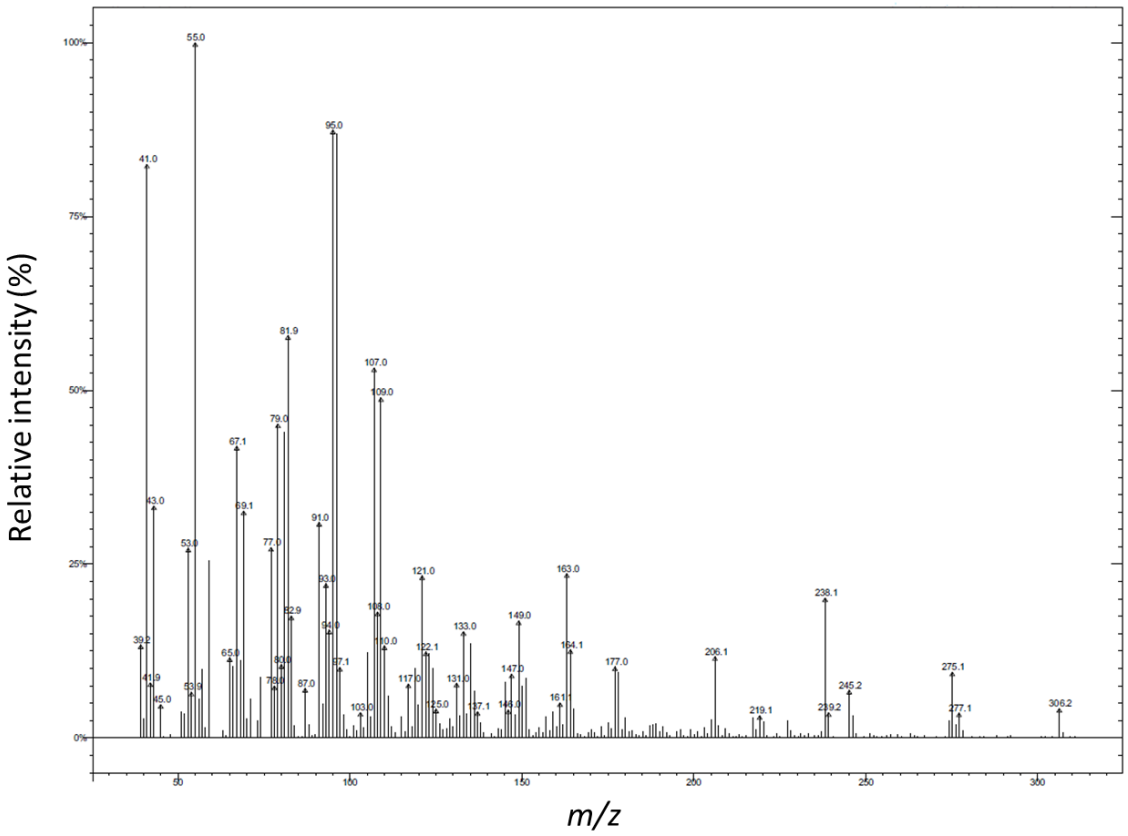

Fig. 13. GC-MS spectrum of methyl ester of (+)-*trans*-OPDA.

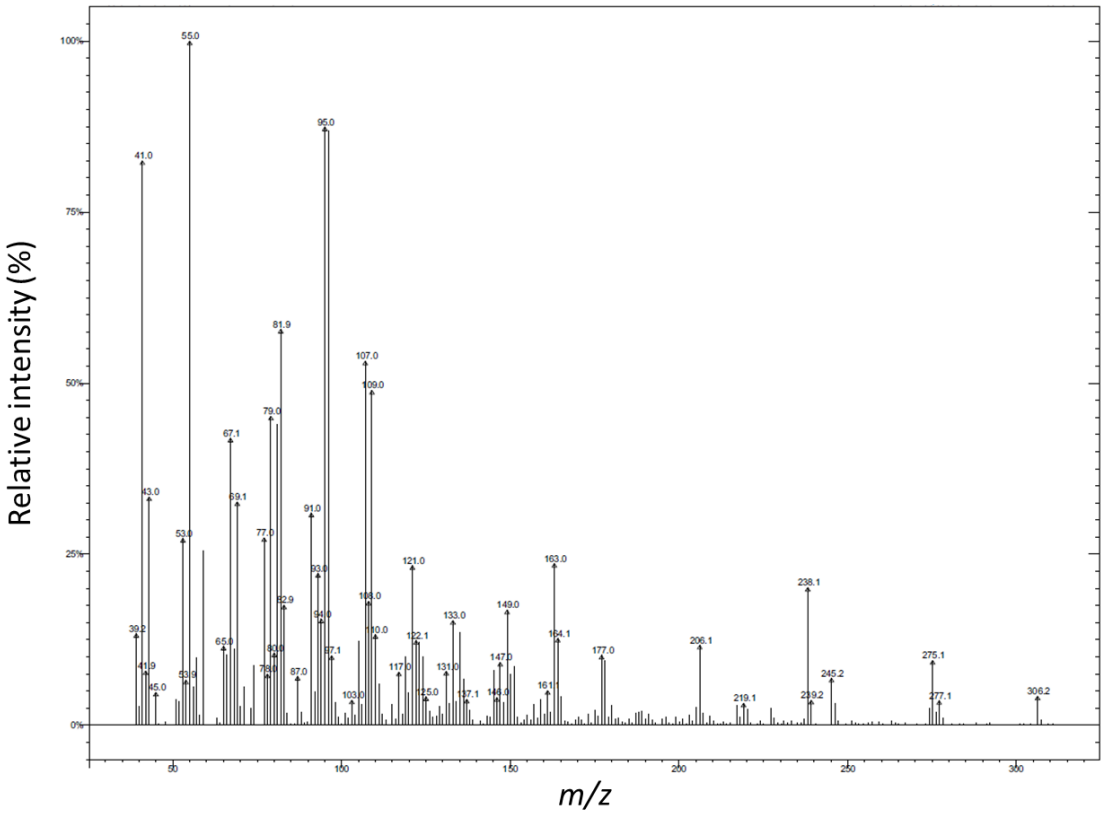

Fig. 14. GC-MS spectrum of methyl ester of (-)-*trans*-OPDA.

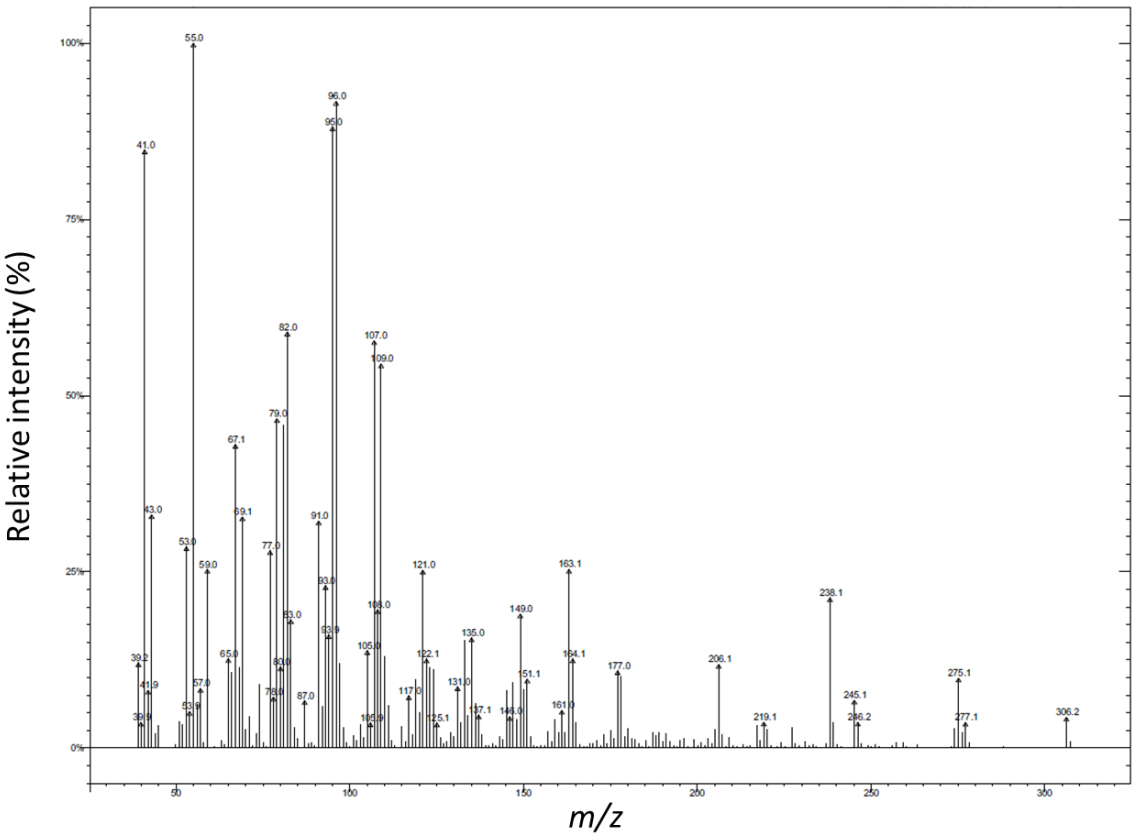

Fig. 15. GC-MS spectrum of methyl ester of standard (±)−OPDA.

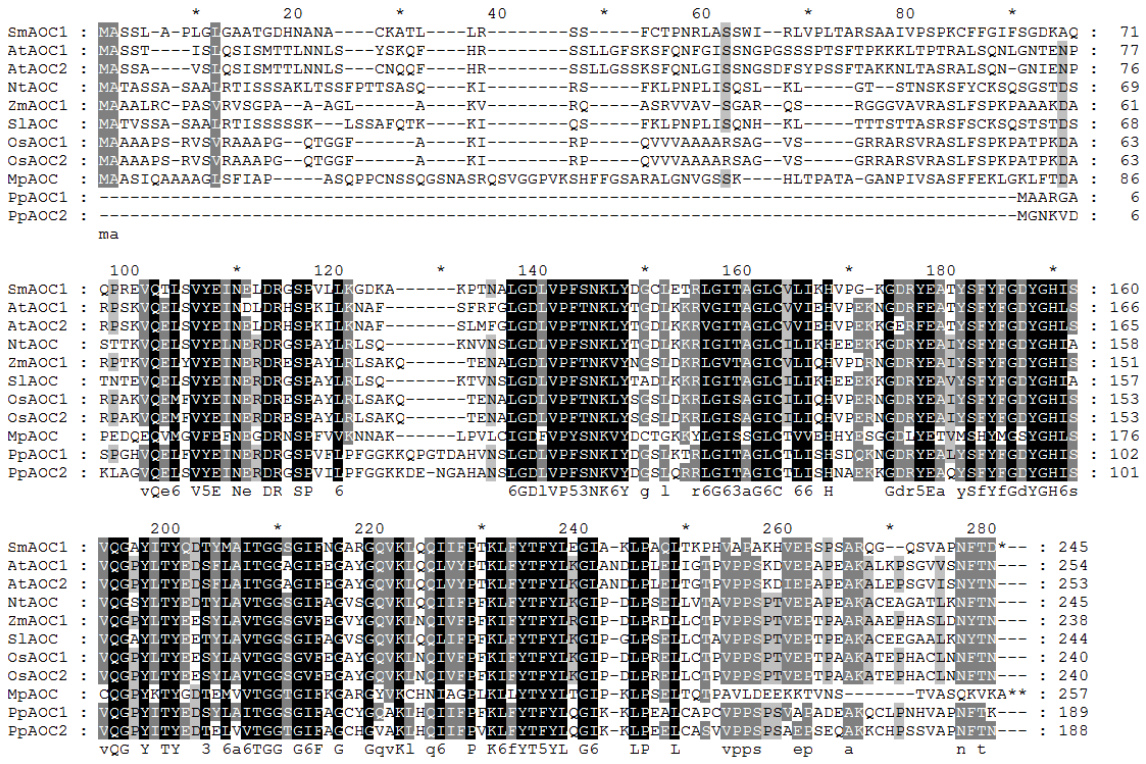

Fig. 16. Amino acid sequence alignment of SmAOC1 with the previous reported AOCs. Amino acid sequences were aligned using Clustal Omega. Identical and similar amino acids are highlighted in black and gray, respectively. The aligned sequences include SmAOC1 (*Selaginella moellendorffii*, Sm_91887), PpAOC1 (*Physcomitrella patens*, CAD48752), PpAOC2 (*P. patens*, CAD48753), MpAOC (*Marchantia polymorpha*, BAO93687), AtAOC1 (*Arabidopsis thaliana*, AEE77065.1), AtAOC2 (*A. thaliana*, AEE77066.1), ZmAOC (*Zea mays*, NP_001105245), OsAOC1 (*Oryza sativa*, ABV03555), OsAOC2 (*O. sativa*, ABV45432), SlAOC (*Solanum lycopersicum*, AAK62358), and NtAOC (*Nicotiana tabacum*, CAC83765).

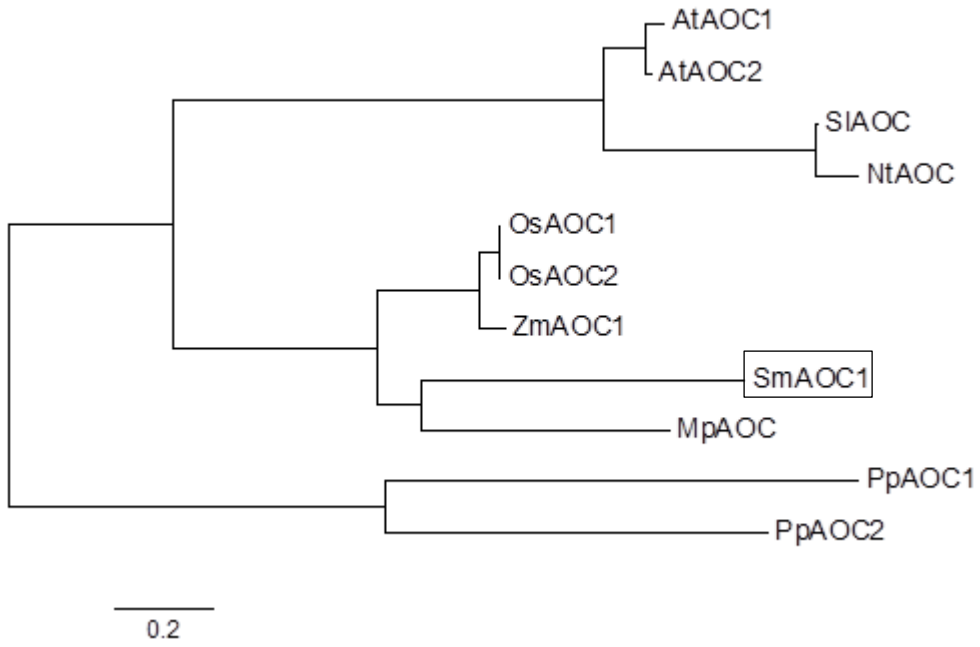

Fig. 17. Phylogenetic tree of SmAOC1 and previously reported AOCs.

Phylogenetic tree was constructed using the neighbor-joining method with MEGA 5.2 program based on amino acid sequence alignment. The bars represent evolutionary distance. The reliability of the tree measured by bootstrap analysis with 1,000 replicates. The analysis was performed with following: SmAOC1 (*Selaginella moellendorffii*, Sm_91887), PpAOC1 (*Physcomitrella patens*, CAD48752), PpAOC2 (*P. patens*, CAD48753), MpAOC (*Marchantia polymorpha*, BAO93687), AtAOC1 (*Arabidopsis thaliana*, AEE77065.1), AtAOC2 (*A. thaliana*, AEE77066.1), ZmAOC (*Zea mays*, NP_001105245), OsAOC1 (*Oryza sativa*, ABV03555), OsAOC2 (*O. sativa*, ABV45432), SlAOC (*Solanum lycopersicum*, AAK62358), and NtAOC (*Nicotiana tabacum*, CAC83765).

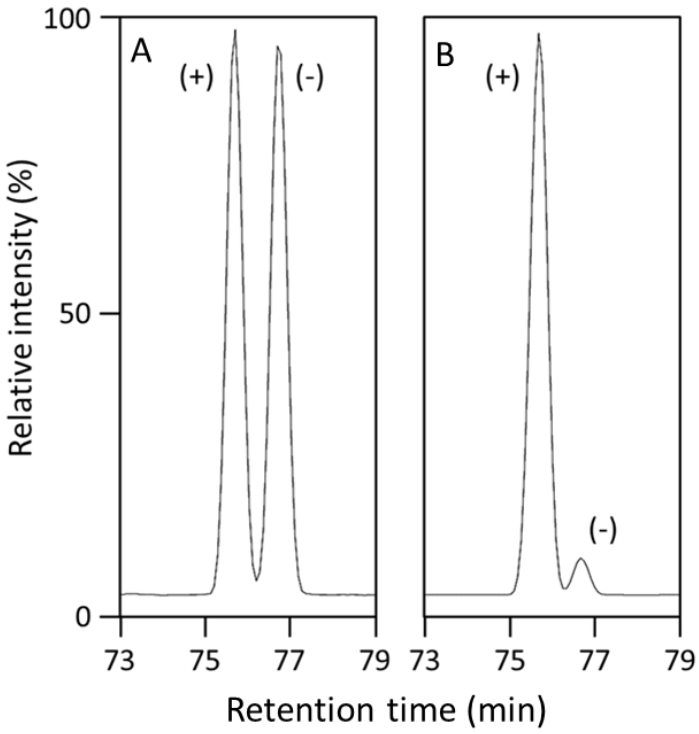

Fig. 18. Chiral GC-MS analysis of the OPDA methyl ester.

Recombinant SmAOC1 was reacted with the substrate 13-HPOT and an allene oxide synthase (PpAOS1), directly treated with alkaline solution and then methylated by ethereal diazomethane. The methylated OPDA was analyzed by GC-MS using a chiral capillary column. The molecular ion peak of the OPDA methyl ester at *m/z* 306 was monitored. The former and latter peaks represent the *trans*-(+)- and (-)-OPDA methyl ester, respectively (Laudert et al. 1997). (A) Racemic OPDA standard. (B) Product of the SmAOC1 enzymatic reaction.

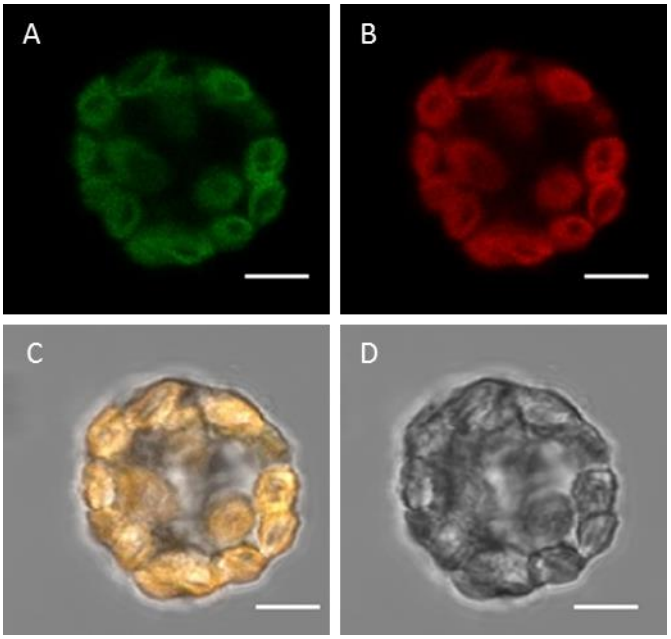

Fig. 19. Expression of SmAOC1-GFP fusion protein in the chloroplast of *P. patens* protoplast.

The sub-cellular localization of SmAOC1 was analyzed by constructing the SmAOC1-GFP plasmid, which was introduced into the prepared protoplast of *P. patens* using PEG-mediated transformation method. Images were taken with a confocal laser-scanning microscope with an excitation of 488 nm and emission of 530 nm for detecting GFP and an emission above 655 nm for detecting autofluorescence from chlorophyll. (A) Green fluorescence of SmAOC1-GFP. (B) Red chlorophyll autofluorescence. (C) Merge of the green fluorescence and the red chlorophyll autofluorescence. (D) Bright field. Scale bar: 10 μm.

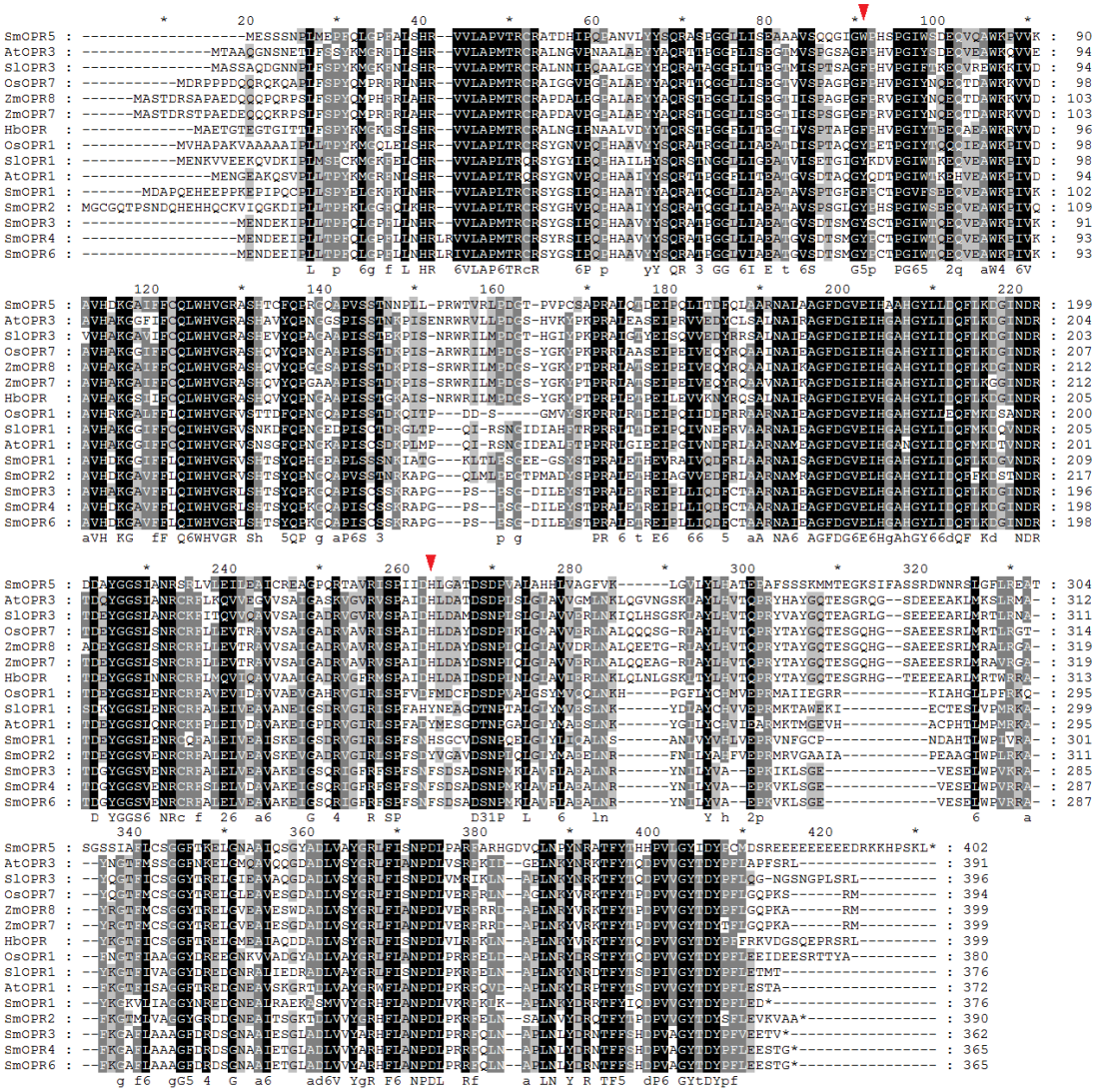

Fig. 20. Amino acid sequence alignment of SmOPRs and other known OPRs.

Amino acid sequences were aligned using Clustal Omega. Identical and similar amino acids are highlighted in black and gray, respectively. The two specificity-determining residues are marked by red arrows. The aligned sequences include OPR3-like enzymes (AtOPR3: *Arabidopsis thaliana* OPR3, AEC06000; HbOPR: *Hevea brasiliensis* OPR, AAY27752; OsOPR7: *Oryza sativa* OPR7, Q6Z965; SlOPR3: *Solanum lycopersacum* OPR3, NP_001233873; ZmOPR7: *Zea mays* OPR7, NP_001105910; ZmOPR8, NP_001105833), OPR1-like enzymes (AtOPR1: *Arabidopsis thaliana* OPR1, AEE35875; OsOPR1: *Oryza sativa* OPR1, Q84QK0; SlOPR1: *Solanum lycopersacum* OPR1, NP_001234781), and SmOPRs. The numbering of SmOPRs was in accordance with that previously described by Li et al. (2009).

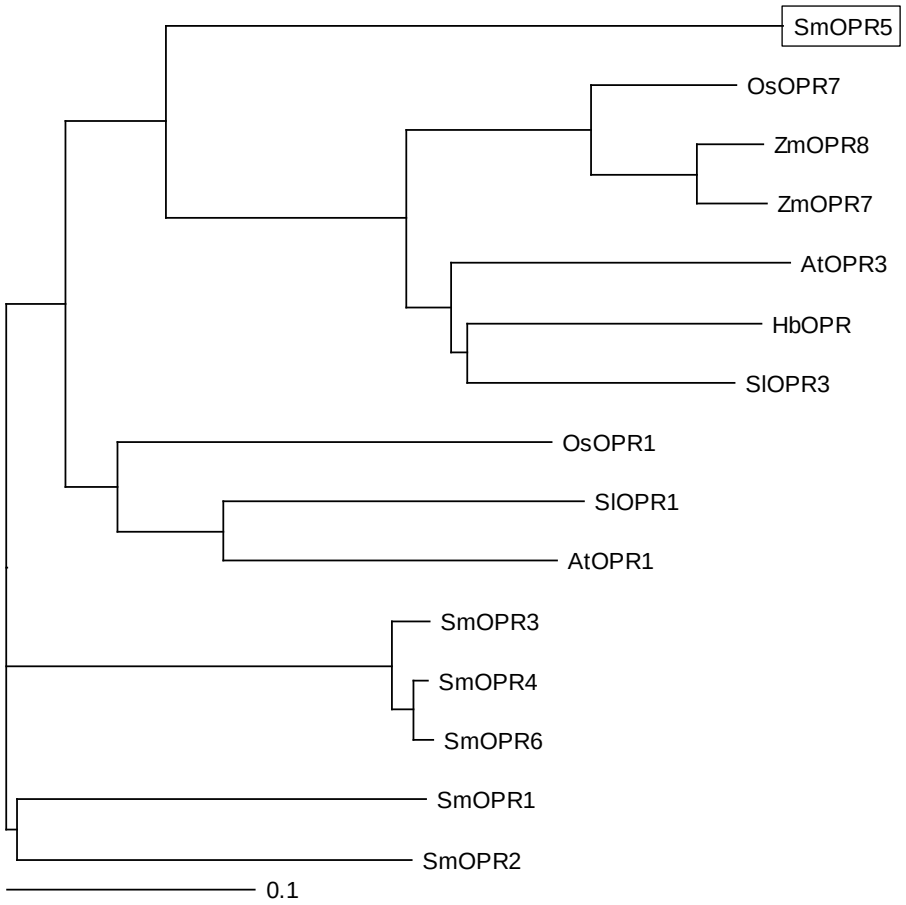

Fig. 21. Phylogenetic tree of SmOPRs and previously reported OPRs.

The OPR amino acid sequences were compared using Clustal Omega. The phylogenetic tree was visualized from the resulting alignment using TreeView X program. The analysis was performed with the following: OPR3-like enzymes (AtOPR3: *Arabidopsis thaliana* OPR3, AEC06000; HbOPR: *Hevea brasiliensis* OPR, AAY27752; OsOPR7: *Oryza sativa* OPR7, Q6Z965; SlOPR3: *Solanum lycopersacum* OPR3, NP_001233873; ZmOPR7: *Zea mays* OPR7, NP_001105910; ZmOPR8, NP_001105833), OPR1-like enzymes (AtOPR1: *Arabidopsis thaliana* OPR1, AEE35875; OsOPR1: *Oryza sativa* OPR1, Q84QK0; SlOPR1: *Solanum lycopersacum* OPR1, NP_001234781), and SmOPRs. The numbering of SmOPRs was in accordance with that previously described by Li et al. (2009).

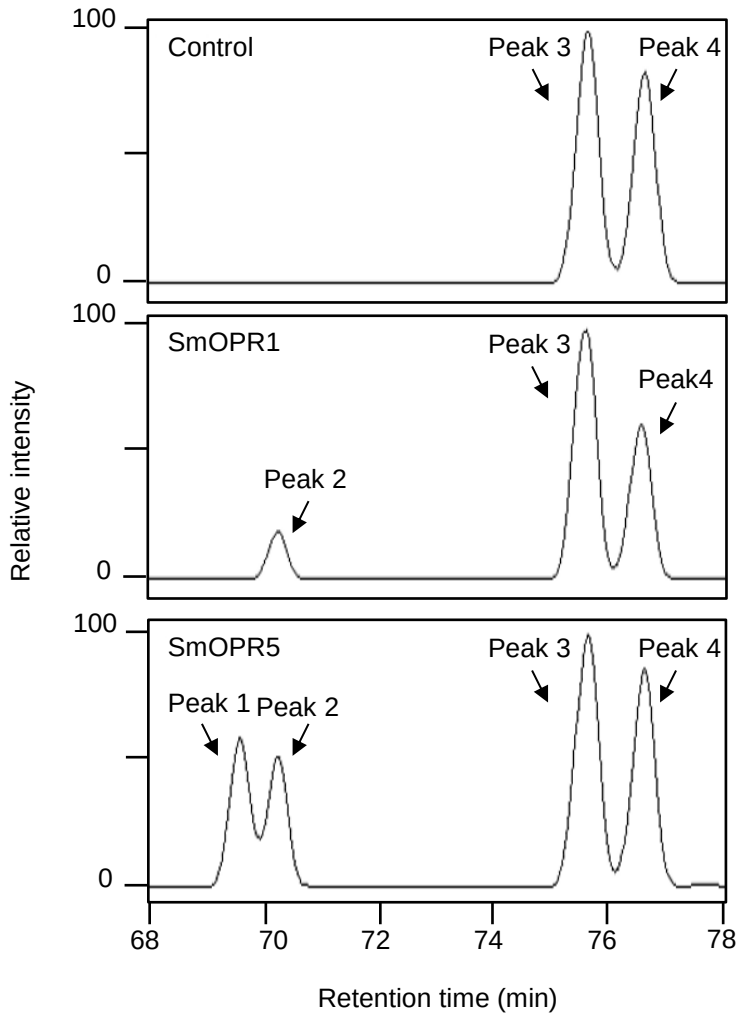

Fig. 22. Chiral GC-MS analysis of the reaction products catalyzed by SmOPR1 and SmOPR5.

Recombinant SmOPR1 and SmOPR5 were each reacted with racemic OPDA, directly treated with alkaline solution and then methylated by ethereal diazomethane. The methylated reaction products were analyzed by GC-MS using a chiral capillary column. The data are presented as the total ion current chromatogram. Peaks 1 to 4 represent trans-isomers of (+)-OPC-8:0 (natural type), (-)-OPC-8:0, (+)-OPDA (natural type) and (-)-OPDA, respectively, that were derived from *cis*-isomers of these compounds.

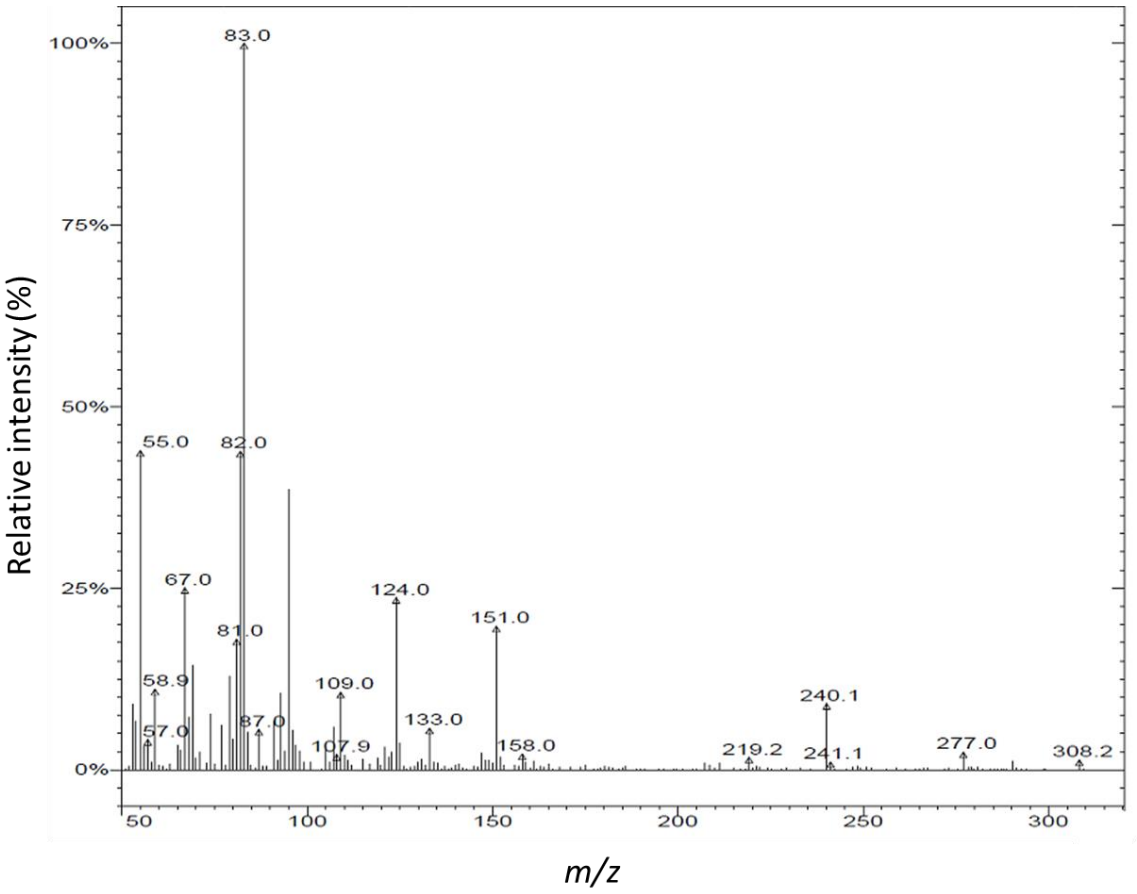

Fig. 23. GC-MS spectrum of the peak 1 of Fig. 22

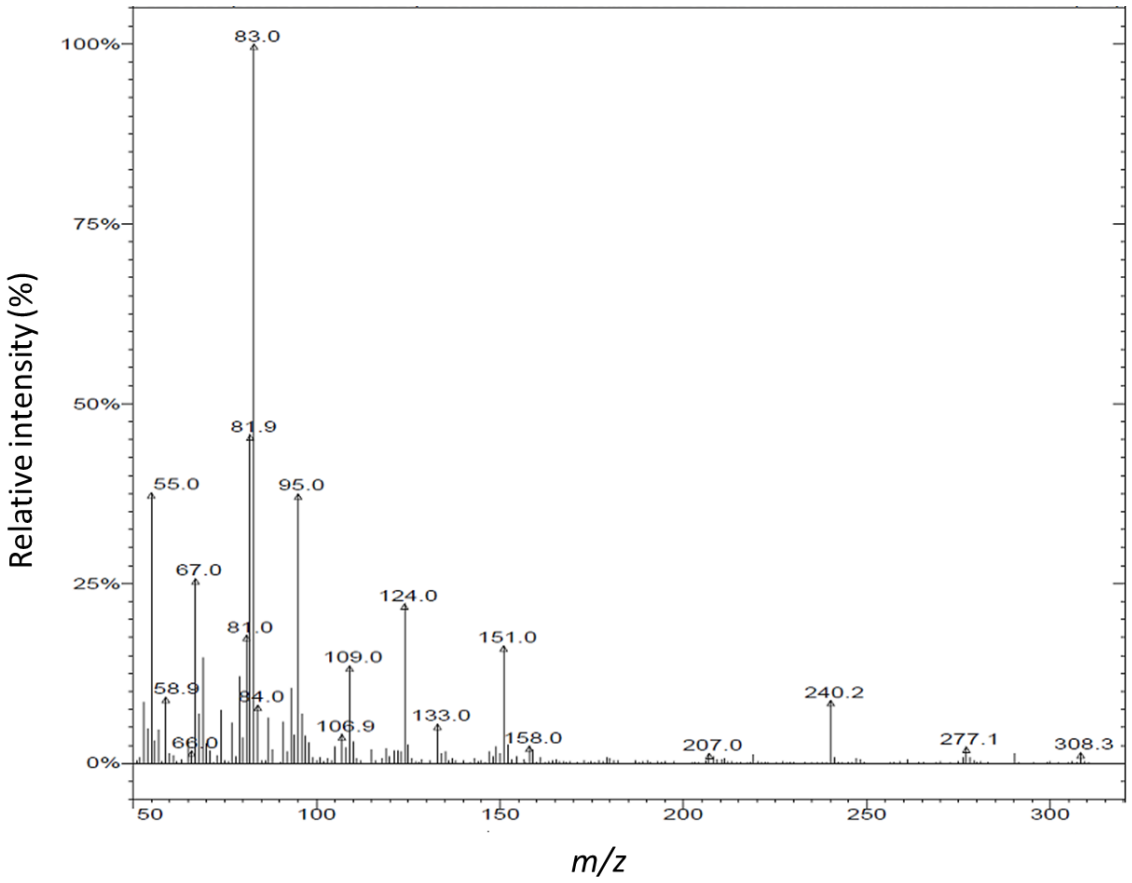

Fig. 24. GC-MS spectrum of the standard methyl ester of OPC-8:0.

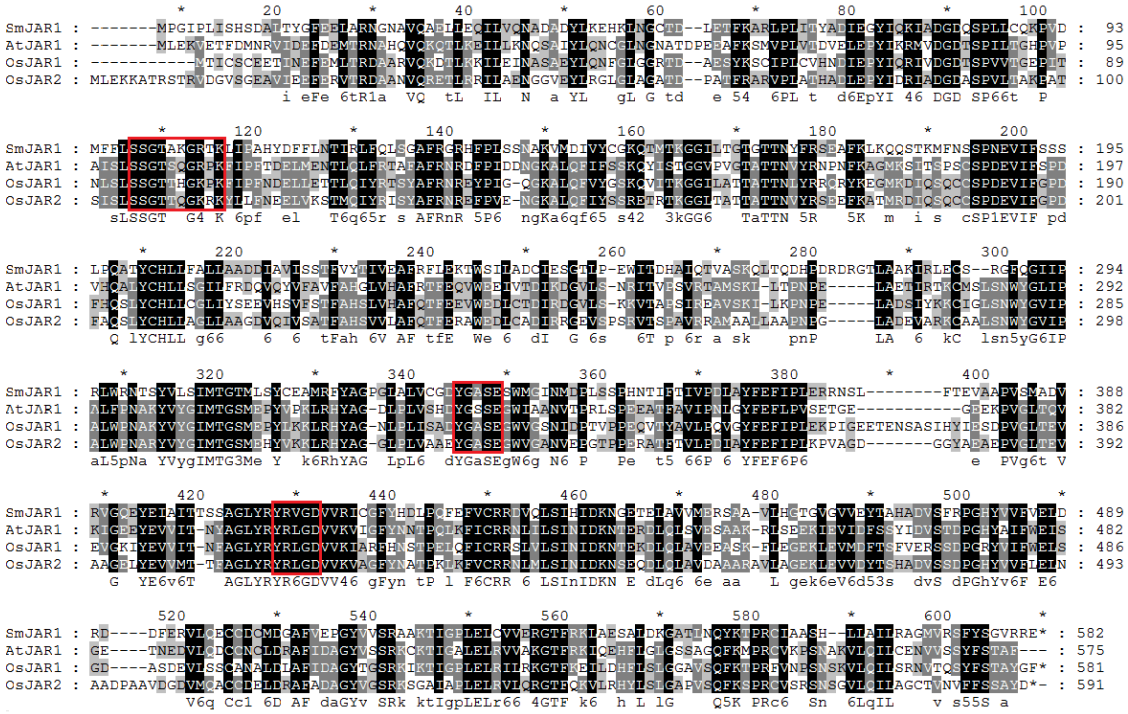

Fig. 25. Amino acid sequence alignment of SmJAR1 with three GH3 family members. Amino acid sequences were aligned using Clustal Omega. Identical and similar amino acids are highlighted in black and gray, respectively. The boxes indicate the three important motifs for enzymatic activity of GH3 proteins. The aligned sequences include AtJAR1 (*Arabidopsis thaliana*, AEC10684), OsJAR1 (*Oryza sativa*, LOC_Os05g50890.1), and OsJAR2 (*O.sativa*, LOC_Os01g12160.1).

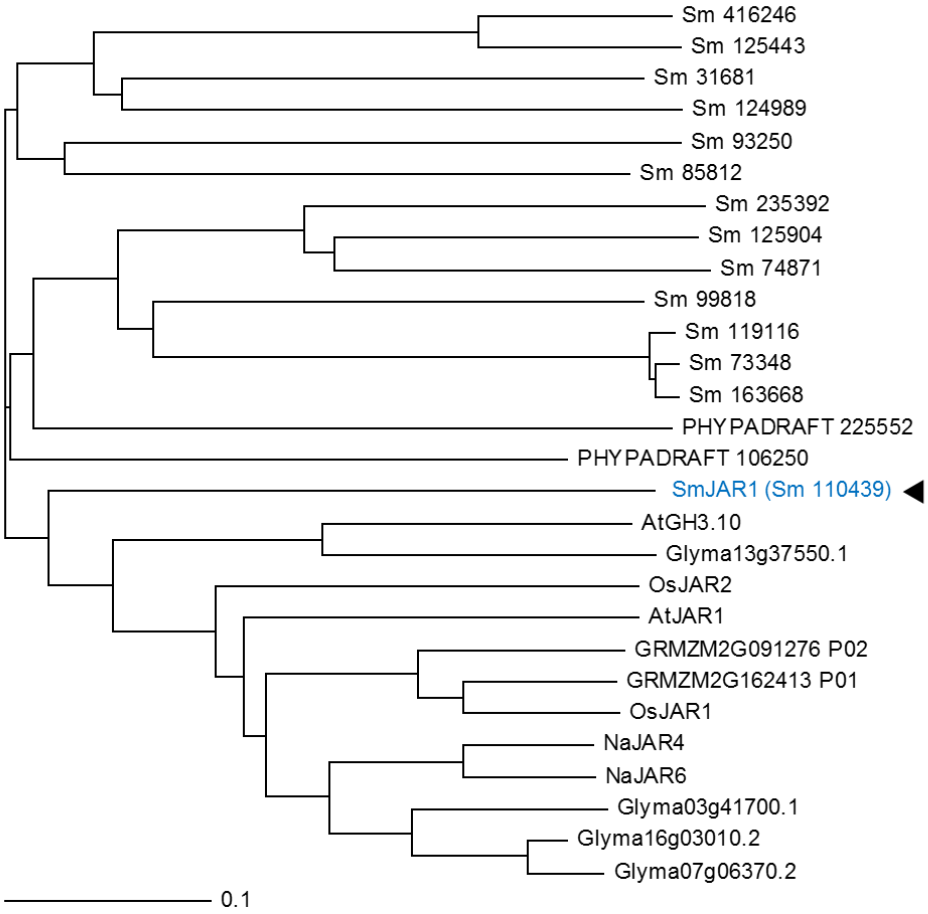

Fig. 26. Phylogenetic tree of JAR1 homologous proteins in *S. moellendorffii* with other JAR1s.

The tree was generated from amino acid alignment and constructed using Clustal Omega before visualizing with TreeView X program. The analysis was performed with the following: AtJAR1 (*Arabidopsis thaliana*, AEC10684), AtGH3.10 (*Arabidopsis thaliana*, At4g03400), OsJAR1, OsJAR2 (*Oryza sativa*, LOC_Os05g50890.1), OsJAR2 (*O. sativa*, LOC_Os01g12160.1), Glyma16g03010.2 (*Glycine max*), Glyma07g06370.2 (*G. max*), Glyma03g41700.1 (*G. max*), Glyma13g37550.1 (*G. max*), NaJAR4 (*Nicotiana attenuate*, ABC87760.1), NaJAR6 (*N. attenuate*, ABC87761.1), GRMZM2G091276_P02 (*Zea mays*), GRMZM2G162413_P01 (*Z. mays*), PHYPADRAFT_106250 (*Phsycomitrella patens*), and PHYPADRAFT_225552 (*P. patens*).

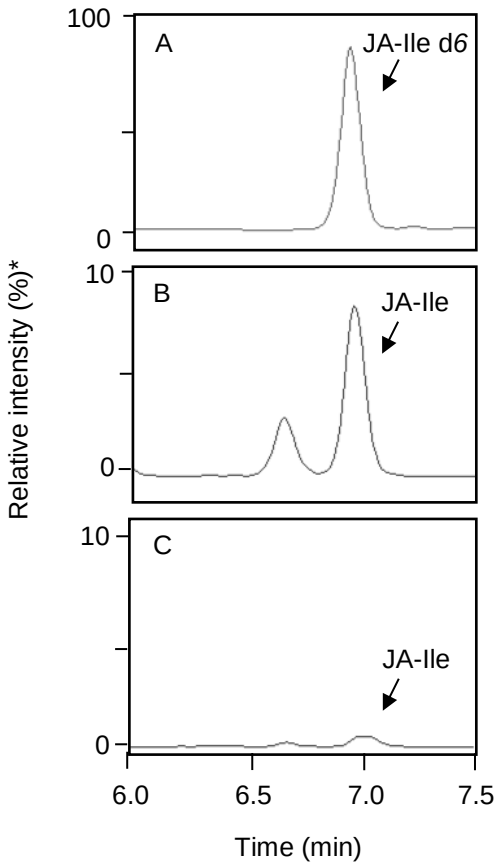

Fig. 27. UPLC-MS/MS analysis of JA-Ile in *E. coli* overexpressing SmJAR1.
MRM mode analysis of a specific daughter peak of JA-Ile-d_6 at *m/z* 129.68 that was derived from the peak at *m/z* 328.03 $[M-H]^-$ and of the peak at *m/z* 129.68 that was derived from the peak of JA-Ile at *m/z* 322.03 $[M-H]^-$. (A) Internal standard JA-Ile-d_6. (B) Culture supernatant of *E. coli* overexpressing SmJAR1. (C) Culture supernatant of *E. coli* containing pET23a as a control. *The value of 100% is equal to 9×10^5 counts, which was converted by the algorithm in Mass Lynx software (Waters Corporation, Milford, MA, USA).

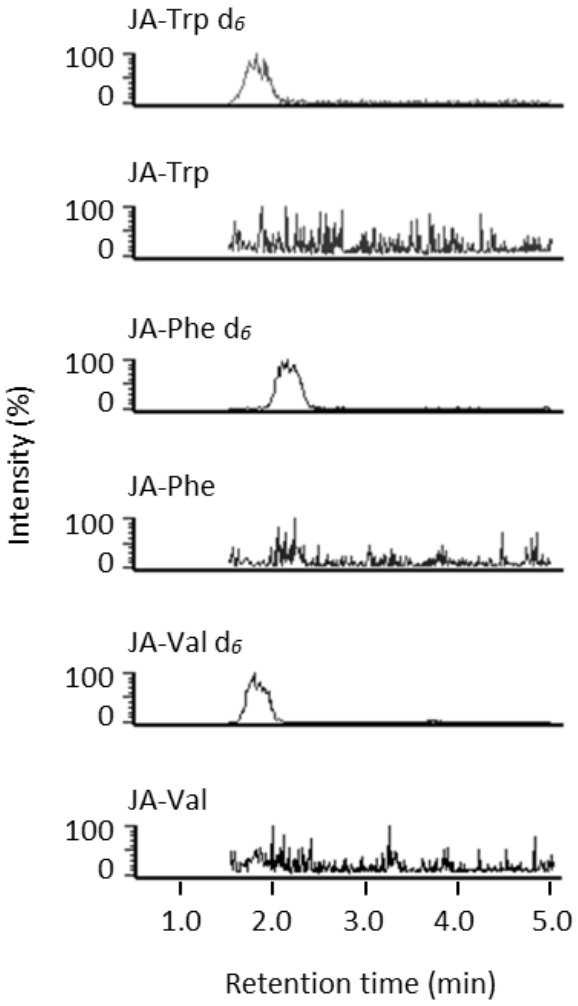

Fig. 28. UPLC-MS/MS analysis of conjugates of JA and amino acid (JA-Trp, JA-Phe, and JA-Val) in *S. moellendorffii*.
No obvious peak corresponding to JA-Trp, JA-Phe and JA-Val was detected in the extract of *S. moellendorffii*.

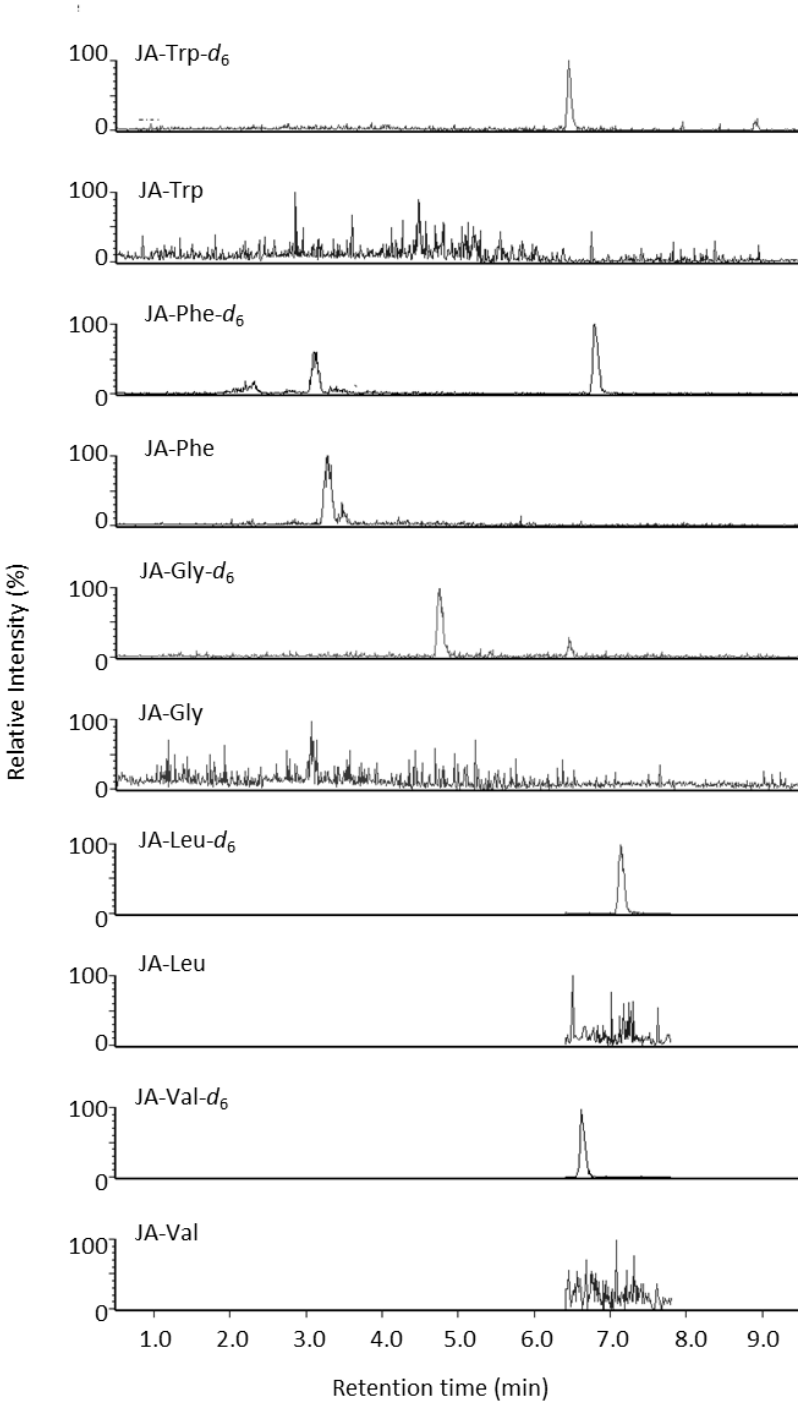

Fig. 29. UPLC-MS/MS analysis of endogenous JA conjugation with other amino acid (Trp, Phe, Gly, Leu, and Val) in wounded *S. moellendorffii*.
No obvious peak corresponding to JA-Trp, JA-Phe and JA-Val was detected in the extract of wounded *S. moellendorffii*.

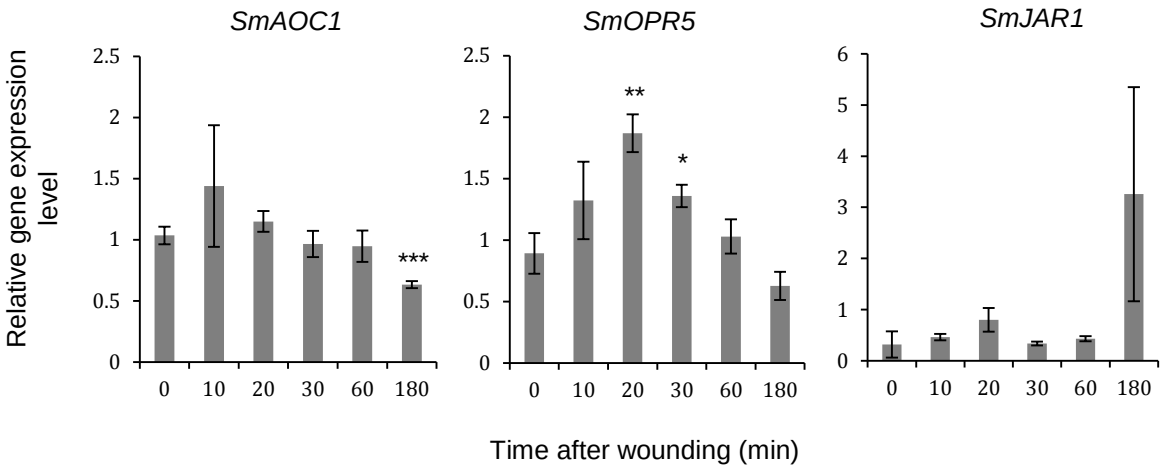

Fig. 30. Quantitative RT-PCR analysis of *SmAOC1*, *SmOPR5*, and *SmJAR1* in wounded *S. moellendorffii.*

Plants were subjected to mechanical wounding and then collected at the indicated times after wounding. To evaluate the transcript levels of *SmAOC1*, *SmOPR5*, and *SmJAR1*, qRT-PCR was performed using RNA isolated from control and wounded plants. The data are presented as the mean ± SD (n = 3). The asterisks represent a significant difference between the treated and control plants (Student's t test, $*p < 0.05$; $**p < 0.01$). Each target gene was calculated and expressed as fold regulation in comparison to the housekeeping actin gene (XM_002976966).

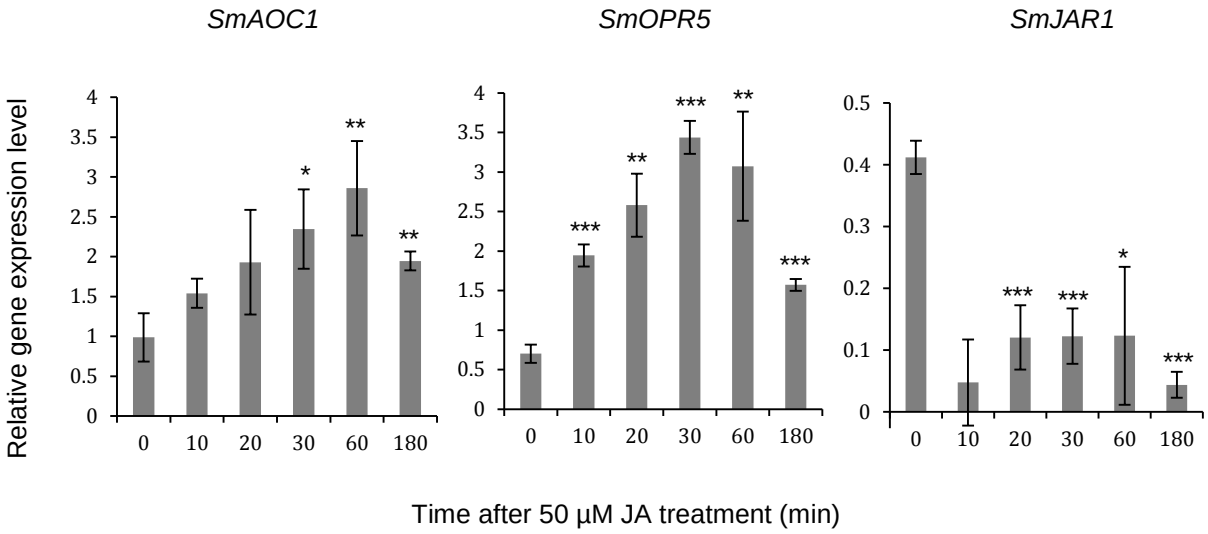

Fig. 31. Quantitative RT-PCR analysis of *SmAOC1*, *SmOPR5*, and *SmJAR1* in *S. moellendorffii* treated with JA.

Plants were treated with 50 μM JA and then collected at the indicated times after JA treatment. To evaluate the transcript levels of *SmAOC1*, *SmOPR5*, and *SmJAR1*, qRT-PCR was performed using RNA isolated from control and JA-treated plants. The data are presented as the mean ± SD (n = 3). The asterisks represent a significant difference between the treated and control plants (Student's t test, $*p < 0.05$; $**p < 0.01$; $***p < 0.001$). Each target gene was calculated and expressed as fold regulation in comparison to the housekeeping ubiquitin EST (DN839032).

3.3 Materials and methods

3.3.1 Bioinformatics analysis

All of the putative genes in *S. moellendorffii* were screened in the Phytozome v 11.0 database (https://phytozome.jgi.doe.gov/pz/portal.html) using the *Arabidopsis* amino acid sequence as a query (Table 2). Multiple sequence analysis was performed using Clustal Omega and viewed in the GeneDoc software program. A phylogenetic tree was generated using Mega version 5.2 (Neighbor-joining method). Bootstrap analysis was performed by resampling the datasets 1,000 times. The sub-cellular localization of *SmAOC1* was predicted using ChloroP v 1.1 (http://www.cbs.dtu.dk /services/ChloroP/) and TargetP (http://www.cbs.dtu.dk/services /TargetP/). The theoretical pI and molecular weight were analyzed using the Compute pI/Mw tool (http://web.expasy.org/compute_pi/) (Table 3).

3.3.2 SmAOS

3.3.2.1 Cloning of *SmAOS2*

Total RNA and cDNA of *S. moellendorffii* were obtained according to the method described in Chapter 7. The primer set of *SmAOS2*, SmAOS2-F and SmAOS2-R, was used to amplify the open reading frame (ORF) of *SmAOS2*. To afford the ORF of *SmAOS2*, the PCR reaction was performed in 50 μl per tube, containing 10 μl of dNTP mixture (2.0 mM each), 1 μl each from forward and reverse primer (5 μM), 0.5 μl of cDNA, 25 μl of 2 × PCR buffer, 0.5 μl of KOD FX DNA polymerase (Toyobo, Japan) and 12 μl of Milli-Q water under following conditions; pre-denaturation at 94°C for 2 min followed by 40 cycles of denaturing at 98°C for 10 s, annealing at 56°C for 30 s, and extension at 68°C for 1 min, and then a final extension at 68°C for 10 min. The obtained PCR product was purified and inserted into the pBlueScript SK II (+) vector

(Stratagene, USA), which was digested with *Eco*RV to obtain the plasmid of pSK-SmAOS2. DNA sequencing was performed to confirm that the target gene was successfully inserted into the plasmid. The primers used in this study are listed in Table 4.

3.3.2.2 Synthesis of a recombinant SmAOS2 in *E. coli*

The primer set for overexpression of SmAOS2 in *E. coli*, SmAOS2NdeI-F with *Nde*I site and SmAOS2XhoI-R with *Xho*I site was designed according to a *SmAOS2* sequence. PCR was performed in 15 µl of a reaction mixture containing 1.5 µl of dNTP mixture (2.0 mM each dNTP), 0.9 µl of 25 mM $MgSO_4$, 1.5 µl of KOD plus neo buffer (10 ×), 0.9 µl of each primer (SmAOS2NdeI-F and SmAOS2XhoI-R, 5 µM), 1 µl of pSK-SmAOS2 (200 ng/ µl), 0.3 µl of KOD plus neo DNA polymerase (Toyobo, Japan), and 8 µl of Milli-Q water. PCR was conducted with the following conditions: 2 min at 94°C for pre-denaturation; 30 cycles of 98°C for 10 s, 58°C for 30 s, and 68°C for 90 s and then final extension at 68°C for 10 min. The PCR product then was purified and ligated into pET23a vector (Merck, USA) using Ligation Mix (Takara, Japan) according to the standard procedure. The constructed plasmid, pET23a-SmAOS2, was transformed in *E. coli* BL21 (DE3) according to standard procedure and was subsequently grown in LB agar medium supplemented with 100 µg/ml of ampicillin. A single colony was inoculated into 10 ml of LB medium containing 100 µg/ml of ampicillin and then incubated at 37°C for overnight. A 10 ml aliquot was transferred into 1 l of LB medium containing 100 µg/ml of ampicillin and then incubated at 37°C until the OD_{600} reached 0.4, and then the sample was finally induced by 1 mM of IPTG for overnight at 25°C. The bacterial cells were collected by centrifugation at 5,000 × *g* for 20 min and lysed by ultrasonication in 50 mM phosphate buffer pH 7.8, 0.3 M NaCl,

and 20 mM imidazole. Cell debris was removed by centrifugation at 14,000 × *g* for 15 min. The supernatant was subjected to Ni-NTA agarose column chromatography (2 mL, GE Healthcare, USA). SmAOS2, fused with a His-tag, was eluted with 50 mM phosphate buffer (pH 7.8) containing 100 mM imidazole and 0.3 M NaCl. The resulting recombinant protein solution was dialyzed with 50 mM phosphate buffer (pH 7.8) containing 0.1 M NaCl. The purity was checked by SDS-PAGE (Fig. 11). The primers used in this study are listed in Table 4.

3.3.2.3 Enzyme assay of SmAOS2

To measure AOS activity, SmAOS2 was reacted with 13(*S*)-HPOT according to Bandara et al. (2009) with some modifications. Five milligrams of recombinant SmAOS2 was reacted with 6 μg of 13(*S*)-HPOT as a substrate in a total volume of 0.1 ml of 50 mM phosphate buffer (pH 7.0). The reaction mixture was incubated at 25°C for 1 h. To terminate the enzymatic reaction, the mixture was treated with 1 M HCl until it reached pH 3. To convert *cis*-OPDA to *trans*-OPDA, the reaction mixture was subjected to alkaline treatment by stirring with 1 ml of 1 M NaOH for 30 min. After acidification, the resulting solution was extracted three times with an identical volume of ethyl acetate, evaporated, and methylated using ethereal diazomethane. After incubation for 30 min on ice, the reaction was terminated with the addition of 1 or 2 drops of acetic acid until the color changed from yellow to colorless. The methylated residue was dissolved in 100 μl of $CHCl_3$ for chiral GC-MS analysis (1200 L GC-MS/MS system, Varian, USA) equipped with a β–DEX fused silica capillary column (0.25 mm × 30 m × 0.25 μm, Supelco, USA). Helium was used as the carrier gas at a constant flow rate of 1.0 ml/min. The ion source and vaporizing chamber were heated to 200°C and 220°C, respectively, and the ionization voltage was 70 eV. The column was

initially heated to 50°C and held isothermally for 1 min, and then the temperature was subsequently increased at a rate of 10°C/min to a final temperature of 190°C, which was held for 80 min.

3.3.3 SmAOC

3.3.3.1 Cloning of *SmAOC1*

Total RNA and cDNA of *S. moellendorffii* were obtained according to the method described in Chapter 7. Full length cDNA of *SmAOC1* (Sm_91887) was obtained with 5'-Full RACE Core Set according to the manufacturer's instructions (see Chapter 7). Subsequently, the primer set of *SmAOC1*, SmAOC1-F and SmAOC1-R, was used to amplify the ORF of *SmAOC1*. The PCR reaction was performed in 50 μl per tube, containing 10 μl of dNTP mixture (2.0 mM each), 1 μl each from forward and reverse primer (5 μM), 0.5 μl of cDNA, 25 μl of 2 × PCR buffer, 0.5 μl of KOD FX DNA polymerase (Toyobo, Japan) and 12 μl of Milli-Q water under following conditions: pre-denaturation at 94°C for 2 min followed by 40 cycles of denaturing at 98°C for 10 s, annealing at 55°C for 30 s, and extension at 68°C for 1 min, and then a final extension at 68°C for 10 min. The obtained PCR product was purified and inserted into the pBlueScript SK II (+) vector (Stratagene, USA), which was digested with *Eco*RV to obtain the plasmid of pSK-SmAOC1. DNA sequencing was performed to confirm that the target gene was successfully inserted into the plasmid. The primers used in this study are listed in Table 4.

3.3.3.2 Synthesis of a recombinant SmAOC1 in *E. coli*

ChloroP v 1.1 and TargetP predicted that the fifty amino acids at the N-terminus of SmAOC1 was a chloroplast transit peptide. The primer set for overexpression of

SmAOC1, SmAOC1SphI-F with *Sph*I site and SmAOC1SalI-R with *Sal*I site, in *E. coli* was designed according to a *SmAOC1* sequence, which had 150 nucleotides deleted from the codon for the first methionine. PCR was performed in 15 µl of a reaction mixture containing 1.5 µl of dNTP mixture (2.0 mM each dNTP), 0.9 µl of 25 mM $MgSO_4$, 1.5 µl KOD plus neo buffer (10 ×), 0.9 µl of each primer (SmAOC1SphI-F and SmAOC1SalI-R, 5 µM), 1 µl of pSK-SmAOC1 (200 ng/ µl), 0.3 µl of KOD plus neo DNA polymerase (Toyobo, Japan), and 8 µl of Milli-Q water. PCR was conducted with the following conditions: 2 min at 94°C for pre-denaturation; 30 cycles of 98°C for 10 s, 60°C for 30 s, and 68°C for 90 s and then final extension at 68°C for 10 min. The PCR product was then purified and ligated into pQE30 vector (Qiagen, USA) using T4 DNA ligase according to the standard procedure. The constructed plasmid, pQE30-SmAOC1, was transformed in *E. coli* M15 according to a standard procedure and was subsequently grown in LB agar medium supplemented with 100 µg/ml of ampicillin.

A single colony was inoculated into 10 ml of LB medium containing 100 µg/ml of ampicillin and then incubated at 37°C for overnight. A 10 ml aliquot was transferred into 1 l of LB medium containing 100 µg/ml of ampicillin and then incubated at 25°C until the OD_{600} reached 0.5, the sample was finally induced by 0.2 mM of IPTG for 4 h at 25°C. The bacterial cells were collected by centrifugation at 7,000 × *g* for 20 min and lysed by ultrasonication in 50 mM phosphate buffer pH 7.8, 0.3 M NaCl, and 20 mM imidazole. Cell debris was removed by centrifugation at 15,000 × *g* for 15 min; then, the supernatant was subjected to Ni-NTA agarose column chromatography (2 ml, GE Healthcare, USA). SmAOC1, fused with a His-tag, was eluted with 50 mM phosphate buffer (pH 7.8) containing 200 mM imidazole and 0.3 M NaCl. The resulting recombinant protein solution was dialyzed with 50 mM Tris-HCl (pH 8.0) containing 20 mM NaCl. The purity was checked by SDS-PAGE (Fig. 11). The dialyzed product

was concentrated using Amicon Ultra-15 Centrifugal Filter Device 10K (Merck Millipore Ltd., Germany) and then used for evaluation of enzymatic activity. The primers used in this study are listed in Table 4.

3.3.3.3 Subcellular localization of SmAOC1

To analyze the localization of SmAOC1, PCR was performed using primers, SmAOC1NdeI-F and SmAOC1EcoRV-R, with *Nde*I and *Eco*RV restriction sites, respectively. The PCR reaction mixture contained 1.5 µl of dNTP mixture (2.0 mM each dNTP), 0.9 µl of 25 mM $MgSO_4$, 1.5 µl of KOD plus neo buffer (10 ×), 0.9 µl of each primer (5 µM), 1 µl of pSK-SmAOC1 (200 ng/µl), 0.3 µl of KOD plus neo DNA polymerase (Toyobo, Japan), and an adjusted Milli-Q water level up to a volume of 15 µ1. PCR was conducted for 2 min at 94°C for pre-denaturation; 30 cycles of 98°C for 10 s, 60°C for 30 s, and 68°C for 90 s; final extension was performed at 68°C for 10 min. The PCR product was ligated into the pENTR4 vector using GeneArt Seamless Cloning and Assembly Kit (Invitrogen, USA). The pENTR4-SmAOC1 entry clone was introduced into the pUGWnew5 destination vector by Gateway LR Clonase Mix (Invitrogen, USA) to generate the plasmid encoding 35S::SmAOC1-GFP (pUGWnew5-SmAOC1). The constructed plasmid of 35S::SmAOC1-GFP was transformed into protoplasts of *P. patens*, which were grown in BCDATG medium for 3 days under white fluorescent light using the PEG-mediated transformation technique. Localization of the SmAOC1-GFP fusion protein was observed under a TCS-SP5 confocal laser scanning microscope (Leica, Germany) after 3 days incubation. Images were observed at an excitation of 488 nm and emission of 530 nm for detecting the GFP signal as well as emission over 655 nm for detecting auto-fluorescence from the chloroplasts. The primers used in this study are listed in Table 4.

3.3.3.4 Enzyme assay of SmAOC1 activity

The enzymatic reaction was performed in a mixture of 5 μg of 13-HPOT and 5 μg of PpAOS1 in 1 ml of 10 mM sodium phosphate buffer (pH 7.8) with or without 10 μg of SmAOC1. The reaction mixture was incubated at 25°C for 1 h. The products of the SmAOC1 reaction were analyzed according to the method of OPDA analysis described in the previous section.

3.3.4 SmOPR

3.3.4.1 Cloning of *SmOPR1*

Total RNA and cDNA of *S. moellendorffii* were obtained according the method described in Chapter 7. The primer set of *SmOPR1*, SmOPR1-F and SmOPR1-R, was used to amplify the ORF of *SmOPR1*. To afford the ORF of *SmOPR1*, the PCR reaction was performed in 50 μl per tube, containing 10 μl of dNTP mixture (2.0 mM each), 1 μl each from forward and reverse primer (5 μM), 0.5 μl of cDNA, 25 μl of 2 × PCR buffer, 0.5 μl of KOD FX DNA polymerase (Toyobo, Japan) and 12 μl of Milli-Q water under following conditions; pre-denaturation at 94°C for 2 min followed by 40 cycles of denaturing at 98°C for 10 s, annealing at 60°C for 30 s, and extension at 68°C for 1 min, and then a final extension at 68°C for 10 min. The obtained PCR product was purified and inserted into the pBlueScript SK II (+) vector (Stratagene, USA), which was digested with *Eco*RV to obtain the plasmid of pSK-SmOPR1. DNA sequencing was performed to confirm that the target gene was successfully inserted into the plasmid. The primers used in this study are listed in Table 4.

3.3.4.2 Synthesis of a recombinant SmOPR1 in *E. coli*

The primer set for overexpression of SmOPR1, SmOPR1EcoRI-F with *Eco*RI site and SmOPR1NotI-R with *Not*I site, in *E. coli* was designed according to a *SmOPR1* sequence. PCR was performed in 15 µl of a reaction mixture containing 1.5 µl of dNTP mixture (2.0 mM each dNTP), 0.9 µl of 25 mM $MgSO_4$, 1.5 µl of KOD plus neo buffer (10 ×), 0.9 µl of each primer (SmOPR1EcoRI-F and SmOPR1NotI-R, 5 µM), 1 µl of pSK-SmOPR1 (200 ng/ µl), 0.3 µl of KOD plus neo DNA polymerase (Toyobo, Japan), and 8 µl of Milli-Q water. PCR was conducted with the following conditions: 2 min at 94°C for pre-denaturation; 30 cycles of 98°C for 10 s, 60°C for 30 s, and 68°C for 90 s and then final extension at 68°C for 10 min. The PCR product then was purified and ligated into pET23a vector (Merck, USA) using Ligation Mix (Takara, Japan) according to the manufacturer's instruction. The constructed plasmid, pET23a-SmOPR1, was transformed in *E. coli* BL21 (DE3) according to standard procedure and was subsequently grown in LB agar medium supplemented with 100 µg/ml of ampicillin.

A single colony was inoculated into 10 ml of LB medium containing 100 µg/ml of ampicillin and then incubated at 37°C for overnight. A 10 ml aliquot was transferred into 1 l of LB medium containing 100 µg/ml of ampicillin and then incubated at 25°C until the OD_{600} reached 0.4; the sample was finally induced by 1 mM of IPTG for overnight at 18°C. The bacterial cells were collected by centrifugation at 7,000 × *g* for 20 min and lysed by ultrasonication in 50 mM phosphate buffer pH 7.4, 0.3 M NaCl, and 20 mM imidazole. Cell debris was removed by centrifugation at 15,000 × *g* for 15 min; then, the supernatant was subjected to Ni-NTA agarose column chromatography (2 mL, GE Healthcare, USA). SmOPR1, fused with a His-tag, was eluted with 50 mM phosphate buffer (pH 7.4) containing 200 mM imidazole and 0.3 M NaCl. The resulting recombinant protein solution was dialyzed with 50 mM Tris-HCl (pH 7.8) containing

20 mM NaCl. The purity was checked by SDS-PAGE (Fig. 11). The dialyzed product was concentrated using Amicon Ultra-0.5ml Centrifugal Filter Units 30K and 50K (Merck Millipore Ltd., Germany) and then used for evaluation of enzymatic activity. The primers used in this study are listed in Table 4.

3.3.4.3 Cloning of *SmOPR5*

Total RNA and cDNA of *S. moellendorffii* were obtained according the method described in Chapter 7. The primer set of *SmOPR5*, SmOPR5-F and SmOPR5-R, was used to amplify the ORF of *SmOPR5*. To afford the ORF of *SmOPR5*, the PCR reaction was performed in 50 μl per tube, containing 10 μl of dNTP mixture (2.0 mM each), 1 μl each from forward and reverse primer (5 μM), 0.5 μl of cDNA, 25 μl of 2 × PCR buffer, 0.5 μl of KOD FX DNA polymerase (Toyobo, Japan) and 12 μl of Milli-Q water under following conditions; pre-denaturation at 94°C for 2 min followed by 40 cycles of denaturing at 98°C for 10 s, annealing at 60°C for 30 s, and extension at 68°C for 1 min, and then a final extension at 68°C for 10 min. The obtained PCR product was purified and inserted into the pBlueScript SK II (+) vector (Stratagene, USA), which was digested with *Eco*RV to obtain the plasmid of pSK-SmOPR5. DNA sequencing was performed to confirm that the target gene was successfully inserted into the plasmid. The primers used in this study are listed in Table 4.

3.3.4.4 Synthesis of a recombinant SmOPR5 in *E. coli*

The primer set for overexpression of SmOPR5, SmOPR5BamHI-F with *Bam*HI site and SmOPR5XhoI-R with *Xho*I site, in *E. coli* was designed according to a *SmOPR5* sequence. PCR was performed in 15 μl of a reaction mixture containing 1.5 μl of dNTP mixture (2.0 mM each dNTP), 0.9 μl of 25 mM $MgSO_4$, 1.5 μl of KOD plus

neo buffer (10 ×), 0.9 µl of each primer (SmOPR5BamHI-F and SmOPR5XhoI-R, 5 µM), 1 µl of pSK-SmOPR5 (200 ng/ µl), 0.3 µl of KOD plus neo DNA polymerase (Toyobo, Japan), and 8 µl of Milli-Q water. PCR was conducted with the following conditions: 2 min at 94°C for pre-denaturation; 30 cycles of 98°C for 10 s, 60°C for 30 s, and 68°C for 90 s and then final extension at 68°C for 10 min. The PCR product then was purified and ligated into pET23a vector (Merck, USA) using In-Fusion HD Cloning Kit (Takara, Japan) according to the manufacturer's instruction. The constructed plasmid, pET23a-SmOPR5, was transformed in *E. coli* BL21 (DE3) according to standard procedure and was subsequently grown in LB agar medium supplemented with 100 µg/ml of ampicillin.

A single colony was inoculated into 10 ml of LB medium containing 100 µg/ml of ampicillin and then incubated at 37°C for overnight. A 10 ml aliquot was transferred into 1 l of LB medium containing 100 µg/ml of ampicillin and then incubated at 25°C until the OD_{600} reached 0.4; the sample was finally induced by 1 mM of IPTG for overnight at 18°C. The bacterial cells were collected by centrifugation at 7,000 × *g* for 20 min and lysed by ultrasonication in 50 mM phosphate buffer pH 7.4, 0.3 M NaCl, and 20 mM imidazole. Cell debris was removed by centrifugation at 15,000 × *g* for 15 min; then, the supernatant was subjected to Ni-NTA agarose column chromatography (2 mL, GE Healthcare, USA). SmOPR5, fused with a His-tag, was eluted with 50 mM phosphate buffer (pH 7.4) containing 200 mM imidazole and 0.3 M NaCl. The resulting recombinant protein solution was dialyzed with 50 mM Tris-HCl (pH 7.8) containing 20 mM NaCl. The purity was checked by SDS-PAGE (Fig. 11). The dialyzed product was concentrated using Amicon Ultra-0.5mL Centrifugal Filter Units 30K and 50K (Merck Millipore Ltd., Germany) and then used for evaluation of enzymatic activity. The primers used in this study are listed in Table 4.

3.3.4.5 Enzyme assays for OPR activity

The enzymatic reaction was performed according to the method of Schaller et al. (1998) with some modifications. Five micrograms of affinity-purified recombinant SmOPR1 or SmOPR5 was incubated in 50 mM potassium phosphate buffer (pH 7.4) containing 7.5 μg of (±)-*cis*-OPDA as a substrate and 1.0 mM NADPH in a total volume of 0.1 ml for 1 h at 25°C. At the end of the incubation, (±)-*cis*-OPDA and (±)-*cis*-OPC-8:0 were converted to methylated *trans*-isomers according to the method described above. OPC-8:0 was evaluated by chiral GC-MS analysis (same conditions as the enzymatic analysis for SmAOC1).

3.3.5 SmJAR1

3.3.5.1 Cloning of *SmJAR1*

Total RNA and cDNA of *S. moellendorffii* were obtained according the method described in Chapter 7. The primer set of *SmJAR1*, SmJAR1-F and SmJAR1-R, was used to amplify the ORF of *SmJAR1*. To afford the ORF of *SmJAR1*, the PCR reaction was performed in 50 μl per tube, containing 10 μl of dNTP mixture (2.0 mM each), 1 μl each from forward and reverse primer (5 μM), 0.5 μl of cDNA, 25 μl of 2 × PCR buffer, 0.5 μl of KOD FX DNA polymerase (Toyobo, Japan) and 12 μl of Milli-Q water under following conditions; pre-denaturation at 94°C for 2 min followed by 40 cycles of denaturing at 98°C for 10 s, annealing at 60°C for 30 s, and extension at 68°C for 1 min, and then a final extension at 68°C for 10 min. The obtained PCR product was purified and inserted into the pBlueScript SK II (+) vector (Stratagene, USA), which was digested with *Eco*RV to obtain the plasmid of pSK-SmJAR1. DNA sequencing was

performed to confirm that the target gene was successfully inserted into the plasmid. The primers used in this study are listed in Table 4.

3.3.5.2 Construction of *E. coli* transferred with an overexpression vector of *SmJAR1*

The primer set for overexpression of SmJAR1, SmJAR1BamHI-F with *Bam*HI site and SmJAR1XhoI-R with *Xho*I site, in *E. coli* was designed according to a *SmJAR1* sequence. PCR was performed in 15 µl of a reaction mixture containing 1.5 µl of dNTP mixture (2.0 mM each dNTP), 0.9 µl of 25 mM $MgSO_4$, 1.5 µl of KOD plus neo buffer (10 ×), 0.9 µl of each primer (SmJAR1BamHI-F and SmJAR1XhoI-R, 5 µM), 1 µl of pSK-SmJAR1 (200 ng/ µl), 0.3 µl of KOD plus neo DNA polymerase (Toyobo, Japan), and 8 µl of Milli-Q water. PCR was conducted with the following conditions: 2 min at 94°C for pre-denaturation; 30 cycles of 98°C for 10 s, 60°C for 30 s, and 68°C for 90 s and then final extension at 68°C for 10 min. The PCR product then was purified and ligated into pET23a vector (Merck, USA) using In-Fusion HD Cloning Kit (Takara, Japan) according to the manufacturer's instruction. The constructed plasmid, pET23a-SmJAR1, was transformed in *E.coli* BL21 (DE3) according to standard procedure. The resultant strain was used for an assay of JA-Ile synthetic activity. The primers used in this study are listed in Table 4.

3.3.5.3 Enzyme assays for JAR1 activity

SmJAR1 activity was assayed according to Wakuta et al. (2011) with some modifications. *E. coli* BL21 (DE3) cells carrying pET23a-SmJAR1 were cultured overnight in 5 ml of LB medium with 100 µg/ml of ampicillin at 37°C. A portion of the culture was inoculated into 2 ml of fresh selective LB medium, incubated until the OD_{600} reached 0.2, and treated with 1 mM IPTG. The culture was incubated at 37°C for

5 h to induce protein production. Subsequently, 0.2 mM JA was added to the culture. The incubation was continued at 37°C for 3 h with shaking. JA-Ile in the culture was analyzed using the UPLC-MS/MS system as previously described (Sato et al. 2009).

3.3.6 Quantitative RT-PCR for *SmAOC1*, *SmOPR5*, and *SmJAR1* in *S. moellendorffii* subjected to wounding stress and JA treatments

The coding sequences (CDSs) for *SmAOC1*, *SmOPR5*, and *SmJAR1* were used to design specific primers for quantitative RT-PCR (qRT-PCR). The primers used to amplify these genes are listed in Table 4. Total RNA of *S. moellendorffii* was extracted 0, 10, 20, 30, 60, and 180 min after wounding or 50 µM JA treatment. The first-strand cDNA was used as a template. In the present study, KOD SYBR® qPCR Mix (Toyobo, Japan) was used according to the manufacturer's protocol. Each reaction mixture contained 12.5 µl of KOD SYBR® qPCR Mix, 1 µl of each primer (10 mM), 1 µl of cDNA, and 9.5 µl of MilliQ water qRT-PCR was performed on a Thermal Cycler Dice Real Time system (Takara TP800, Japan). The qRT-PCR conditions were as follows: pre-incubation at 95°C for 30 s, followed by 40 cycles of 95°C for 5 s and 60°C for 30 s. The specificity of each PCR amplicon was assessed with a dissociation curve (95°C for 15 s, 60°C for 30 s, and 95°C at 15 s). Each target gene was calculated and expressed as fold regulation in comparison to the housekeeping genes, an actin gene (XM_002976966) for the wounding treatment and a ubiquitin EST (DN839032, Kirkbride et al. 2013) for the JA treatment.

CHAPTER 4

EFFECT OF EXOGENOUSLY APPLIED JASMONATES ON THE GROWTH OF *S. MOELLENDORFFII*

4.1 Introduction

Terrestrial plants potentially got injured or destroyed from environmental conditions thus threaten their survival. Jasmonates are crucial compounds as a signaling molecule in regulating these dynamic and adaptive responses. Among other jasmonates, OPDA, JA, and JA-conjugated isoleucine (JA-Ile) are widespread in the plant kingdom. However, the different group of plants occupies different jasmonates derivatives to activate the response genes related to plant growth and fitness (Weiler et al. 1993; Stelmach et al. 1998; Stintzi and Browse 2000; Staswick and Tiryaki 2004). To understand how specific chemical forms of this hormone affect the plant development, this chapter describes the responds of *S. moellendroffii* upon various forms of jasmonates. It is important to distinguish the identity of specific component that acts as a signal signature in *S. moellendorffii* as a basal vascular plant model.

4.2 Results and discussion

4.2.1 Effect of exogenous OPDA, JA, and JA-Ile on the growth of *S. moellendorffii* shoots

Growth inhibition caused by exogenously applied JA is one of the most significant physiological responses in seed plants. To examine the ability of OPDA, JA, and JA-Ile to inhibit the growth of *S. moellendorffii*, bulbils of *S. moellendorffii* (Fig. 6) were sprinkled onto soil, and the germinated plants were grown with or without treatment with OPDA, JA, or JA-Ile at concentrations of 25, 50, and 100 µM. After four

weeks, the lengths of the shoots of *S. moellendorffii* were measured. All jasmonates tested in this study were shown to have growth inhibitory effects on shoots of *S. moellendorffii* (Fig. 32). Both OPDA and JA inhibited growth in a dose-dependent manner, with a stronger effect with OPDA than with JA. JA-Ile also retarded the growth of the shoots of this plant, but the growth inhibitory effect did not depend on the concentrations of JA-Ile. This is the first report that OPDA, JA, and JA-Ile inhibit the growth of seedless vascular plants, such as lycophytes.

P. patens and *M. polymorpha* cannot produce JA, and JA does not induce any significant physiological responses; instead, OPDA inhibits their growth and elevates the expression of genes encoding enzymes in the octadecanoid pathway such as AOS and AOC (Stumpe et al. 2010; Yamamoto et al. 2015). However, *P. patens* responds to methyl jasmonate, which has not been detected in *P. patens*, to show reducing its colony size (Ponce de León et al. 2012). Many studies have reported the growth inhibitory activity of JA in seed plants (Avanci et al. 2010). OPDA, JA, and JA-Ile treatment retarded the growth of *S. moellendorffii* in a manner similar to that of seed plants (Figs. 32 and 33). This study provides the first evidence that JA and JA-Ile inhibit the growth of non-seed vascular plants. The growth inhibitory activity of JA and JA-Ile is probably a characteristic physiological response that is conserved in vascular plants. During plant evolution, JA biosynthesis and signaling in vascular plants might have developed due to the need of adaption to continue living on land and/or to organize more complicated physiological processes.

Recently, it has been reported that the genes encoding proteins homologous to COI1 and JAZ, which are essential for JA signaling system, are present in bryophytes and lycophytes (Wang et al. 2015). Since exogenously applied JA inhibited the growth of *S. moellendorffii*, it was likely that JA functions through a signal transduction

mechanism similar to the COI1-JAZ system in seed plants. Given that JA does not have any significant effect in Bryophytes, vascular plants may have developed the COI1-JAZ system, which is suitable for JA signaling. Investigation of the functional difference in the COI1-JAZ system between bryophytes and lycophytes is important for understanding the functional evolution of JA signal transduction in plants. *S. moellendorffii* will be a key plant for understanding the function of JA in vascular plants.

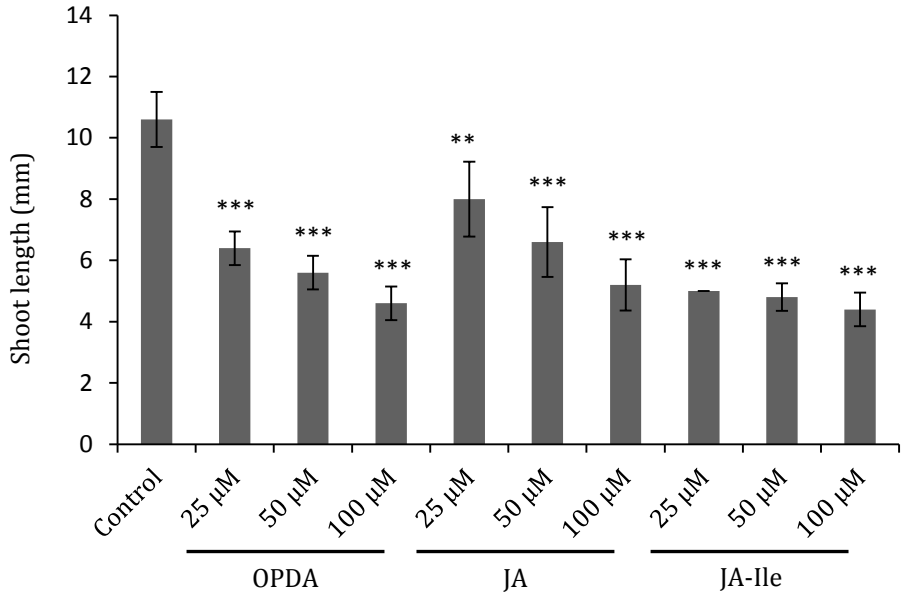

Fig. 32. Growth inhibitory activities of OPDA, JA, and JA-Ile in *S. moellendorffii*. *S. moellendorffii* was treated with OPDA, JA, and JA-Ile for four weeks, and then the length of shoots were measured. The data are presented as the mean ± SD (n= 5). The asterisks represent a significant difference between the treated and control plants (Student's t test, $^{**}p < 0.01$; $^{***}p < 0.001$).

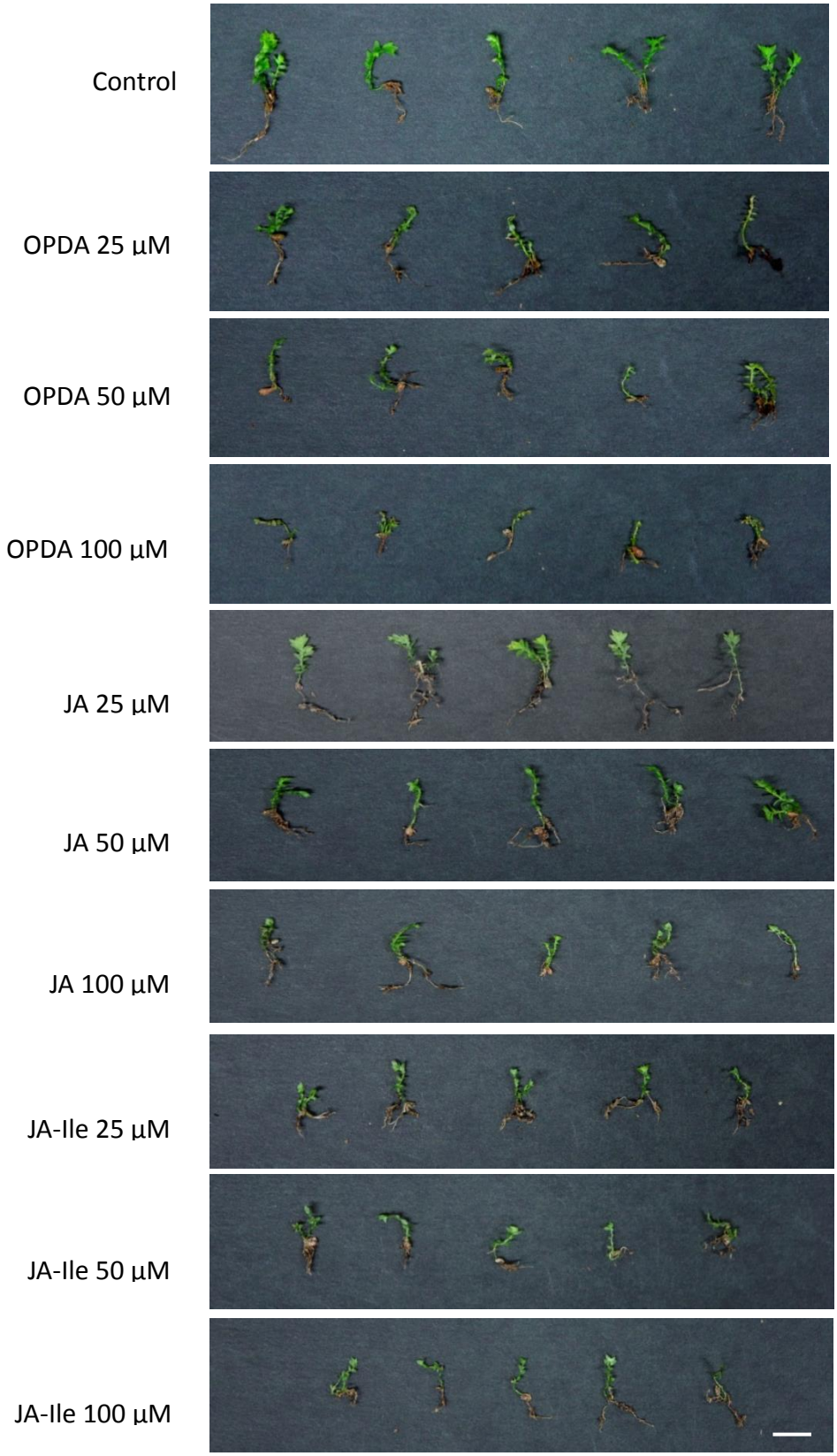

Fig. 33. Growth inhibitory activities of OPDA, JA, and JA-Ile in *S. moellendorffii*. *S. moellendorffii* was treated with OPDA, JA, or JA-Ile at concentration of 25, 50, and 100 μM.

4.3 Materials and methods

4.3.1 Assay of growth inhibitory activity in *S. moellendorffii*

S. moellendorffii bulbils (Fig. 6) were sprinkled onto a Jiffy-7 pellet (Sakata Seed Corporation, Japan). The bulbils were grown at 25°C under white fluorescent light with a photoperiod of 14 h light/10 h dark. After germination and one week of growth, each germinated plants were treated with applying a drop (± 50-100 µl) of OPDA, JA, or JA-Ile solution at concentrations of 25 µM, 50 µM, and 100 µM every other day for four weeks. The shoot growth of the plants was evaluated by morphometric analysis.

CHAPTER 5

JASMONOYL-ISOLEUCINE CATABOLISM

5.1 Introduction

JA-Ile functions as a signal molecule to induce formation of COI1-JAZ co-receptor complex to control JA-response genes. In the presence of JA-Ile, COI1 receptor interacts with JAZ protein and leads to the ubiquitination and degradation by 26S proteasome, resulting to de-repression of transcription of target genes. To maintain physiological action of JA-Ile, attenuation of JA-Ile is important to keep a homeostasis level when the stress levels have subsided. JA and JA-Ile probably play an important role in JA-dependent mediated responses against wounding stresses in *S. moellendorffii*. SmJAR1, which catalyzes the conjugation of JA with Ile, was also shown in previous chapter. Thus, this chapter reports the identification of 12-hydroxyJA-Ile (12-OH-JA-Ile) as well as a wound-induced gene that encodes JA-Ile-12-hydroxylase as the catabolism product to inactivate JA-Ile in *S. moellendorffii*.

5.2 Results and discussion

5.2.1 Identification of 12-OH-JA-Ile and 12-COOH-JA-Ile

The bioactive JA-Ile as one of JA derivatives is converted by the action of JAR1 enzyme that conjugate JA to isoleucine. The conjugated molecules, JA-Ile, then will be perceived by COI1-JAZ receptor leading to de-repressing JA-responsive genes transcription. Two JA-Ile derivatives, 12-OH-JA-Ile and 12-carboxyJA-Ile (12-COOH-JA-Ile) are known as inactive forms of JA-Ile and already have been well studied in *Arabidopsis*. Here, 12-OH-JA-Ile and 12-COOH-JA-Ile in wounded *S. moellendorffii* extract were analyzed by UPLC-MS/MS. The analytical data of 12-OH-JA-Ile (*m/z*

129.7 derived from the peak at *m/z* 338.3 $[M-H]^-$) showed that predominant peaks at a retention time of 5.39 min in standard, *S. moellendorffii* product, and co-injection were overlapped (Figs. 34A, 34B, and 34C). The analytical data of 12-COOH-JA-Ile demonstrated the peak at the same retention time of 5.49 min in standard, *S. moellendorffii* product, and a mixed sample of standard and *S. moellendorffii* product (*m/z* 129.7 that was derived from the peak at *m/z* 352.24 $[M-H]^-$; Figs. 34D, 34E, and 34F). These data revealed that *S. moellendorffii* metabolized JA-Ile into 12-OH-JA-Ile and 12-COOH-JA-Ile.

.

5.2.2 Kinetic analysis of wound-induced accumulation of 12-OH-JA-Ile

12-OH-JA-Ile is accumulated in damaged leaf of *Arabidopsis* as a response to mechanical wounding (Kitaoka et al. 2011; Koo et al. 2011). To examine whether wounding induces the accumulation of 12-OH-JA–Ile in a similar manner to flowering plants, the endogenous amount of 12-OH-JA-Ile in wounded microphylls of *S. moellendorffii* were analyzed by UPLC-MS/MS. *S. moellendorffii* were wounded by tweezer and the damaged microphylls were harvested after 0, 1, 3, 5, and 7 h. The results showed that the concentrations of 12-OH-JA-Ile were significantly elevated at 7 h after wounding (Fig. 35). It was suggested that 12-OH-JA-Ile is an inactive form in JA signaling pathway in *S. moellendorffii* as well as flowering plants.

5.2.3 Application of 12-OH-JA-Ile to *S. moellendorffii*

Previous study of *Arabidopsis* by Koo et al. (2011) showed that 12-OH-JA-Ile is an inactive form of JA-Ile because 12-OH-JA-Ile cannot prompt to form COI1-JAZ complex, which is essential to JA signal transduction. Therefore, 12-OH-JA-Ile does not show JA activity such as growth inhibitory activity in *Arabidopsis*. In previous

section, JA and JA-Ile were indicated to suppress the growth of *S. moellendorffii*. To examine whether 12-OH-JA-Ile is also an inactive form of JA-Ile in *S. moellendorffii*, the growth inhibitory activity of 12-OH-JA-Ile was evaluated in *S. moellendorffii*. The result revealed that 12-OH-JA-Ile inhibited the growth of *S. moellendorffii* much less than JA-Ile (Fig. 36). Therefore, 12-OH-JA-Ile in *S. moellendorffii* was shown to be an inactive form of JA-Ile as well as that in *Arabidopsis*. The weak activity of 12-OH-JA-Ile may be caused by the lower affinity of 12-OH-JA-Ile to act as a ligand to COI1-JAZ receptor compared to JA-Ile (Koo et al. 2011). Thus, weak signal stimulated by 12-OH-JA-Ile seems to increase JA-responsive genes expression slightly. Interestingly, phenotypic analysis of *S. moellendorffii* treated with 12-OH-JA-Ile indicated that 12-OH-JA-Ile promoted the development of two microphylls from a bulbis in *S. moellendorffii* (Fig. 37). This phenomenon was not found in JA-Ile treated plants. It is likely that the double emergence of microphylls is a specific activity of 12-OH-JA-Ile in *S. moellendorffii*. There is a possibility that 12-OH-JA-Ile has its own signaling system to induce the formation of double microphylls in *S. moellendorffii*.

5.2.4 Functional analysis of CYP94J1 and CYP94J2

Transient accumulation of JA-Ile in response to wounding stresses implies the existence of pathway to remove and/or inactivate JA-Ile. The known pathway in catabolism of JA-Ile is oxidation of JA-Ile into 12-OH-JA-Ile, which is catalyzed by CYP94B3 in *Arabidopsis* (Kitaoka et al. 2011; Koo et al. 2011). Moreover, this reaction is considered to be important to adjust JA-Ile concentration in *Arabidopsis* where JA activity is properly controlled in physiological steps for stress adaptation and development process. In *Arabidopsis*, CYP86 clan consists of four CYP families. The CYP86, CYP94, and CYP704 families are conserved in *Arabidopsis*, *S. moellendorffii*,

and *P. patens*; whereas CYP96 is only found in angiosperms (Banks et al. 2011). Among thirteen CYP86 genes found in *S. moellendorffii*, five of them are CYP94Js families and located in the same cluster with JA-Ile hydroxylase genes from *Arabidopsis* (Banks et al. 2011).

Here, two of five SmCYP94Js homologs (CYP94J1 and CYP94J2) were successfully cloned. Sequencing data of CYP94J1 in this study revealed that thymine, which positioned at 846, was different from cytosine in database, but does not alter the amino acid translation (Asp). Because the sequence of CYP94J2 showed almost similar to amino acid sequence CYP94J4, therefore only CYP94J1 and CYP94J2 that will be analyzed further.

A method according to Kitaoka et al. (2011) was used to identify *CYP94J1* and *CYP94J2* encoding JA-Ile-12-hydroxylase by feeding JA-Ile as a substrate to *Pichia pastoris* containing the *Arabidopsis* CPR (ATR) to overexpress those genes, and then the resultant products were identified. The ATR encoded NADPH-cytochrome P450 reductase that is important to maintain the P450 enzyme activity. The data of UPLC-MS/MS analysis showed two dominant peaks of 12-OH-JA-Ile (*m/z* 129.7 derived from the peak at *m/z* 338.3 $[M-H]^-$). However, the intensity of both peaks between the extracts of *P. pastoris* strains that expressed CYP94J1 or CYP94J2 and an extract of vector control were not significantly different (Fig. 38). The same intensity of two peaks of products in each yeast strains expressing CYP94J1 and CYP94J2 was probably due to the weak activity of CYP94J1 and CYP94J2. Thus, CYP94J1 and CYP94J2 could not overcome the oxidation activity of JA-Ile, which were derived from enzymatic activity of *P. pastoris.* In contrast, a strong peak derived from 12-OH-JA-Ile was appeared in an extract of a *P. pastoris* strain expressing *Arabidopsis* CYP94B3 compared to that in an extract of vector control. These results demonstrated that weak

activities of CYP94J1 and CYP94J2 in *P. pastoris* made difficult to detect 12-OH-JA-Ile in UPLC-MS/MS analysis. Therefore, this method would not be suitable for expression of CYP94Js. The research of other groups used microsome fractions of *Saccharomyces cerevisiae* to analyze the activity of JA-Ile-12-hydroxylase in *Arabidopsis* (Koo et al. 2011; Heitz et al. 2012) and successfully shows the activity toward JA-Ile. Further investigation of CYP94Js in *S. moellendorffii* by using this system is proposed to inquire more accurate data. There are also possibilities that the other CYP94J enzymes are involved in the oxidation of JA-Ile.

Hydroxylation is important in controlling plant hormone activities, such as ABA catabolism by CYP707A, brassinosteroid catabolism by CYP73A1, gibberellin biosynthesis by CYP88A, JA biosynthesis by CYP74A, and JA-Ile inactivation by CYP94 (Helliwell et al. 2001; Park et al. 2002; Turk et al. 2005; Umezawa et al. 2006). *Arabidopsis* contains six CYP94s. Among them, CYP94B3 has been shown to catalyze ω-hydroxylation reactions on long chain fatty acid. In plants, ω-hydroxylation of fatty acid is important for the cuticle synthesis and might be involved in plant signaling (Benveniste et al. 1998; Pinot and Beisson 2011). Overexpression of CYP94B3 showed phenotype of JA-Ile deficiency: defects in male sterility, resistance to jasmonate-induced growth inhibition, and susceptibility to herbivory attack. On the other hand, the loss-of-function in *cyp94b3* mutant increased the amount of JA-Ile and enhanced expression of jasmonate-responsive genes (Kitaoka et al. 2011; Koo et al. 2011; Heitz et al. 2012). In soybean and rice contain 14 and 18 members CYP94s in the non-A-type P450 family, respectively (Nelson et al. 2004; Guttikonda et al. 2010). Phylogeny analysis displays that *CYP94* genes are conserved in dicots, monocots, and non-vascular plant such as *P. patens*, but not in photosynthetic aquatic organisms (Nelson et al. 2004; Pinot and Beisson 2011). Thus, it implies the importance of CYP94 function in land

plants. However, in the present study, CYP94J1 and CYP94J2 did not clearly display activity to convert JA-Ile into 12-OH-JA-Ile. Identification of these CYP94Js function will shed a new light to elucidate the function of P450 family that most of their physiological function remains unknown. Moreover, extensive characterization of other functions in CYP94 is needed since the functional activity of CYP94 homologs in non-vascular plants has not been conducted and neither JA nor JA-Ile is able to be produced in *P. patens*.

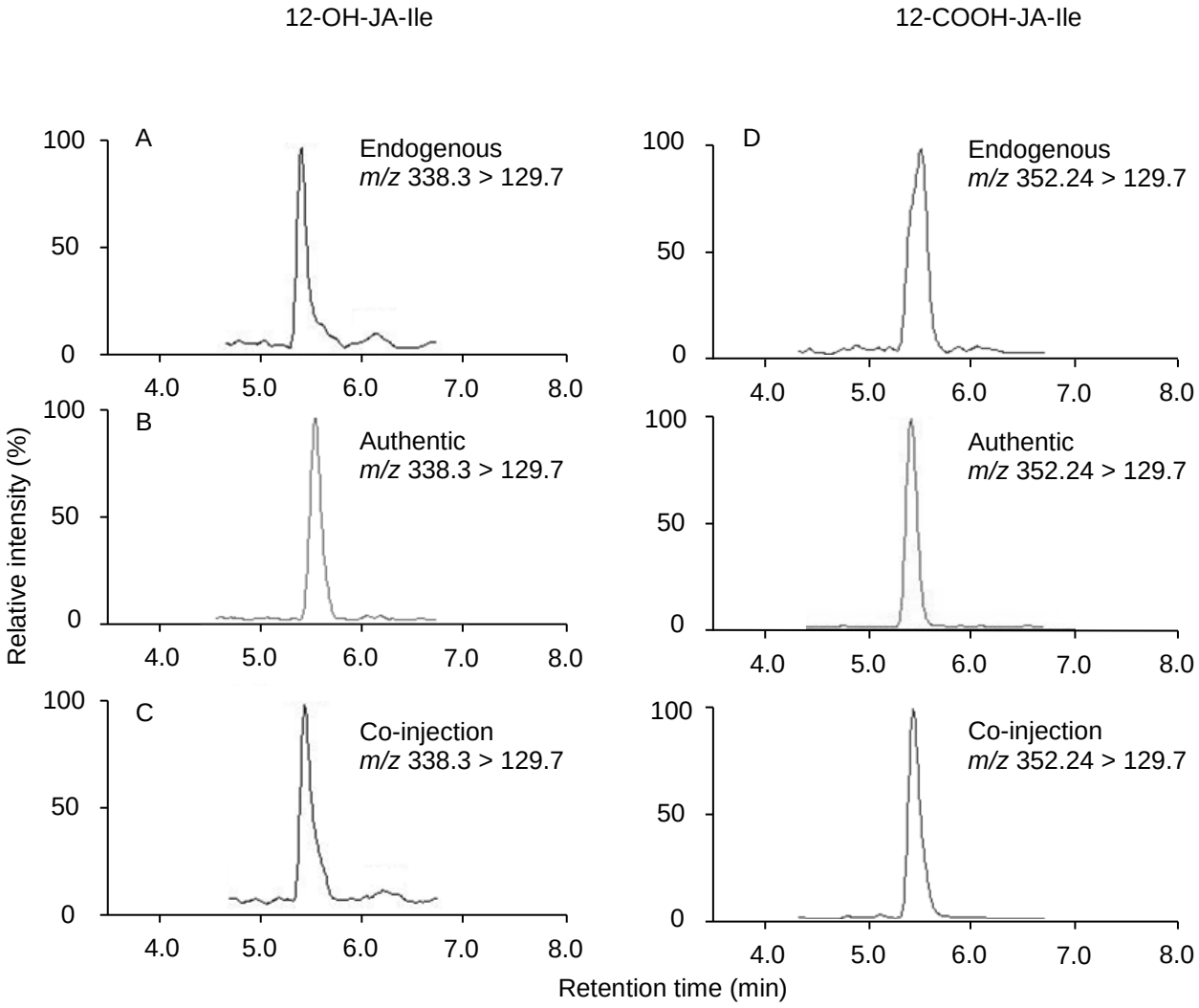

Fig. 34. UPLC-MS/MS analysis 12-OH-JA-Ile and 12-COOH-JA-Ile in wounded *S. moellendorffii*.

(A-C) MRM mode analysis of a specific daughter peak at *m/z* 129.7 that was derived from the peak at *m/z* 338.3 $[M-H]^-$. (D-F) MRM mode analysis of a specific daughter peak at *m/z* 352.24 that was derived from the peak at *m/z* 129.7 $[M-H]^-$. (A, D) Endogenous product of wounded *S. moellendorffii*. (B, E) Authentic compound. (C, F) Co-injection of endogenous product of *S. moellendorffii* extract and authentic compound.

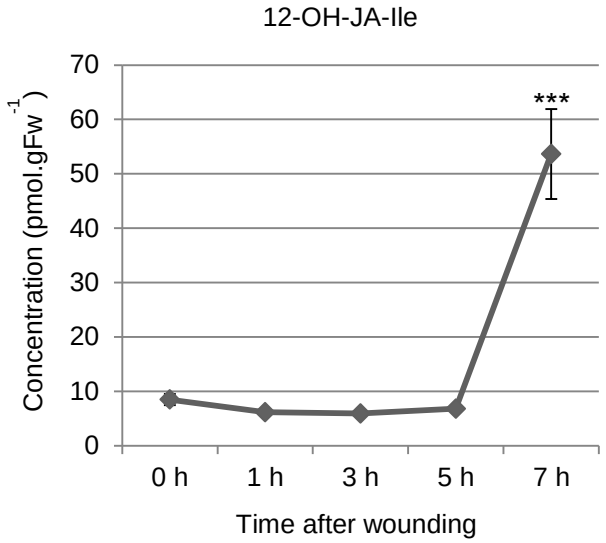

Fig. 35. Kinetics analysis of 12-OH-JA-Ile in *S. moellendorffii*.

S. moellendorffii was harvested after 0, 1 3, 5, and 7 h wounding by tweezer and the amount of 12-OH-JA-Ile was measured by UPLC-MS/MS analysis. The data represents the mean of three replications, and error bars indicate the SD. (Student's t test, ***$p < 0.001$).

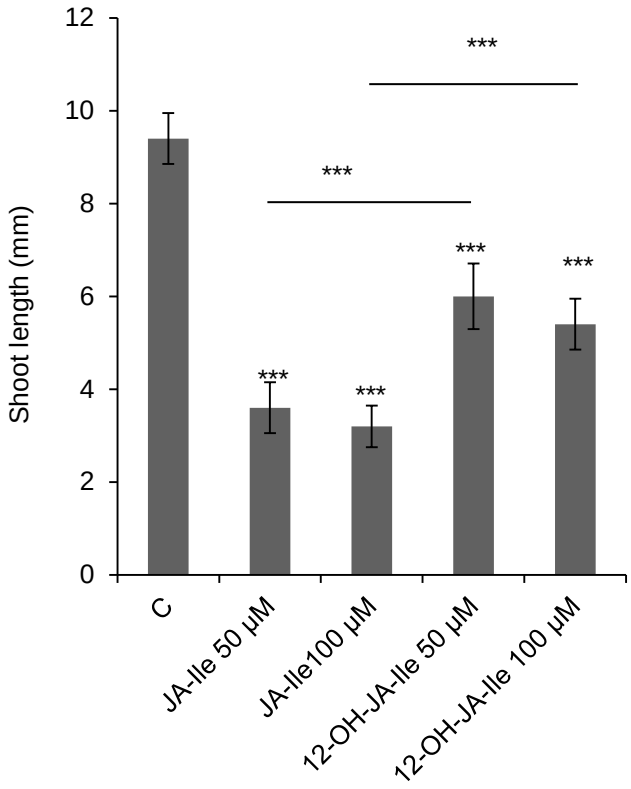

Fig. 36. Effect of exogenous JA-Ile and 12-OH-JA-Ile to the growth of *S. moellendorffii*. 12-OH-JA-Ile slightly inhibited the growth of *S. moellendorffii* compare to JA-Ile application due to the weak affinity of 12-OH-JA-Ile to cooperate with CO1-JAZ receptor. The data represents the mean of five replications, and error bars indicate the SD. (Student's t test, ***$p < 0.001$).

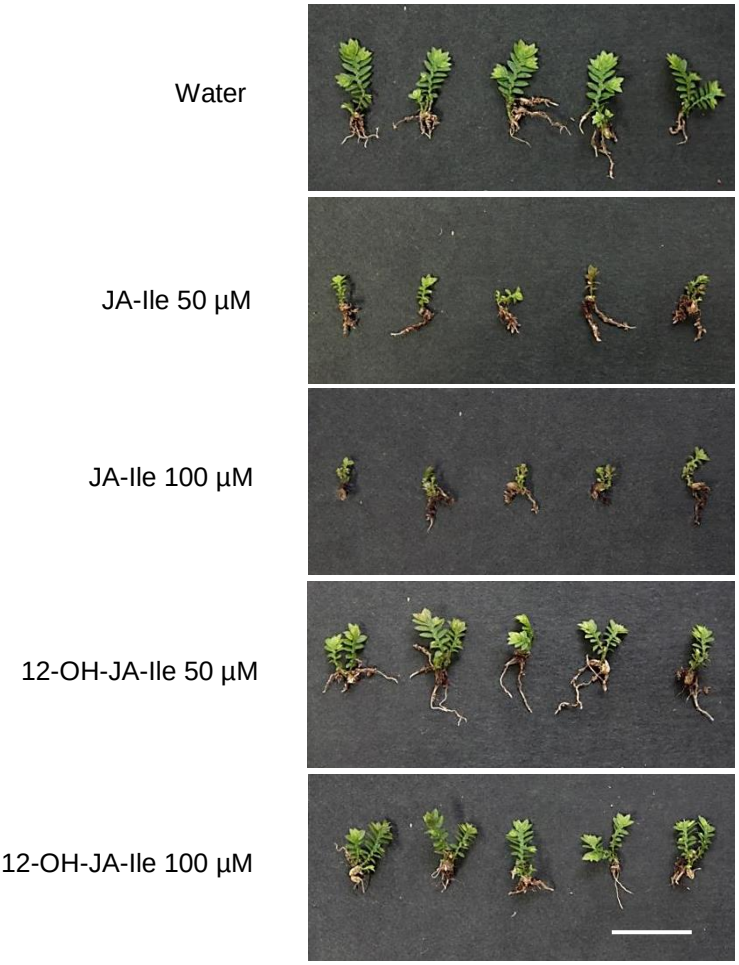

Fig. 37. Phenotype of *S. moellendorffii* after JA-Ile or 12-OH-JA-Ile application.
After germinated, *S. moellendorffii* was sprayed every other day with of JA-Ile or 12-OH-JA-Ile for five weeks and the shoot lengths was subjected to morphometric analysis. Scale bar: 1 cm.

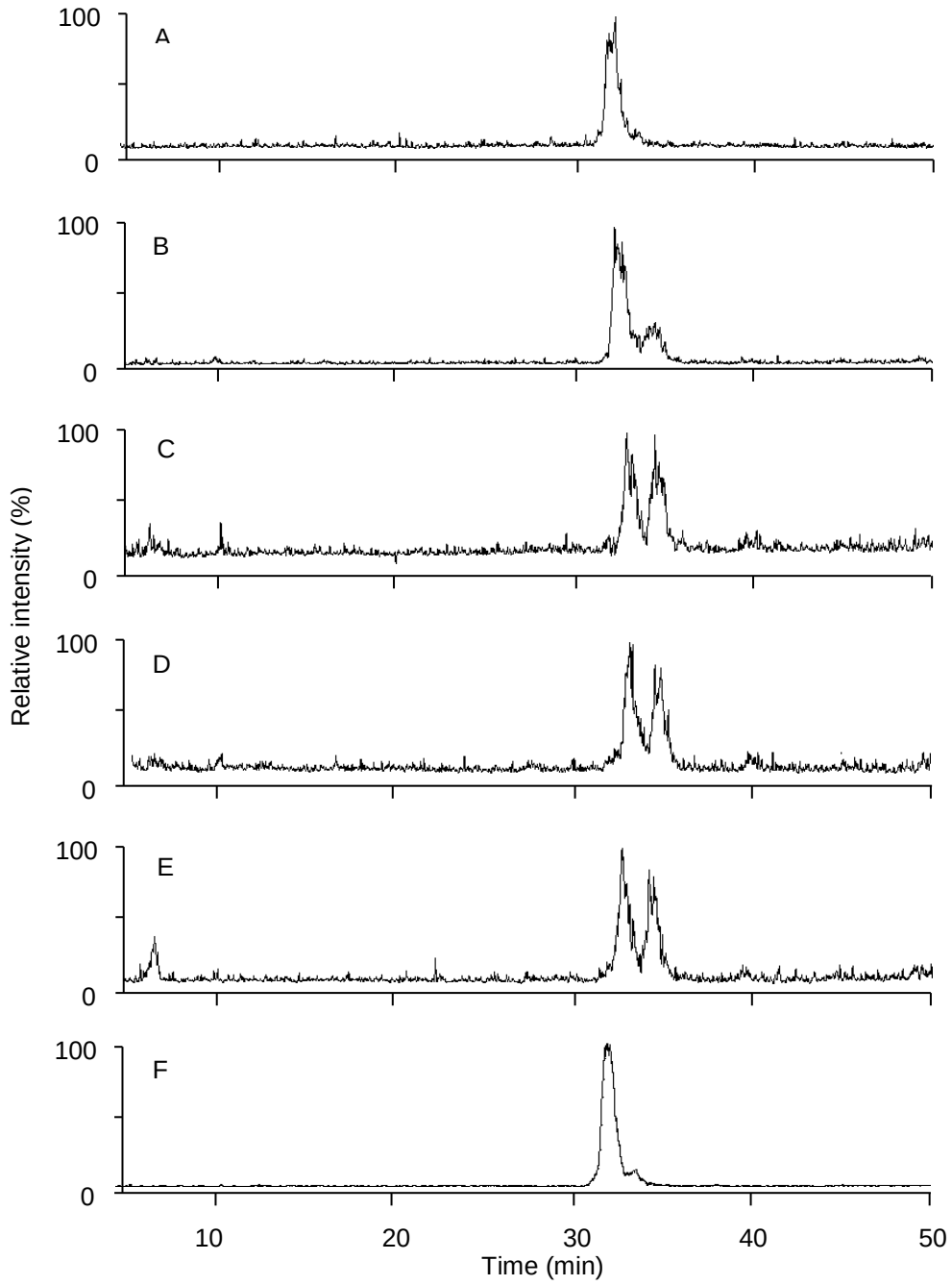

Fig. 38. *In vivo* formation of 12-OH-JA-Ile in strains of *P. pastoris* expressing *CYP94*s. *P. pastoris* transformed with respective *CYP94* gene or vector control were cultured in medium supplemented with JA-Ile as a substrate. After 3 days incubation, resultant products were analyzed by UPLC-MS/MS. The calculated molecular weight for 12-OH-JA-Ile and 12-OH-JA-[$^{13}C_6$]Ile are *m/z* 338.3 and 344.3, respectively. (A) Synthetic 12-OH-JA-Ile. (B-D) 12-OH-JA-Ile in respective strains of *P. pastoris* expressing *CYP94B3*, *CYP94J1*, and *CYP94J* after feeding JA-Ile. (E) vector control (F) Synthetic 12-OH-JA-[$^{13}C_6$]Ile.

5.3 Materials and methods

5.3.1 12-OH-JA-Ile and 12-COOH-JA-Ile profiling

Identification of 12-OH-JA-Ile and 12-COOH-JA-Ile was analyzed by UPLC-MS/MS according to the method of Sato et al. (2009) with some modifications. The plants were wounded using tweezer and were sprayed with JA-Ile. After 3 h, the damaged microphylls (ca. 1 g) were soaked in 20 ml ethanol for 24 h, the extract was added with 12-OH-JA-[$^{13}C_6$]Ile and 12-COOH-JA-[$^{2}H_3$]Leu as an internal standard, then was evaporated. The resultant residue was dissolved in 80 % aq. MeOH and loaded on to a column (Bond Elut C18, 6 ml, 1 g, Agilent Technologies, USA). The column was successively washed with 2 ml of 80 % aq. MeOH, three times. The volatile components of the eluents were removed *in vacuo*. The obtained residue was dissolved with 300 µl of 80 % aq. MeOH, and 5 µl of the solution was subjected to UPLC-MS/MS analysis as described previously.

For kinetic analysis of wound-induced accumulation of 12-OH-JA-Ile, the plants were wounded using tweezer for 0, 1, 3, 5, and 7 h and harvested at the indicated time after wounding treatment. The endogenous amount of 12-OH-JA-Ile was detected by UPLS-MS/MS analysis with the same methods described previously.

5.3.2 Exogenous application of 12-OH-JA-Ile to *S. moellendorffii*

S. moellendorffii bulbils (Fig. 6) were sprinkled onto a Jiffy-7 pellet (Sakata Seed Corporation, Japan). The bulbils were grown at 25°C until one week, and treated with a drop (30-50 µl) of JA-Ile or 12-OH-JA-Ile at concentrations of 50 µM and 100 µM every other day for five weeks. The shoot growth of the plants was evaluated by morphometric analysis.

5.3.3 Predicted genes encoding enzymes for oxidation of JA-Ile

Phylogenetic analysis of *Selaginella* CYP86 clan P450 (Banks et al. 2011) showed that SmCYP94Js (SmCYP94J1, SmCYP94J2, SmCYP94J3, SmCYP94J4) were located in the same cluster with AtCYP94B3 and AtCYP94C1 that are important for JA-Ile oxidation. Therefore, four putative SmCYP94Js were analyzed based on sequence result from GenBank (CYP94J1, XM_002979639; CYP94J2, XM_002988596; CYP94J3, XM_002979293; CYP94J4, XM_002964729).

5.3.4 Cloning of CYP94J1

Total RNA and cDNA of *S. moellendorffii* were obtained according the method described in Chapter 7. The primer set of *CYP94J1*, CYP94J1-F and CYP94J1-R, was used to amplify the ORF of *CYP94J1*. To afford the ORF of *CYP94J1*, the PCR reaction was performed in 50 μl per tube, containing 10 μl of dNTP mixture (2.0 mM each), 1 μl each from forward and reverse primer (5 μM), 0.5 μl of cDNA, 25 μl of 2 × PCR buffer, 0.5 μl of KOD FX DNA polymerase (Toyobo, Japan) and 12 μl of Milli-Q water under following conditions; pre-denaturation at 94°C for 2 min followed by 40 cycles of denaturing at 98°C for 10 s, annealing at 60°C for 30 s, and extension at 68°C for 1 min, and then a final extension at 68°C for 10 min. The obtained PCR product was purified and inserted into the pBlueScript SK II (+) vector (Stratagene, USA), which was digested with *Eco*RV to obtain the plasmid of pSK-CYP94J1. DNA sequencing was performed to confirm that the target gene was successfully inserted into the plasmid. The primers used in this study are listed in Table 4.

5.3.5 Cloning of CYP94J2

Total RNA and cDNA of *S. moellendorffii* were obtained according the method described in Chapter 7. The primer set of *CYP94J2*, CYP94J2-F and CYP94J2-R, was used to amplify the ORF of *CYP94J2*. To afford the ORF of *CYP94J2*, the PCR reaction was performed in 50 µl per tube, containing 10 µl of dNTP mixture (2.0 mM each), 1 µl each from forward and reverse primer (5 µM), 0.5 µl of cDNA, 25 µl of 2 × PCR buffer, 0.5 µl of KOD FX DNA polymerase (Toyobo, Japan) and 12 µl of Milli-Q water under following conditions; pre-denaturation at 94°C for 2 min followed by 40 cycles of denaturing at 98°C for 10 s, annealing at 60°C for 30 s, and extension at 68°C for 1 min, and then a final extension at 68°C for 10 min. The obtained PCR product was purified and inserted into the pBlueScript SK II (+) vector (Stratagene, USA), which was digested with *Eco*RV to obtain the plasmid of pSK-CYP94J2. DNA sequencing was performed to confirm that the target gene was successfully inserted into the plasmid. The primers used in this study are listed in Table 4.

5.3.6 Functional analysis of CYP94J1

The primer set for overexpression of CYP94J1 in *P. pastoris*, CYP94J1EcoRI-F with *Eco*RI site and CYP94J1NotI-R with *Not*I site, were designed according to *CYP94J1* sequence. PCR was performed in 15 µl of a reaction mixture containing 1.5 µl of dNTP mixture (2.0 mM each dNTP), 0.9 µl of 25 mM $MgSO_4$, 1.5 µl of KOD plus neo buffer (10 ×), 0.9 µl of each primer (CYP94J1EcoRI-F and CYP94J1NotI-R, 5 µM), 1 µl of pSK-CYP94J1 (200 ng/ µl), 0.3 µl of KOD plus neo DNA polymerase (Toyobo, Japan), and 8 µl of Milli-Q water. PCR was conducted with the following conditions: 2 min at 94°C for pre-denaturation; 30 cycles of 98°C for 10 s, 58°C for 30 s, and 68°C for 90 s and then final extension at 68°C for 10 min. After the PCR product was digested with *Eco*RI and *Not*I, the gene fragment was ligated into the expression

vector pPICZ-B, which was previously digested with *Eco*RI and *Not*I, to obtain pPICZ-CYP94J1. The constructed plasmid, pPICZ-CYP94J1, was transformed in *E.coli* DH5α according to standard procedure and was subsequently grown in LB agar medium supplemented with 25 μg/ml of zeocin. The colony was isolated, and purified plasmid was linearized with *Nsi*I then was used to construct a *P. pastoris strain* expressing *SmCYP94J1*. The linearized pPICZ-CYP94J1 gene was integrated into this transformants and the transformants were selected for YPDS plates containing blasticidin S (300 μg/ml) and zeocin (100 μg/ml) (See Chapter 7 for detail method). The primers used in this study are listed in Table 4.

5.3.7 Functional analysis of CYP94J2

The primer set for overexpression of CYP94J1 in *P. pastoris*, CYP94J2EcoRI-F with *Eco*RI site and CYP94J2NotI-R with *Not*I site was designed according to a *CYP94J2* sequence. PCR was performed in 15 μl of a reaction mixture containing 1.5 μl of dNTP mixture (2.0 mM each dNTP), 0.9 μl of 25 mM $MgSO_4$, 1.5 μl of KOD plus neo buffer (10 ×), 0.9 μl of each primer (CYP94J2EcoRI-F and CYP94J2NotI-R, 5 μM), 1 μl of pSK- CYP94J2 (200 ng/ μl), 0.3 μl of KOD plus neo DNA polymerase (Toyobo, Japan), and 8 μl of Milli-Q water. PCR was conducted with the following conditions: 2 min at 94°C for pre-denaturation; 30 cycles of 98°C for 10 s, 58°C for 30 s, and 68°C for 90 s and then final extension at 68°C for 10 min. After the PCR product was digested with *Eco*RI and *Not*I, the gene fragment was ligated into the expression vector pPICZ-B, which was previously digested with *Eco*RI and *Not*I, to obtain pPICZ-CYP94J2. The constructed plasmid, pPICZ-CYP94J2, was transformed in *E.coli* DH5α according to standard procedure and was subsequently grown in LB agar medium supplemented with 25 μg/ml of zeocin. The colony was isolated, and purified plasmid

was linearized with *Nsi*I, then was used to construct a *P. pastoris* strain expressing *SmCYP94J2*. The linearized pPICZ-CYP94J2 gene was integrated into this transformant, and the transformants were selected for YPDS plates containing blasticidin S (300 μg/ml) and zeocin (100 μg/ml) (See Chapter 7 for detail method). The primers used in this study are listed in Table 4.

5.3.8 Enzyme assay of CYP94J1 and CYP94J2

The heterologous production of CYP94J1 and CYP94J2 was conducted according to Kitaoka et al. (2011). Each transformant was incubated in 3 ml of minimal glycerol medium (MGY medium) containing blasticidin S (300 μg/ml) and zeocin (100 μg/ml) at 28°C, 160 rpm. After 24 h incubation, the culture was centrifuged at 5,000 × *g* for 10 min. The collected cells were added into 3 ml of minimal MeOH medium (MM medium) containing blasticidin S (300 μg/ml), zeocin (100 μg/ml), and JA-Ile (40 nmol) as a substrate. Production of CYP94J1 and ATR was induced by addition of 0.5% (v/v) MeOH every 24 h. After incubation at 28°C for three days, the products were retrieved from the culture broth by centrifugation 5,000 × *g* for 10 min. The supernatant was added an internal standard 12-OH-JA-[$^{13}C_6$]Ile then applied to the cartridge column of a Bond Elut C_{18}. The column was washed with water (2 ml x 3) and extracted with 2 ml MeOH:H_2O (80:20) for three times. The volatile components of the eluents were removed *in vacuo*. The obtained residue was dissolved with 300 μl of 80 % aq. MeOH, and 5 μl of the solution was subjected to UPLC-MS/MS analysis. The analytes were eluted with solvent A (20% aq. methanol with 0.05% acetic acid) and solvent B (methanol with 0.05% acetic acid) using linear gradient mode. The ratio of solvent A to solvent B was 100:0 from 0 min to 2 min, and linearly converted from

100:0 to 80:20 between 2 min to 54 min. Finally the column was eluted with solvent B from 54 min to 60 min at flow rate of 0.25 ml/min.

CHAPTER 6

GENERAL DISCUSSION

6.1 Jasmonates biosynthesis in *S. moellendorffii*

Since the first discovery of jasmonate over 50 years ago by Demole group (Demole et al. 1962), the understanding of biosynthesis, signaling pathway, and physiological functions of jasmonates has been marked several major developments. By using the *Arabidopsis* as a model plant, identification of genes encoding most of JA biosynthetic enzymes and the discovery of a versatile bioactive JA-Ile have been revealed successfully. JAs have been ubiquitously produced in seed plants but not in *P. patens* and *M. polymorpha*. These findings raise a question when JA is firstly synthesized by plant for developments and stress responses that might be related to one of the adaptation process during plant evolutionary history. In this study, *S. moellendorffii* as the earliest non-seed vascular plant model is used to elucidate JA biosynthesis, metabolism, and functions. A significant result of JA and JA-Ile detection in *S. moellendorffii* suggested that the appearance of JA and JA-Ile are probably related to development of vascular system during plant evolution process to adapt to environmental changes.

The level of JA in plants varies in developmental stages and different tissues upon different environmental stimuli (Creelman and Mullet 1997). The kinetic analysis of jasmonates accumulation in wounded *S. moellendorffii* showed an extremely high concentration of OPDA that is not common in seed plants while the stress-induced level of JA-Ile generally is lower than that of JA (~10%) (Koo and Howe 2012). The transient accumulation of OPDA, JA, and JA-Ile in the kinetic analysis of wounded *S. moellendorffii* could be assumed that there are other metabolic pathways to generate

different JA derivatives, which compete with the main JA biosynthetic pathway. The relatively high accumulation of OPDA possibly plays a main role in adaptation to wounding stress, which is different from JA and JA-Ile in *S. moellendorffii*. Previous studies showed that OPDA activates a set of important genes in seed germination (Dave et al. 2011), seed dormancy (Dave et al. 2016), and embryo development in tomato (*Solanum lycopersicum*) (Goetz et al. 2012), drought stress responses in *Arabidopsis* and tomato (Savchenko and Dehesh 2014), local defense response of tomato (Bosch et al. 2014), and tendril coiling in *Bryonia dioica* and *Phaseolus vulgaris* (Stelmach et al. 1998). However, unlike JA signaling, OPDA signaling is COI1 independent (Taki et al. 2005). Recently, the identification of OPDA-Ile suggest that this compound might mediate OPDA-mediated responses (Arnold et al. 2016; Floková et al. 2016) like those in seed plants that require the conjugation of JA-Ile as the ligand to COI1-JAZ system. The further study to identify OPDA-Ile and its function in *S. moellendorffii* is important to have a better understanding of how plant evolved to adapt land environments.

In *S. moellendorffii,* genes encoding key enzymes in jasmonates biosynthesis (*SmAOS2*, *SmAOC1*, *SmOPR5*, and *SmJAR1*) showed the same characteristics as those in flowering plants: functionally active AOS, AOC, OPR3, and JAR1. Accumulation of *SmAOC1* and *SmOPR5* mRNA by wounding and JA indicates a positive feedback regulation of JA biosynthesis. While the profile of wound-induced expression of *SmJAR1* was tightly correlated with wound-induced JA-Ile accumulation pattern, JA suppressed mRNA accumulation of *SmJAR1*.

The study conducted by Bandara (2011), exhibited the crucial role of OPR3 as the only enzyme to generate JA seems to be not functional in *P. patens*. The *OPR* homologous genes of higher and lower plants were shown to be conserved in phylogenetic analysis. In that analysis, PpOPR3 and PpOPR6 were clustered in

subgroup II which is known as a group OPR3 that involved in JA biosynthesis. The PpOPR3 had a Phe and His that is considered to be a critical amino acid residue responsible for substrate specificity while PpOPR6 were occupied by Phe and Tyr. However, OPR3 functional activity of PpOPR3 enzymes from *P. patens* prefers to consume (-)-*cis*-OPDA over (+)-*cis*-OPDA. The same results was also obtained in SmOPR1 that possessed Phe and His but does not have the ability to catalyze the reduction of *cis*-(+)-OPDA, a natural JA precursor. While in SmOPR5 harbors Trp and His as the active side residue, the GC-MS data analysis represented positive activity to generate both (±)-OPC-8:0 enantiomers. These results imply that the substrate specificity does not solely depend on gate keeping residues. In 3D modeling study of OsOPR in rice revealed that two middle variable region: MVR i and MVR ii determined a specific substrate binding with the OPR protein and affected the substrate entrance into the substrate-binding pocket, respectively (Li et al. 2011). Considering that OPR3-like enzymes are important for JA biosynthesis, it is suggested that OPR3 activity is one of key factors to acquire JA signaling pathway in the transition process from Bryophytes to seedless vascular plants.

6.2 Inactivation of JA-Ile in *S. moellendorffii*

Most of the stress related hormones in plants and animals needs to be switched off when stress levels are reduced. As a major regulator in defense responses, bioactive JA-Ile levels are controlled dynamically when plants are stimulated during stresses and then undergo modification process when signaling must be turned off. UPLC-MS/MS analysis depicts that wounded *S. moellendorffii* produces inactive form of JA-Ile: 12-OH-JA-Ile and 12-COOH-JA-Ile. Attenuation of JA-Ile responses is likely conserved in vascular plants. In flowering plants, wound also induced the formation of 11-OH-JA,

12-OH-JA, 12-OH-JA-Ile, 12-COOH-JA-Ile and 12-HSO_4-JA (Wasternack and Hause 2013). The concentration of JA metabolites described above often shows several times higher than that of JA and/or OPDA in each organ and each plant (Miersch et al. 2007). The same phenomenon was observed in kinetic analysis of wounded *S. moellendorffii* where wound-induced accumulation of 12-OH-JA-Ile (Fig. 35) showed relative higher level compared to that in JA-Ile (Fig. 8).

The recent discover of cytochrome P450 CYP94B3 (a JA-Ile-12hydroxylase) in *Arabidopsis* suggests that CYP94B3 manipulates JA-Ile levels for plant resistance to environmental stress by oxidizing JA-Ile into 12-OH-JA-Ile, which is less active than JA-Ile in promoting COI1-JAZ interaction (Koo et al. 2011). This observation showed that ω-oxidation is a crucial and conserved pathway for catabolism of lipid-derived molecules in plants. In this study, the JA-Ile-12hydroxylase homologs in *S. moellendorffii* CYP94J1 and CYP94J2 did not clearly show activity to oxidize JA-Ile into 12-OH-JA-Ile. Interestingly, *P. patens* possess the homologs of these enzymes but it only has the ability to synthesize OPDA and lack the ability to produce JA and JA-Ile. Therefore, further study of functional characterization of CYP94 in *S. moellendorffii* and *P. patens* may provide a new insight of the evolutionary origins of oxylipin signaling and catabolism.

In plants, oxygenated fatty acid derivatives, which are mostly catalyzed by cytochrome P450 enzymes, are involved in various biological functions. Cytochrome P450 proteins comprise one of the largest protein families that estimated up to 1% of the total gene annotations of each plant species. The cytochrome P450 families are conserved in land plants and establish roles in a wide variety of biochemical pathways, such as synthesis and metabolism of plant hormones. In JA biosynthetic pathway, CYP74s is involved in JA biosynthesis, and CYP94 as a JA-Ile-12-hydroxylase to

inactivate JA-Ile where their expressions were enhanced by wounding at the transcriptional level. The identification of these two enzymes contributed the elucidation of cytochrome P450 family, however physiological role of them in plants remains largely unknown. Functional elucidation of various genes involved in JA biosynthesis and catabolism in *S. moellendorffii* as well as comparison of those genes between *S. moellendorffii*, *Arabidopsis* and *Physcomitrella* will be the key to understanding the evolution of plants.

6.3 Jasmonates function in *S. moellendorffii*

The biological roles of JA have been extensively investigated in seed plants. In *Arabidopsis* and tomato, JA are involved in vegetative growth, senescence, stamen and trichome development, and responses to various biotic and abiotic stresses (Creelman and Mullet 1997; Wasternack 2007; Avanci et al. 2010). Many of these responses were identified by application of jasmonate to plants (Creelman and Mullet 1997). Non-vascular plant models of moss *P. patens* and liverwort *M. polymorpha* responded to the application of OPDA by reducing their growth size (Ponce de león et al. 2012; Yamamoto et al. 2015). Application of OPDA, JA, and JA-Ile to the germinated *S. moellendorffii* reduced their growth significantly with the strongest effect of JA-Ile followed by OPDA and JA. This growth inhibition in response to mechanically wounding are probably caused by inhibition of the mitotic cycle of G1/S transition thus reducing cell number and repressing the onset of endoreduplication which affects cell size (Noir et al. 2013; Larrieu and Vernoux 2016).

In conclusion, this study provides the first evidence of the biosynthesis of OPDA, JA, and JA-Ile as well as the JA-Ile metabolites, 12-OH-JA-Ile and 12-COOH-JA-Ile, in the model Lycophytes *S. moellendorffii*, which is taxonomically positioned between

Bryophytes and Euphyllophytes (Fig. 39). Moreover, active enzymes involved in the octadecanoid pathway, including AOS, AOC, OPR3-like enzyme, and JAR1, were also identified in this plant. The application of exogenous OPDA, JA, and JA-Ile significantly inhibited the growth of *S. moellendorffii.* Thus, OPDA, JA, and JA-Ile are probably important signaling molecules in stress responses and growth of *S. moellendorffii*. The unique physiological effect of 12-OH-JA-Ile displays a promotion of two microphylls from a single bulbis of *S. moellendorffii*. These observations suggested that *S. moellendorffii* is an important transition model between lower and higher plants that can be used to clarify the plant adaptation to the changing environmental conditions.

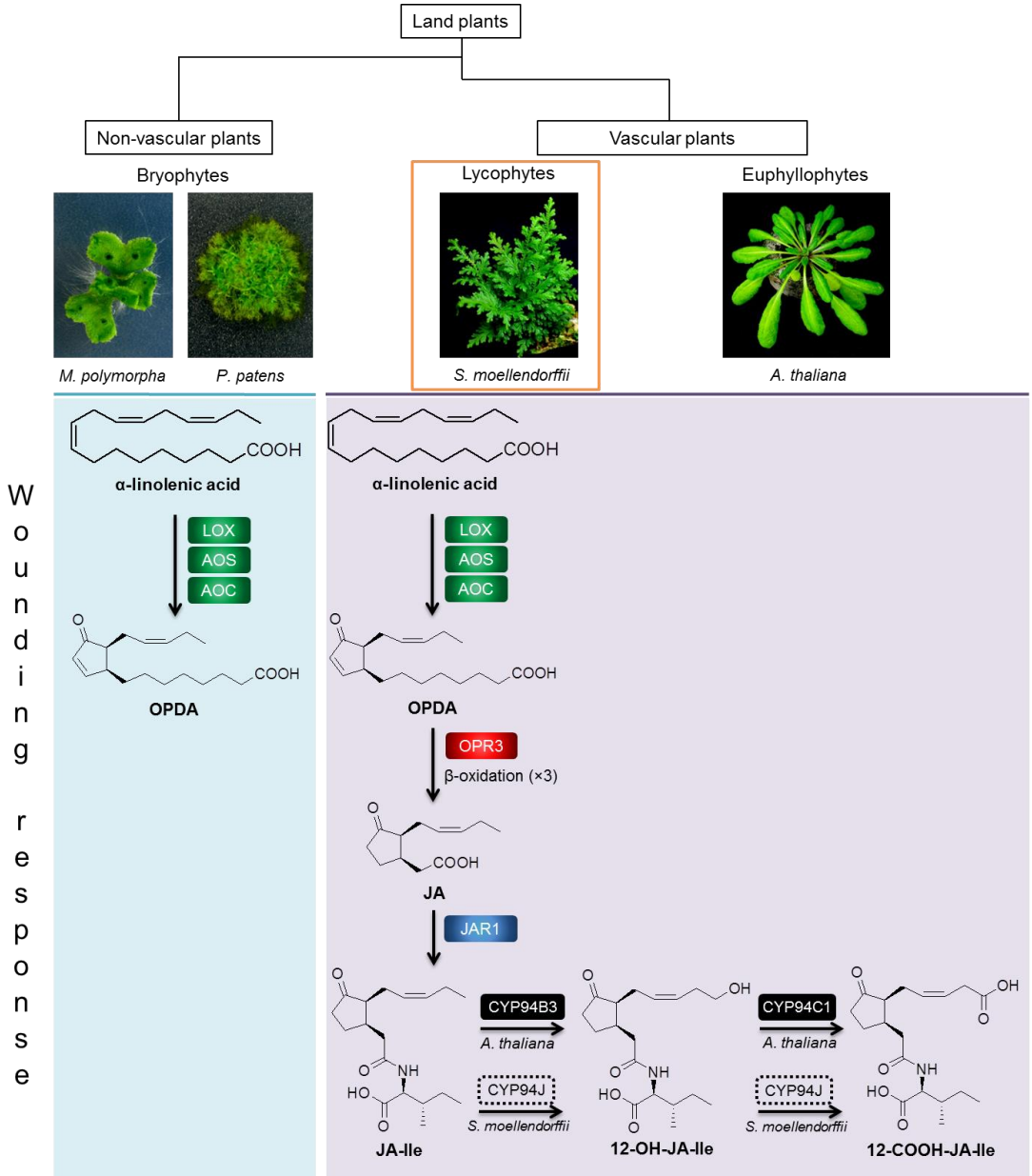

Fig. 39. Summary figure.

Biosynthesis of jasmonates in response to wounding stresses in non-vascular plants and vascular plants. *S. moellendorffii* has an ability to produce JA, JA-Ile, 12-OH-JA-Ile, and 12-COOH-JA-Ile like those in seed plants (e.g. *A. thaliana*). Green box indicated JA biosynthetic enzymes located in chloroplast, red box indicated a JA biosynthetic enzyme located in peroxisome, blue box indicated an enzyme located in cytoplasm, black box indicated enzymes that are involved in JA-Ile oxidation in *A. thaliana*, black dotted box indicated predicted enzymes that are involve in JA-Ile oxidation in *S. moellendorffii*. Abbreviation: AOC, allene oxide cyclase; AOS, allene oxide synthase; JA, jasmonic acid; JA-Ile, jasmonoyl-isoleucine; JAR1, jasmonate resistant 1; LOX, lipoxygenase; OPDA, 12-oxo-phytodienoic acid; OPR3, OPDA reductase; 12-OH-JA-Ile, 12-hydroxyJA-Ile; 12-COOH-JA-Ile, 12-carboxyJA-Ile.

CHAPTER 7

GENERAL METHODS

7.1 5'-RACE PCR

The protocol of 5'-Full RACE Core Set (Takara, Japan) can be divided into four steps: first strand cDNA synthesis, degradation of hybrid RNA, ligation reaction, and PCR reaction.

a. First strand cDNA synthesis

The reaction mixture was prepared in a 1.5 ml microtube contains these following reagents and PCR conditions:

Poly $(A)^+$ RNA or Total RNA	5 µg	30°C 10 min
10x RT buffer	1.5 µl	50°C 60 min
RNase inhibitor (40 U/ µl)	0.5 µl	80°C 2 min
AMV reverse transcriptase XL (5U/ µl)	1.0 µl	4°C ∞
SmAOC1_RT (100 pmol/ µl)	2.0 µl	
RNase free dH_2O	up to 15 µl	
Total	15 µl	

b. Degradation of hybrid RNA

The following reaction mixture was prepared. RNase H (1 µl) was added to the reaction mixture and gently mixed by tapping the tube. After incubation for 1 h at 30°C, ethanol precipitation was performed.

1^{st} strand cDNA solution obtained at (a)	15 µl
5x hybrid RNA degradation buffer	15 µl

dH_2O	45 µl
Total	75 µl

c. Ligation reaction

After preparing the reaction mixture below, it was added into the resultant product which has been collected at (b). T4 RNA ligase (1 µ) was added. The reaction mixture was incubated at 15°C for 15-18 h.

5x RNA (ssDNA) ligation buffer	8 µl
40% PEG #6000	20 µl
dH_20	12 µl
Total	40 µl

d. PCR reaction

The first PCR reaction was done using KOD FX Neo (Toyobo, Japan) with the template obtained from the result of Ligation reaction (c) and the primer set of SmAOC1_A1 and SmAOC1_S1 (Table 4). To confirm the PCR product, electrophoresis was performed. The obtained band at approximately 2.5 kbp was isolated and used as the template for the second PCR. Second PCR was also performed using KOD FX Neo with the primer set SmAOC1_A2 and SmAOC1_S2 (Table 4).

7.2 Sub-cellular localization of SmAOC1 in protoplast of *P. patens*

7.2.1 General method of sub-cellular localization of SmAOC1

PCR was carried out using a set of primers, SmpENTR4-F and SmpENTR4-R (Table 2) with the *Nde*I and *Eco*RV restriction site, respectively. PCR reaction contains

dNTP mixture (2.0 mM each dNTP), 0.9 µl of 25 mM $MgSO_4$, 1.5 µl KOD plus neo buffer (10 x), 0.9 µl of each primer (5 µM), 1 µl of pSK-SmAOC1 (200 ng/ µl), 0.3 µl of KOD plus neo DNA polymerase (Toyobo, Japan), and adjusted of Milli-Q water until volume reached 15 µl. PCR was conducted under the conditions of 2 min at 94^{o}C for pre-denaturation; 30 cycles of 98°C for 10 s, 60°C for 30 s, and 68°C for 1.5 min; and final extension of 68°C for 10 min. PCR product was ligated into the pENTR4 vector using GeneArt® Seamless Cloning and Assembly Kit (Invitrogen, USA). Entry clone of pENTR4-SmAOC1 was introduced to pUGWnew5 destination vector and Gateway LR Clonase Mix (Invitrogen, USA) to generate the plasmid encoding 35S::SmAOC1-GFP (pUGWnew5-SmAOC1). Trasnformation was carried out into the protoplast prepared from *P. Patens* (grown in BCDATG medium for 3 days) by PEG-mediated transformation technique (Liu and Vidali, 2011). After incubation for 3 days, localization of SmAOC1-GFP was observed by using a TCS-SP5 confocal laser scaning microscope (Leica, Germany). Images were observed under the excitation at 488 nm and emission 530 nm for detection of the GFP signal, and emission over 655 nm for detection of aoutofluorscence from chloroplast.

7.2.2 GeneArt® Seamless Cloning Reaction

Seamless Cloning Reaction was carried out according to manufacturer's instruction (Invitrogen, USA). The reaction mixture was prepared according to the composition described below, was mixed and was centrifuged. After adding 0.5 µl of Enzyme mix (×10). The resultant reaction mixture was incubated at room temperature for 30 min. The reaction mixture was transferred into One Shot®TOP10 chemically competent *E. coli*. Transformation mixture solution was incubated on ice for 30 min. The cells were heat-shocked at 42°C for 30 min without shaking. Then the tube was immediately

transferred to ice and incubated on ice for 2 min. S.O.C medium (250 µl, room temperature) was added to the transformation mixture solution then was shaken reciprocally (200 rpm) at 37^{o}C for I h. The transformation mixture solution was spread into a LB agar medium supplemented with an antibiotic suitable for selection and incubated at 37°C for overnight.

5x reaction buffer	1 µl
Insert (SKII::SmAOC1)	1 µl
Vector pENTR4	1 µl
Milli-Q	1.5 µl
Total	4.5 µl

7.2.3 LR Reaction

LR Reaction was carried out using Gateway LR Clonase Mix (Invitrogen, USA) according to manufacturer's instruction. The following components were added to a 1.5 ml microctube. The reaction was incubated at 25°C for 1 h. Proteinase K solution (1 µl) was added to the solution to terminate the reaction. The resultant solution was incubated at 37°C for 10 min and continued to transformation into *E. coli* DH5α in LB medium containing 100 µl/ml of ampicillin.

LR Clonase II mix	2 µl
pUGW/NEW5	120 ng
pENTR4-SmAOC1	120 ng
TE buffer (pH 8.0)	up to 10 µl
Total	10 µl

7.2.3 Transformation to protoplast of *P. patens*

Transformation of *SmAOC1* was done using PEG-mediated transformation technique. A 2% driselase (w/v) in 8% mannitol (1 ml) and two plates of mosses were put into microtube and covered with aluminium for 25 min while turn in the other way every 5 min. The mixture was centrifuged at 1,500 rpm for 2 min with slow acceleration and deceleration. After supernatant was removed, the pellet was resuspended with 1 ml of 8% mannitol and was centrifuged (1,500 rpm, 2 min, slow acceleration and deceleration), and repeated for two times. After protoplasts were obtained in a good condition by counting the cells under the microscope using hemacytometer, centrifugation was done for one more time. Supernatant was removed and the pellet was slowly resuspended by 400 µl of MMM solution. DNA (6 µg) and 300 µl of protoplast suspension was added into round-bottom tube in 300 µl of PEG6000 and T solution mixture. The mixture was incubated at 45°C for 5 min followed by further incubation at 20°C for 10 min. The mixture was added with 4 ml of 8% mannitol and subsequently was centrifuged (1,000 rpm, 3 min, slow acceleration and deceleration). After supernatant was removed, the pellet was resuspended by pipetting with 8 ml of 8% mannitol. The solution was spread into petri dishes. Observation with a TCS-SP5 confocal laser scanning can be done after incubation the plate at 15°C for 3 days.

T solution[*]

8% mannitol	2.25 ml
1 M $Ca(NO_3)_2$	250 µl
1 M Tris-HCl (pH 8.0)	25 µl

MMM solution[*]

Mannitol	0.3 g
1 M $MgCl_2$	50 µl
1% MES	333 µl
Milli-Q	2.95 ml

[*]Solution was filter-sterilized before use

7.3 Solid phase extraction

Mycrophyll (500 mg) was homogenized under liquid nitrogen and extracted with 20 ml of ethanol for 24 h. Before subjecting to solid phase extraction, the mixture was added by OPC-8-d_6 (100 ng/g fresh weight of plants), JA-d_6 (100 ng/g fresh weight of plants), JA-Ile d_6 (12.5 ng/g fresh weight of plants), and/or 12-OH-JA-[$^{13}C_6$]Ile (200 ng/g fresh weight of plants). The ethanol extracted solution was evaporated, and the crude extract was put into a cartridge column Bond Elute C18. The column was successively washed with 2 ml solution of methanol for three times. The volatile components of the eluents were removed *in vacuo*. Finally, the residue was dissolved with 300 µl solution methanol:water (80:20) and 5 µl of sample solution was subjected to UPLC-MS/MS analysis.

7.4 Basic method for molecular biological study

7.4.1 Total RNA isolation

A sample (120 mg) was frozen in liquid nitrogen and ground at 1,500 rpm for 15 s using Multi-Beads Shocker® (Yasui Kikai, Japan). RNA extraction buffer [500 µl, 1 M Tris-HCl (pH 7.5), 0.5 mM EDTA (pH 8.0), 4 M NaCl, 10% SDS (w/v)] and phenol (150 µl) were added to the sample and ground at 1,500 rpm for 60 s. A mixed solution

of chloroform and isoamyl alcohol (24:1, 250 µl) was added and mixed for 30 s before centrifugation (15,000 rpm, 10 min, 4°C). A supernatant (300 µL) was precipitated by 70 % ethanol aq. and continued by centrifugation (15,000 rpm, 10 min, 4°C). The obtained pellet was mixed with Milli-Q water (90 µl) and DNase I buffer (10 µl, Promega, USA). The mixture was transferred into the new 1.5 ml microtube and incubated at 37°C for 30 min after addition 10 U of DNase I (Promega, USA). Milli-Q water (200 µl) and phenol (300 µl) were added to the mixture, were mixed, and were centrifuged (15,000 rpm, 10 min, 4^{o}C). The supernatant was transferred into new 1.5 ml microtube. After ethanol precipitation, 20 µl of Milli-Q water was added to dissolve the total RNA.

7.4.2 cDNA synthesis

cDNA was synthesized from total RNA using Moloney Murine Leukemia Virus Reverse Transcriptase (M-MLV RT, Invitrogen, USA). The following reagents were mixed in the nuclease-free microtube. The mixture was heated at 65°C for 5 min and subsequently was cooled on ice. M-MLV Reverse Transcriptase (1 µL, 200 U/µl) was added and gently mixed to the reaction mixture. Then the reaction was incubated at 42°C for 60 min, and then was inactivated by heating at 99°C for 1 min. The obtained cDNA was used as a template for amplification in PCR.

Total RNA	5.0 µg
5x PCR buffer	5.0 µl
dNTP (2.5 mM)	4.0 µl
DTT (0.1 M)	4.0 µl
Oligo dT B26 (2.5 µM)	2.0 µl

Milli-Q	up to 19 µl
Total	19 µl

7.4.3 Transformation into competent *E. coli*

The following components were mixed in the 1.5 ml microtube. The mixture was incubated at 16°C for 1 h and transferred into the *E. coli* competent cells. The culture was kept on the ice box for 30 min, heat-shocked at 42°C for 1 min and immediately put on the ice. The transformant was spread in LB agar medium containing appropriate antibiotics.

10x Ligase buffer	1.0 µ1
T4 DNA Ligase	1.0 µ1
Vector DNA (50 ng/ µL)	1.0 µl
Insert DNA	10-20 ng
Milli-Q	up to 10 µl
Total	10 µl

7.4.4 Colony PCR

To ensure that the target gene has inserted into the vector, colony PCR was performed. The following PCR reaction mixtures were prepared in the PCR tube. A single colony was inoculated into the reaction mixture as a template and part of the same colony was transferred into the new LB agar medium containing appropriate antibiotics then subsequently incubated at 37°C for overnight. The reaction mixture was amplified under PCR condition described below.

2× GoTaq GreenMaster Mix	6.25 µl	95°C	2 min	
Primer forward (5 µM)	0.5 µl	95°C	30 s	30×
Primer reverse (5 µM)	0.5 µl	58°C	30 s	
Milli-Q	5.25 µl	72°C	1 min	
Total	12.5 µL	72°C	10 min	
		4°C	∞	

7.4.5 Gel and PCR isolation

Isolation of PCR products from gel were performed using Wizard® SV Gel and PCR Clean-Up System (Promega, USA). After electrophoresis, PCR product was excised from gel and placed in 1.5 ml microtube. Membrane Binding Solution was added per 10 mg of gel slice. The sliced gel was mixed and incubated at 55^{o}C until it was completely dissolved. The dissolved gel mixture was transferred into the assembled Minicolumn and incubated at room temperature for 1 min. The assembled Minicolumn was centrifuged at 16,000 × *g* for 1 min; the flowthrough was discarded. For washing, Membrane Wash Solution (700 µL) was added and centrifuged at 16,000 x g for 1 min; the flow-through was discarded. Membrane Solution (500 µL) was added; then was continued for centrifugation at 16,000 × *g* for 5 min. Additional centrifuge at 16,000 × *g* for 1 min was done to remove the remaining ethanol. The Minicolumn was transferred into a new 1.5 ml microtube. The DNA was eluted with 50 µl of Nuclease-Free Water after incubation at room temperature for 3 min.

7.4.6 Plasmid isolation

A single colony was grown in 5 ml of LB medium containing appropriate antibiotics at 3°C overnight with shaking. A 5 ml of culture was transferred into two 1.5

ml microtubes and centrifuged (15,000 rpm, 3 min, 4°C) to precipitate cells. Supernatant was removed before the addition of Sol. I [200 µl, 25 mM Tris-HCl (pH 8.0), 10 mM EDTA, 50 mM glucose]. After the cell completely was dissolved, Sol. II (400 µl, 0.2 M NaOH, 1% SDS) was added, gently mixed by inverting the tubes for 5 times, and put on ice for 4 min. Sol. III [300 µl, 3.0 M KOAc (pH 4.8)] was added, gently mixed by inverting the tubes for 5 times, and put on ice for 10 min. The tubes were centrifuged (15,000 rpm, 10 min, 4°C) and carefully transferred the supernatant into new 1.5 ml microtubes. Isopropanol (600 µl) was added, put on ice for 10 min, and centrifuged (15,000 rpm, 10 min, 4°C); and the supernatant was removed. The precipitate DNA was added by 70% ethanol aq. then centrifuged (15,000 rpm, 5 min, 4°C). To remove the remaining liquids, the tubes were air-dried for 5 min. The pellet was resuspended with RNase A (100 µl, 20 µg/mL) solution and incubated at 37°C for 45 min. $MgCl_2$ (30 µl, 1 M) was added into the mixture and put on ice for 10 min before centrifugation (15,000 rpm, 10 min, 4°C). The supernatant from two microtubes were transferred into one new 1.5 ml microtube, added by PEG/NaCl (120 µl), and put on ice for 45 min. The tube was centrifuged (15,000 rpm, 15 min, 4°C). The obtained pellet was added by 70% ethanol aq. (1 ml) and centrifuged (15,000 rpm, 5 min, 4^oC). The DNA pellet was resuspended with Milli-Q water (50 µl).

7.4.7 Sequencing

Sequencing was performed using BigDye Terminator v3.1 cycle sequencing kit (Applied Biosystems). Before doing the sequencing, preparation method was performed. PCR mixture was described in below paragraph with conditions for PCR-sequencing: pre-denaturation at 96°C for 1min, 25 cycles of 96°C for 10 s, 50°C for 5 s, and 60°C for 4 min. The PCR product was purified by ethanol precipitation. Incubation at room

temperature in dark was done for 10 min before centrifugation (15,000 rpm, 15 min, 4°C). The supernatant was discarded carefully. The obtained pellet was added by 1 ml of 70% ethanol aq. and continued for centrifugation (15,000 rpm, 10 min, 4°C). To remove all the remain liquid, the pellet was air-dried for 25 min followed by resuspending with 20 µl of HiDi (Applied Biosystems, USA) and boiled up at 95°C for 2 min and subsequently cooled on ice.

Template DNA (plasmid)	100 ng
5x sequencing buffer	2.0 µl
BigDye reaction mix	0.5 µl
Primer (1.6 µM)	1.0 µl
Milli-Q	up to 10 µl
Total	10 µl

7.5 Pichia expression

Pichia ATR was inoculated into 5 ml YPD medium containing 300 µg/ml blasticidin S and incubated at 30°C for two days. A 5 ml aliquot was transferred into 40 ml of YPD medium supplemented with 300 µg/ml blasticidin S and then incubated at 30°C until the OD_{600} reached between 1.0-1.3. The cells were collected by centrifugation at 1,500 × *g* for 5 min at 4°C. The cells were dissolved in LiAc DTT solution and incubate at room temperature for 30 min. The collected cells were washed in 1 ml solution of 1 M sorbitol for three times at 0°C and finally resuspended in 250 µl of 1 M sorbitol. The linearized pPICZ-B carrying CYP94J genes was transformed by using electroporation into the prepared *Pichia* and incubated at 30°C for 3 h without shaking. The successful

transformants were selected in YPD agar medium containing 300 µg/ml blasticidin S and 100 µg/ml zeocin.

7.6 Medium compositions

Yeast Extract Peptone Dextrose Medium (YPD)

1% yeast extract

2% peptone

Sterile water

2% agar (optional for making YPD plates)

2% dextrose (glucose)

Minimal Glycerol Medium

1.34% yeast nitrogen base

1% glycerol

4 x 10^{-5}% biotin

Minimal MeOH Medium

1.34% yeast nitrogen base

4 x 10^{-5}% biotin

0.5% methanol

Luria Broth (LB)

10 g/l tryptone

5 g/l yeast extract

5 g/l NaCl

BCDATG

H_2O	900 ml
Stock solution B	10 ml
Stock solution C	10 ml
Stock solution D	10 ml
Alternative TES	1 ml
500 mM ammonium tartrate	10 ml（final concentration 5 mM）
50 mM CaCl2・2H2O	20 ml（final concentration 1 mM）
Agar (Sigma A6924）	8 g（final concentration 0.8%）
Glucose	5 g
H_2O	up to 1000 ml

Sock solution B (x100)

$MgSO_4$・7 H_2O	25 g (0.1 mM)
H_2O	up to 1000 ml

Stock solution C (x100)

KH_2PO_4	25 g (1.84 mM)
4 M KOH	adjust pH to 6.5
H_2O	up to 1000 ml

Stock solution D (x100)

KNO_3	101 g (1 M)

$FeSO_4 \cdot 7\ H_2O$	1.25 g (4.5 mM)
H_2O	up to 1000 ml

S.O.C

2% tryptone

0.5% yeast extract

10 mM NaCl

2.5 mM KCl

10 mM $MgCl_2$

10 mM $MgSO_4$

20 mM glucose

Table 4. Oligonucleotide primers.

Primer Name	Sequence 5’ to 3’	Purpose
SmAOC1-RT	GGAGCAACGGACTGC	5’-RACE PCR
SmAOC1_A1	GAGATGTGGCCGTAGTCCC	5’-RACE PCR
SmAOC1_S1	GGATACGTACATGGCGATCA	5’-RACE PCR
SmAOC1_A2	AAGCTGTAGGTGGCCTCGTA	5’-RACE PCR
SmAOC1_S2	CTTCTACTTGGAGGGCATCG	5’-RACE PCR
SmAOC1-F	ATGGCAAGTTCCCTGGCG	ORF SmAOC1
SmAOC1-R	TTAATCTGTGAAGTTTGGAGCAAC	ORF SmAOC1
SmAOC1SphI-F	TAGCATGCTCAGCTGCCATTGTCCC	Hetero-overexpression of SmAOC1
SmAOC1SalI-R	CGGTCGACTTAATCTGTGAAGTTTGGAG	Hetero-overexpression of SmAOC1
SmAOC1NdeI-F	AAAAGCAGGCTCCACCATGGCAAGTTCCCT	Subcellular localization of SmAOC1
SmAOC1EcoRV-R	AAGCTGGGTCTAGATTTAATCTGTGAAGTT	Subcellular localization of SmAOC1
SmOPR1-F	ATGGATGCGCCCCAGGAGCA	ORF SmOPR1
SmOPR1-R	AGCTATCGTTTTTCTTAATCTTCAAGGAAAGGA	ORF SmOPR1
SmOPR1EcoRI-F	GAATTCATGGATGCGCCCCAGG	Hetero-overexpression SmOPR1
SmOPR1NotI-R	GCGGCCGCATCTTCAAGGAAAGG	Hetero-overexpression SmOPR1
SmOPR5-F	ATGGAAAGCTCATCAAATCCTCTGA	ORF SmOPR5
SmOPR5-R	CTAAAGTTTGCTGGGGTGTTTCTT	ORF SmOPR5
SmOPR5BamHI-F	ATGGGTCGCGGATCCATGGAAAGCTCATCA	Hetero-overexpression SmOPR5
SmOPR5IXhoI-R	GTGGTGGTGCTCGAGAAGTTTGCTGGGGTG	Hetero-overexpression SmOPR5
SmJAR1-F	ATGCCAGGGATTCCATTGAT	ORF SmJAR1
SmJAR1-R	CTACTCTCTCCTCACTCCCG	ORF SmJAR1
SmJAR1BamHI-F	ATGGGTCGCGGATCCATGCCAGGGATTCCA	Hetero-overexpression SmJAR1
SmJAR1IXhoI-R	GTGGTGGTGCTCGAGCTCTCTCCTCACTCC	Hetero-overexpression SmJAR1
SmAOS1_F	CTTAGCAGCTCACACTTCAC	ORF SmAOS1
SmAOS1_R	GACATACACACTAGTGCATTTC	ORF SmAOS1
SmAOS2_F	CTTAGCAGCTCATACTTCACTTC	ORF SmAOS2
SmAOS2_R	GACAACGAACACAGGTGATTGTG	ORF SmAOS2

SmAOS3_F	CTTAGCAGCTCAAACTTCAC	ORF SmAOS3
SmAOS3_R	GCATTTCATTTCATGCTCGC	ORF SmAOS3
SmAOS1EcoRI-F	CCGAATTCATGAGCAACGACAGGAACCT	Hetero-overexpression SmAOS1
SmAOS1XhoI-R	TGCTCGAGTGCTCGCTTCTTGAGCTCGG	Hetero-overexpression SmAOS1
SmAOS2NdeI-F	TACATATGAGCAACGACAGGAACCT	Hetero-overexpression SmAOS2
SmAOS2XhoI-R	TGCTCGAGTGCTCGCTTCTTGAGCTCGG	Hetero-overexpression SmAOS2
qSmAOC1-F	TTCCCGACCAAGCTCTTCTA	Expression analysis of SmAOC1
qSmAOC1-R	AAGTTTGGAGCAACGGACTG	Expression analysis of SmAOC1
qSmOPR5-F	AGCTGTGCATGACAAAGGTG	Expression analysis of SmOPR5
qSmOPR5-R	GGACTGTCCATCTGGGAAGA	Expression analysis of SmOPR5
qSmJAR1-F	AGTATACCGCCCATGCTGAC	Expression analysis of SmJAR1
qSmJAR1-R	CCATGCAATCACAACACTCC	Expression analysis of SmJAR1
qSmUbi1-F	ATACCATCGGCGATTTGAAG	Reference gene ubiquitin
qSmUbi1-R	CGCTTACAAGGAAAGCACCT	Reference gene ubiquitin
SmActin-F	ACTGGGACGACATGGAGAAG	Reference gene actin
SmActin-R	CGCCTGAATAGCAACGTACA	Reference gene actin
CYP94J1-F	ATGGAGCAAGGTACTTTAGCTGCTG	ORF CYP94J1
CYP94J1-R	TTACTCTCGAGCTCTCGGAATCACT	ORF CYP94J1
CYP94J2-F	ATGTTGTGGAGCTTGAGCTTTGTTC	ORF CYP94J2
CYP94J2-R	CTAACGAAGCTTGGGAACAACGGGA	ORF CYP94J2
CYP94J1EcoRI-F	GAATTCATGGAGCAAGGTACTTTAGCTG	Hetero-overexpression CYP94J1
CYP94J1NotI-R	GCGGCCGCTTACTCTCGAGCTCTCGGAA	Hetero-overexpression CYP94J1
CYP94J2EcoRI-F	GAATTCATGTTGTGGAGCTTGAGCTTTG	Hetero-overexpression CYP94J2
CYP94J2NotI-R	GCGGCCGCCTAACGAAGCTTGGGAACAACG	Hetero-overexpression CYP94J2

ACKNOWLEDGEMENTS

Having a chance to study abroad is like a dream comes true to me, especially in Japan. I am so grateful to the Special English Program provided by Hokkaido University and the financial support from MEXT for making it all possible for me to study in here.

First and foremost, I would like to express my biggest gratitude to the most superb supervisor Dr. Kosaku Takahashi for his guidance, immense knowledge, and understanding that added considerably to my graduate experience. For always motivate me so that I became more focus and interest in my research area. My deepest appreciation is addressed to Prof. Hideyuki Matsuura for giving me valuable suggestions, insightful comments, and difficult questions. My sincere thanks are also addressed to Prof. Yasuyuki Hashidoko for his contribution to the accomplishment of this thesis.

Thank to my undergraduate thesis supervisor in Indonesia, Dr. Susan Soka; and Dr. Hanny Wijaya to share the information about this Special English Program in Hokkaido University. Thank to Dr. Eri Fukushi and Mr. Yusuke Takata for helping me doing the GC-MS analysis. Thank to Dr. Mitsuyasu Hasebe for kindly providing pUGWnew5 plasmid. Thank to Prof. Koichi Yoneyama and Dr. Xiaonan Xie from Utsunomiya University for kindly providing *S. moellendorffii*.

Thanks to all members in the Laboratory of Natural Product Chemistry. I am very lucky to have a chance to become a part of this laboratory. During these five years, your kindness to teach me patiently, to welcome and always try to speak in English with me is priceless.

To my lovely parents Mr. Tan Jan Boen and Mrs. Fransiska Andriaty, and also my brother Priyo Pratomo that I have been blessed with, thank you for always support me spiritually through my life and their unconditional love during my ups and downs. Last but not least thanks to all my beloved friends, especially Albert who always encourages me to stay strong for going through the tough life in Japan and also for listening to and having to tolerate me over the past three years.

BIBLIOGRAPHY

Agrawal GK, Jwa N-S, Agrawal SK, Tamogami S, Iwahashi H and Rakwal R (2003) Cloning of novel rice allene oxide cyclase (OsAOC): mRNA expression and comparative analysis with allene oxide synthase (OsAOS) gene provides insight into the transcriptional regulation of octadecanoid pathway biosynthetic genes in rice. *Plant Sci.*, 164(6): 979–992.

Aldridge DC, Galt S, Giles D and Turner WB (1971) Metabolites of *Lasiodiplodia theobromae*. *J. Chem. Soc. C Org.*, 1623.

Arnold MD, Gruber C, Floková K, Miersch O, Strnad M, Novák O, Wasternack C and Hause B (2016) The recently identified isoleucine conjugate of *cis*-12-oxo-phytodienoic acid is partially active in *cis*-12-oxo-phytodienoic acid-specific gene expression of *Arabidopsis thaliana*. *PLOS ONE*, 11(9): e0162829.

Avanci NC, Luche DD, Goldman GH and Goldman MHS (2010) Review Jasmonates are phytohormones with multiple functions, including plant defense and reproduction. *Genet. Mol. Res.*, 9(1): 484–505.

Bandara PKGSS, Takahashi K, Sato M, Matsuura H and Nabeta K (2009) Cloning and functional analysis of an allene oxide synthase in *Physcomitrella patens*. *Biosci. Biotechnol. Biochem.*, 73(10): 2356–2359.

Banks JA, Nishiyama T, Hasebe M, Bowman JL, Gribskov M, dePamphilis C, Albert VA, Aono N, Aoyama T, Ambrose BA, et al. (2011) The *Selaginella* genome identifies genetic changes associated with the evolution of vascular plants. *Science*, 332(6032): 960–963.

Bannenberg G, Martínez M, Hamberg M and Castresana C (2009) Diversity of the enzymatic activity in the lipoxygenase gene family of *Arabidopsis thaliana*. *Lipids*, 44(2): 85–95.

Benveniste I, Tijet N, Adas F, Philipps G, Salaün J-P and Durst F (1998) CYP86A1 from *Arabidopsis thaliana* encodes a cytochrome P450-dependent fatty acid omega-hydroxylase. *Biochem. Biophys. Res. Commun.*, 243(3): 688–693.

Bosch M, Wright LP, Gershenzon J, Wasternack C, Hause B, Schaller A and Stintzi A (2014) Jasmonic acid and its precursor 12-oxophytodienoic acid control different aspects of constitutive and induced herbivore defenses in tomato. *Plant Physiol.*, 166(1): 396–410.

Breithaupt C, Kurzbauer R, Schaller F, Stintzi A, Schaller A, Huber R, Macheroux P and Clausen T (2009) Structural basis of substrate specificity of plant 12-oxophytodienoate reductases. *J. Mol. Biol.*, 392(5): 1266–1277.

Chang KH, Xiang H and and Dunaway-Mariano D (1997) Acyl-adenylate motif of the acyl-adenylate/thioester-forming enzyme superfamily: A site-directed mutagenesis study with the pseudomonas sp. strain CBS3 4-chlorobenzoate:coenzyme a ligase. *Biochem.* 36 (50): 15650-15659.

Chehab EW, Wang Y and Braam J (2011) Mechanical Force Responses of Plant Cells and Plants. Signaling and Communication in Plants Vol. 9. Springer Berlin Heidelberg, pp. 173–194.

Christensen SA, Huffaker A, Kaplan F, Sims J, Ziemann S, Doehlemann G, Ji L, Schmitz RJ, Kolomiets M V, Alborn HT, et al. (2015) Maize death acids, 9-lipoxygenase-derived cyclopente(a)nones, display activity as cytotoxic phytoalexins and transcriptional mediators. *Proc. Natl. Acad. Sci. U.S.A.*, 112(36): 11407–11412.

Creelman RA and Mullet JE (1995) Jasmonic acid distribution and action in plants: regulation during development and response to biotic and abiotic stress. *Proc. Natl. Acad. Sci. U.S.A.*, 92(10): 4114–4119.

Creelman RA and Mullet JE (1997) Biosynthesis and action of jasmonates in plants. *Annu. Rev. Plant Physiol. Plant Mol. Biol.*, 48(1): 355–381.

Dave A, Hernández ML, He Z, Andriotis VME, Vaistij FE, Larson TR and Graham IA (2011) 12-Oxo-phytodienoic acid accumulation during seed development represses seed germination in *Arabidopsis*. *Plant Cell.*, 23(2): 583–599.

Dave A, Vaistij FE, Gilday AD, Penfield SD and Graham IA (2016) Regulation of *Arabidopsis thaliana* seed dormancy and germination by 12-oxo-phytodienoic acid. *J. Exp. Bot.*, 67(8): 2277–2284.

Demole E, Lederer E and Mercier D (1962) Isolement et détermination de la structure du jasmonate de méthyle, constituant odorant caractéristique de l'essence de jasmin. *Helv. Chim. Acta.*, 45(2): 675–685.

Farmaki T, Sanmartin M, Jimenez P, Paneque M, Sanz C, Vancanneyt G, Leon J and Sanchez-Serrano JJ (2006) Differential distribution of the lipoxygenase pathway enzymes within potato chloroplasts. *J. Exp. Bot.*, 58(3): 555–568.

Feussner I and Wasternack C (2002) The lipoxygenase pathway. *Annu. Rev. Plant Biol.*, 53(1): 275–297.

Floková K, Feussner K, Herrfurth C, Miersch O, Mik V, Tarkowská D, Strnad M, Feussner I, Wasternack C and Novák O (2016) A previously undescribed jasmonate compound in flowering *Arabidopsis thaliana* – The identification of *cis*-(+)-OPDA-Ile. *Phytochemistry*, 122: 230–237.

Fonseca S, Chini A, Hamberg M, Adie B, Porzel A, Kramell R, Miersch O, Wasternack C and Solano R (2009) (+)-7-Iso-jasmonoyl-L-isoleucine is the endogenous bioactive jasmonate. *Nat. Chem. Biol.*, 5(5): 344–350.

Fortes AM, Miersch O, Lange PR, Malhó R, Testillano PS, Risueño MDC, Wasternack C and Pais MS (2005) Expression of allene oxide cyclase and accumulation of jasmonates during organogenic nodule formation from hop (*Humulus lupulus* var. Nugget) Internodes. *Plant Cell Physiol.*, 46(10): 1713–1723.

Futuyma DJ (1998) *Evolutionary Biology*. Sinauer Associates. Available at: https://books.google.co.jp/books/about/Evolutionary_Biology.html?id=yGhdGQAACAAJ&redir_esc=y.

Gidda SK, Miersch O, Levitin A, Schmidt J, Wasternack C and Varin L (2003) Biochemical and molecular characterization of a hydroxyjasmonate sulfotransferase from *Arabidopsis thaliana*. *J. Biol. Chem.*, 278(20): 17895–17900.

Goetz S, Hellwege A, Stenzel I, Kutter C, Hauptmann V, Forner S, McCaig B, Hause G, Miersch O, Wasternack C, et al. (2012) Role of cis-12-oxo-phytodienoic acid in tomato embryo development. *Plant Physiol.*, 158(4): 1715–1727.

Guttikonda SK, Trupti J, Bisht NC, Chen H, An Y-QC, Pandey S, Xu D and Yu O (2010) Whole genome co-expression analysis of soybean cytochrome P450 genes identifies nodulation-specific P450 monooxygenases. *BMC Plant Biol.*, 10(1): 243.

Habora MEE, Eltayeb AE, Oka M, Tsujimoto H, Tanaka K, Grimm R, Ganal M, Wasternack C, Wasternack C and Tang K (2013) Cloning of allene oxide cyclase gene from Leymus mollis and analysis of its expression in wheat–Leymus chromosome addition lines. *Breed. Sci.*, 63(1): 68–76.

Hamberg M and Fahlstadius P (1990) Allene oxide cyclase: a new enzyme in plant lipid metabolism. *Arch. Biochem. Biophys.*, 276(2): 518–526.

Hashimoto T, Takahashi K, Sato M, Bandara PKGSS and Nabeta K (2011) Cloning and characterization of an allene oxide cyclase, PpAOC3, in *Physcomitrella patens*. *Plant Growth Regul.*, 65(2): 239–245.

Heitz T, Widemann E, Lugan R, Miesch L, Ullmann P, Desaubry L, Holder E, Grausem B, Kandel S, Miesch M, et al. (2012) Cytochromes P450 CYP94C1 and

CYP94B3 catalyze two successive oxidation steps of plant hormone jasmonoyl-isoleucine for catabolic turnover. *J. Biol. Chem.*, 287(9): 6296–6306.

Helliwell CA, Chandler PM, Poole A, Dennis ES and Peacock WJ (2001) The CYP88A cytochrome P450, *ent*-kaurenoic acid oxidase, catalyzes three steps of the gibberellin biosynthesis pathway. *Proc. Natl. Acad. Sci. U.S.A.*, 98(4): 2065–2070.

Ishiguro S, Kawai-Oda A, Ueda J, Nishida I and Okada K (2001) The defective in anther dehiscience gene encodes a novel phospholipase A1 catalyzing the initial step of jasmonic acid biosynthesis, which synchronizes pollen maturation, anther dehiscence, and flower opening in Arabidopsis. *Plant Cell*, 13(10): 2191–209.

Kang JH, Wang L, Giri A and Baldwin IT (2006) Silencing threonine deaminase and JAR4 in *Nicotiana attenuata* impairs jasmonic acid-isoleucine-mediated defenses against *Manduca sexta*. *Plant Cell*, 18(11): 3303–3320.

Kenrick P and Crane PR (1997) The origin and early evolution of plants on land. *Nature*, 389(6646): 33–39.

Kirkbride RC, Fischer RL, Harada JJ, Zheng X and Qu C (2013) *LEAFY COTYLEDON1*, a key regulator of seed development, is expressed in vegetative and sexual propagules of *Selaginella moellendorffii*. *PLOS ONE*, 8(6): e67971.

Kitaoka N, Matsubara T, Sato M, Takahashi K, Wakuta S, Kawaide H, Matsui H, Nabeta K and Matsuura H (2011) Arabidopsis *CYP94B3* encodes jasmonyl-L-isoleucine 12-hydroxylase, a key enzyme in the oxidative catabolism of jasmonate. *Plant Cell Physiol.*, 52(10): 1757–1765.

Koch T, Bandemer K and Boland W (1997) Biosynthesis ofcis-Jasmone: a pathway for the inactivation and the disposal of the plant stress hormone jasmonic acid to the gas phase? *Helv. Chim. Acta*, 80(3): 838–850.

Koeduka T, Ishizaki K, Mwenda CM, Hori K, Sasaki-Sekimoto Y, Ohta H, Kohchi T and Matsui K (2015) Biochemical characterization of allene oxide synthases from the liverwort *Marchantia polymorpha* and green microalgae *Klebsormidium flaccidum* provides insight into the evolutionary divergence of the plant CYP74 family. *Planta*, 242(5): 1175–1186.

Kombrink E (2012) Chemical and genetic exploration of jasmonate biosynthesis and signaling paths. *Planta*, 236(5): 1351–1366.

Koo AJK, Cooke TF and Howe GA (2011) Cytochrome P450 CYP94B3 mediates catabolism and inactivation of the plant hormone jasmonoyl-L-isoleucine. *Proc. Natl. Acad. Sci. U.S.A*, 108(22): 9298–9303.

Koo AJK and Howe GA (2012) Catabolism and deactivation of the lipid-derived hormone jasmonoyl-isoleucine. *Front. Plant Sci.*, 3: 19.

Larrieu A and Vernoux T (2016) Q&A: How does jasmonate signaling enable plants to adapt and survive? *BMC Biol.*, 14: 79.

Laudert D, Hennig P, Stelmach BA, Müller A, Andert L and Weiler EW (1997) Analysis of 12-oxo-phytodienoic acid enantiomers in biological samples by capillary gas chromatography–mass spectrometry using cyclodextrin stationary phases. *Anal. Biochem.*, 246(2): 211–217.

Li W, Liu B, Yu L, Feng D, Wang H and Wang J (2009) Phylogenetic analysis, structural evolution and functional divergence of the 12-oxo-phytodienoate acid reductase gene family in plants. *BMC Evol. Biol.*, 9(1): 90.

Li W, Zhou F, Liu B, Feng D, He Y, Qi K, Wang H and Wang J (2011) Comparative characterization, expression pattern and function analysis of the 12-oxo-phytodienoic acid reductase gene family in rice. *Plant Cell Rep.*, 30(6): 981–995.

Livingstone B (2014) The Princeton Guide to Evolution, Princeton: Princeton University Press. doi: 10.1111/bij.12257.

Ludwig-Müller J, Jülke S, Bierfreund NM, Decker EL and Reski R (2009) Moss (*Physcomitrella patens*) GH3 proteins act in auxin homeostasis. *New Phytol.*, 181(2): 323–338.

Maucher H, Hause B, Feussner I, Ziegler J and Wasternack C (2000) Allene oxide synthases of barley (*Hordeum vulgare* cv. Salome): tissue specific regulation in seedling development. *Plant J.*, 21(2): 199–213.

Maucher H, Stenzel I, Miersch O, Stein N, Prasad M, Zierold U, Schweizer P, Dorer C, Hause B and Wasternack C (2004) The allene oxide cyclase of barley (*Hordeum vulgare* L.)—cloning and organ-specific expression. *Phytochemistry*, 65(7): 801–811.

Miersch O, Neumerkel J, Dippe M, Stenzel I and Wasternack C (2007) Hydroxylated jasmonates are commonly occurring metabolites of jasmonic acid and contribute to a partial switch-off in jasmonate signaling. *New Phytol.* 177 (1): 114-127.

Mosblech A, Feussner I and Heilmann I (2009) Oxylipins: Structurally diverse metabolites from fatty acid oxidation. *Plant Physiol. Biochem.*, 47(6): 511–517.

Nelson DR, Schuler MA, Paquette SM, Werck-Reichhart D and Bak S (2004) Comparative genomics of rice and Arabidopsis. Analysis of 727 cytochrome P450 genes and pseudogenes from a monocot and a dicot. *Plant Physiol.*, 135(2): 756–

72.

Noir S, Bomer M, Takahashi N, Ishida T, Tsui T-L, Balbi V, Shanahan H, Sugimoto K and Devoto A (2013) Jasmonate controls leaf growth by repressing cell proliferation and the onset of endoreduplication while maintaining a potential stand-by mode. *Plant Physiol.*, 161(4): 1930–1951.

Okrent RA, Brooks MD and Wildermuth MC (2009) Arabidopsis GH3.12 (PBS3) conjugates amino acids to 4-substituted benzoates and is inhibited by salicylate. *J. Biol. Chem.*, 284(15): 9742–9754.

Pan Z, Durst F, Werck-Reichhart D, Gardner HW, Camara B, Cornish K and Backhaus RA (1995) The major protein of guayule rubber particles is a cytochrome P450. Characterization based on cDNA cloning and spectroscopic analysis of the solubilized enzyme and its reaction products. *J. Biol. Chem.*, 270(15): 8487–8494.

Park J-H, Halitschke R, Kim HB, Baldwin IT, Feldmann KA and Feyereisen R (2002) A knock-out mutation in allene oxide synthase results in male sterility and defective wound signal transduction in Arabidopsis due to a block in jasmonic acid biosynthesis. *Plant J.*, 31(1): 1–12.

Pi Y, Liao Z, Jiang K, Huang B, Deng Z, Zhao D, Zeng H, Sun X and Tang K (2008) Molecular cloning, characterization and expression of a jasmonate biosynthetic pathway gene encoding allene oxide cyclase from *Camptotheca acuminata*. *Biosci. Rep.*, 28(6): 349.

Pinot F and Beisson F (2011) Cytochrome P450 metabolizing fatty acids in plants: characterization and physiological roles. *FEBS J.*, 278(2): 195–205.

Ponce de león I, Schmelz EA, Gaggero C, Castro A, Álvarez A and Montesano M (2012) *Physcomitrella patens* activates reinforcement of the cell wall, programmed cell death and accumulation of evolutionary conserved defence signals, such as salicylic acid and 12-oxo-phytodienoic acid, but not jasmonic acid, upon *Botrytis cinerea* infection. *Mol. Plant Pathol.*, 13(8): 960–974.

Radhika V, Kost C, Bonaventure G, David A and Boland W (2012) Volatile emission in bracken fern is induced by jasmonates but not by spodoptera littoralis or strongylogaster multifasciata herbivory. *PLOS ONE*, 7(11): e48050.

Reymond P and Farmer EE (1998) Jasmonate and salicylate as global signals for defense gene expression. *Curr. Opin. Plant Biol.*, 1(5): 404–411.

Sanders PM, Lee PY, Biesgen C, Boone JD, Beals TP, Weiler EW and Goldberg RB (2000) The arabidopsis *DELAYED DEHISCENCE1* gene encodes an enzyme in

the jasmonic acid synthesis pathway. *Plant Cell*, 12(7): 1041–1061.

Santino A, Taurino M, De Domenico S, Bonsegna S, Poltronieri P, Pastor V and Flors V (2013) Jasmonate signaling in plant development and defense response to multiple (a)biotic stresses. *Plant Cell Rep.*, 32(7): 1085–1098.

Sato C, Aikawa K, Sugiyama S, Nabeta K, Masuta C and Matsuura H (2011) Distal transport of exogenously applied jasmonoyl-isoleucine with wounding stress. *Plant Cell Physiol.*, 52(3): 509–517.

Sato C, Seto Y, Nabeta K and Matsuura H (2009) Kinetics of the accumulation of jasmonic acid and its derivatives in systemic leaves of tobacco (*Nicotiana tabacum* cv. Xanthi nc) and translocation of deuterium-labeled jasmonic acid from the wounding site to the systemic site. *Biosci. Biotechnol. Biochem.*, 73(9): 1962–1970.

Savchenko T and Dehesh K (2014) Drought stress modulates oxylipin signature by eliciting 12-OPDA as a potent regulator of stomatal aperture. *Plant Signal. Behav.*, 9(3), e28304.

Schaller A and Stintzi A (2008) Jasmonate biosynthesis and signaling for induced plant defense against herbivory. in *Induc. Plant Resist. to Herbiv.*, pp. 349–366.

Schaller A and Stintzi A (2009) Enzymes in jasmonate biosynthesis – Structure, function, regulation. *Phytochemistry*, 70(13–14): 1532–1538.

Schaller F (2001) Enzymes of the biosynthesis of octadecanoid-derived signalling molecules. *J. Exp. Bot.*, 52(354): 11–23.

Schaller F, Biesgen C, Müssig C, Altmann T and Weiler EW (2000) 12-Oxophytodienoate reductase 3 (OPR3) is the isoenzyme involved in jasmonate biosynthesis. *Planta*, 210(6): 979–984.

Schaller F, Hennig P and Weiler EW (1998) 12-Oxophytodienoate-10,11-reductase: occurrence of two isoenzymes of different specificity against stereoisomers of 12-oxophytodienoic acid. *Plant Physiol.*, 118(4): 1345–1351.

Schaller F and Weiler EW (1997) Enzymes of octadecanoid biosynthesis in plants. 12-Oxo-Phytodienoate 10,11-reductase. *Eur. J. Biochem.*, 245(2): 294–299.

Schaller F and Weiler EW (1997) Molecular cloning and characterization of 12-oxophytodienoate reductase, an enzyme of the octadecanoid signaling pathway from *Arabidopsis thaliana*. Structural and functional relationship to yeast old yellow enzyme. *J. Biol. Chem.*, 272(44): 28066–28072.

Sembdner G and Parthier B (1993) The biochemistry and the physiological and

molecular actions of jasmonates. *Annu. Rev. Plant Physiol. Plant Mol. Biol.*, 44(1): 569–589.

Seo HS, Song JT, Cheong J-J, Lee Y-H, Lee Y-W, Hwang I, Lee JS and Choi YD (2001) Jasmonic acid carboxyl methyltransferase: A key enzyme for jasmonate-regulated plant responses. *Proc. Natl. Acad. Sci. U.S.A.*, 98(8): 4788–4793.

Sheard LB, Tan X, Mao H, Withers J, Ben-Nissan G, Hinds TR, Kobayashi Y, Hsu F-F, Sharon M, Browse J, et al. (2010) Jasmonate perception by inositol-phosphate-potentiated COI1-JAZ co-receptor. *Nature*, 468(7322): 400–405.

Staswick PE, Serban B, Rowe M, Tiryaki I, Maldonado MT, Maldonado MC and Suza W (2005) Characterization of an Arabidopsis enzyme family that conjugates amino acids to indole-3-acetic acid. *Plant Cell*, 17(2): 616–627.

Staswick PE and Tiryaki I (2004) The oxylipin signal jasmonic acid is activated by an enzyme that conjugates it to isoleucine in Arabidopsis. *Plant Cell*, 16(8): 2117–2127.

Stelmach BA, Müller A, Hennig P, Laudert D, Andert L and Weiler EW (1998) Quantitation of the octadecanoid 12-oxo-phytodienoic acid, a signalling compound in plant mechanotransduction. *Phytochemistry*, 47(4): 539–546.

Stenzel I, Hause B, Miersch O, Kurz T, Maucher H, Weichert H, Ziegler J, Feussner I and Wasternack C (2003) Jasmonate biosynthesis and the allene oxide cyclase family of *Arabidopsis thaliana*. *Plant Mol. Biol.*, 51(6): 895–911.

Stintzi A and Browse J (2000) The Arabidopsis male-sterile mutant, opr3, lacks the 12-oxophytodienoic acid reductase required for jasmonate synthesis. *Proc. Natl. Acad. Sci. U.S.A.*, 97(19): 10625–10630.

Stintzi A, Weber H, Reymond P, Browse J and Farmer EE (2001) Plant defense in the absence of jasmonic acid: the role of cyclopentenones. *Proc. Natl. Acad. Sci. U.S.A.*, 98(22): 12837–12842.

Strassner J, Schaller F, Frick UB, Howe GA, Weiler EW, Amrhein N, Macheroux P and Schaller A (2002) Characterization and cDNA-microarray expression analysis of 12-oxophytodienoate reductases reveals differential roles for octadecanoid biosynthesis in the local versus the systemic wound response. *Plant J.*, 32(4): 585–601.

Stumpe M and Feussner I (2006) Formation of oxylipins by CYP74 enzymes. *Phytochem. Rev.*, 5(2–3): 347–357.

Stumpe M, Göbel C, Faltin B, Beike AK, Hause B, Himmelsbach K, Bode J, Kramell R,

Wasternack C, Frank W, et al. (2010) The moss *Physcomitrella patens* contains cyclopentenones but no jasmonates: mutations in allene oxide cyclase lead to reduced fertility and altered sporophyte morphology. *New Phytol.*, 188(3): 740–749.

Suza WP, Rowe ML, Hamberg M and Staswick PE (2010) A tomato enzyme synthesizes (+)-7-iso-jasmonoyl-L-isoleucine in wounded leaves. *Planta*, 231(3): 717–728.

Suza WP and Staswick PE (2008) The role of JAR1 in Jasmonoyl-L-isoleucine production during Arabidopsis wound response. *Planta*, 227(6): 1221–1232.

Swarup R and Péret B (2012) AUX/LAX family of auxin influx carriers-an overview. *Front. Plant Sci.*, 3: 225.

Swiatek A, Van Dongen W, Esmans EL and Van Onckelen H (2004) Metabolic fate of jasmonates in tobacco bright yellow-2 cells. *Plant Physiol.*, 135(1): 161–172.

Taki N, Sasaki-Sekimoto Y, Obayashi T, Kikuta A, Kobayashi K, Ainai T, Yagi K, Sakurai N, Suzuki H, Masuda T, et al. (2005) 12-oxo-phytodienoic acid triggers expression of a distinct set of genes and plays a role in wound-induced gene expression in *Arabidopsis*. *Plant Physiol.*, 139(3): 1268–1283.

Tani T, Sobajima H, Okada K, Chujo T, Arimura S, Tsutsumi N, Nishimura M, Seto H, Nojiri H and Yamane H (2008) Identification of the *OsOPR7* gene encoding 12-oxophytodienoate reductase involved in the biosynthesis of jasmonic acid in rice. *Planta*, 227(3): 517–526.

Thines B, Katsir L, Melotto M, Niu Y, Mandaokar A, Liu G, Nomura K, He SY, Howe GA and Browse J (2007) JAZ repressor proteins are targets of the SCFCOI1 complex during jasmonate signalling. *Nature*, 448(7154): 661–665.

Turk EM, Fujioka S, Seto H, Shimada Y, Takatsuto S, Yoshida S, Wang H, Torres QI, Ward JM, Murthy G, et al. (2005) BAS1 and SOB7 act redundantly to modulate Arabidopsis photomorphogenesis via unique brassinosteroid inactivation mechanisms. *Plant J.*, 42(1): 23–34.

Umezawa T, Okamoto M, Kushiro T, Nambara E, Oono Y, Seki M, Kobayashi M, Koshiba T, Kamiya Y and Shinozaki K (2006) CYP707A3, a major ABA 8′-hydroxylase involved in dehydration and rehydration response in *Arabidopsis thaliana*. *Plant J.*, 46(2): 171–182.

Vick BA and Zimmerman DC (1983) The biosynthesis of jasmonic acid: a physiological role for plant lipoxygenase. *Biochem. Biophys. Res. Commun.*,

111(2): 470–477.

Wakuta S, Suzuki E, Saburi W, Matsuura H, Nabeta K, Imai R and Matsui H (2011) OsJAR1 and OsJAR2 are jasmonyl-L-isoleucine synthases involved in wound- and pathogen-induced jasmonic acid signalling. *Biochem. Biophys. Res. Commun.*, 409(4): 634–639.

Wang C, Liu Y, Li S-S and Han G-Z (2015) Insights into the origin and evolution of the plant hormone signaling machinery. *Plant Physiol.*, 167(3): 872–886.

Wang W, Tanurdzic M, Luo M, Sisneros N, Kim HR, Weng J-K, Kudrna D, Mueller C, Arumuganathan K, Carlson J, et al. (2005) Construction of a bacterial artificial chromosome library from the spikemoss *Selaginella moellendorffii*: a new resource for plant comparative genomics. *BMC Plant Biol.*, 5(1): 10.

Wasternack C (2007) Jasmonates: An Update on biosynthesis, signal transduction and action in plant stress response, growth and development. *Ann. Bot.*, 100(4): 681–697.

Wasternack C and Hause B (2013) Jasmonates: biosynthesis, perception, signal transduction and action in plant stress response, growth and development. An update to the 2007 review in Annals of Botany. *Ann. Bot.*, 111(6): 1021–1058.

Wasternack C and Kombrink E (2010) Jasmonates: Structural Requirements for Lipid-Derived Signals Active in Plant Stress Responses and Development. *ACS Chem. Biol.*, 5: 63–77.

Wasternack C, Parthier B and Mullet JE (1997) Jasmonate-signalled plant gene expression. *Trends Plant Sci.*, 2(8): 302–307.

Weiler EW, Albrecht T, Groth B, Xia Z-Q, Luxem M, Liß H, Andert L and Spengler P (1993) Evidence for the involvement of jasmonates and their octadecanoid precursors in the tendril coiling response of *Bryonia dioica*. *Phytochemistry*, 32(3): 591–600.

Widemann E, Miesch L, Lugan R, Holder E, Heinrich C, Aubert Y, Miesch M, Pinot F and Heitz T (2013) The amidohydrolases IAR3 and ILL6 contribute to jasmonoyl-isoleucine hormone turnover and generate 12-hydroxyjasmonic acid upon wounding in Arabidopsis leaves. *J. Biol. Chem.*, 288(44): 31701–31714.

Woldemariam MG, Onkokesung N, Baldwin IT and Galis I (2012) Jasmonoyl-L-isoleucine hydrolase 1 (JIH1) regulates jasmonoyl-L-isoleucine levels and attenuates plant defenses against herbivores. *Plant J.*, 72(5): 758–767.

Yamamoto Y, Ohshika J, Takahashi T, Ishizaki K, Kohchi T, Matusuura H and

Takahashi K (2015) Functional analysis of allene oxide cyclase, MpAOC, in the liverwort *Marchantia polymorpha*. *Phytochemistry*, 116: 48–56.

Yan Y, Borrego E and V. M (2013) Jasmonate biosynthesis, perception and function in plant development and stress responses. *Lipid Metab.* doi: 10.5772/52675.

Yan Y, Christensen S, Isakeit T, Engelberth J, Meeley R, Hayward A, Emery RJN and Kolomiets M V (2012) Disruption of *OPR7* and *OPR8* reveals the versatile functions of jasmonic acid in maize development and defense. *Plant Cell.*, 24(4): 1420–1436.

Zhang J, Simmons C, Yalpani N, Crane V, Wilkinson H and Kolomiets M (2005) Genomic analysis of the 12-oxo-phytodienoic acid reductase gene family of *Zea mays*. *Plant Mol. Biol.*, 59(2): 323–343.

Ziegler J, Stenzel I, Hause B, Maucher H, Hamberg M, Grimm R, Ganal M and Wasternack C (2000) Molecular cloning of allene oxide cyclase. The enzyme establishing the stereochemistry of octadecanoids and jasmonates. *J. Biol. Chem.*, 275(25): 19132–19138.